Spring 2007

Design and performance of CDMA codes for multiuser communications

Radharani Poluri
New Jersey Institute of Technology

ABSTRACT

DESIGN AND PERFORMANCE OF CDMA CODES FOR MULTIUSER COMMUNICATIONS

by
Radharani Poluri

Walsh and Gold sequences are fixed power codes and are widely used in multiuser CDMA communications. Their popularity is due to the ease of implementation. Availability of these code sets is limited because of their generating kernels. Emerging radio applications like sensor networks or multiple service types in mobile and peer-to-peer communications networks might benefit from flexibilities in code lengths and possible allocation methodologies provided by large set of code libraries.

Walsh codes are linear phase and zero mean with unique number of zero crossings for each sequence within the set. DC sequence is part of the Walsh code set. Although these features are quite beneficial for source coding applications, they are not essential for spread spectrum communications. By relaxing these unnecessary constraints, new sets of orthogonal binary user codes (Walsh-like) for different lengths are obtained with comparable BER performance to standard code sets in all channel conditions.

Although fixed power codes are easier to implement, mathematically speaking, varying power codes offer lower inter- and intra-code correlations. With recent advances in RF power amplifier design, it might be possible to implement multiple level orthogonal spread spectrum codes for an efficient direct sequence CDMA system. A number of multiple level integer codes have been generated by brute force search

method for different lengths to highlight possible BER performance improvement over binary codes.

An analytical design method has been developed for multiple level (variable power) spread spectrum codes using Karhunen-Loeve Transform (KLT) technique. Eigen decomposition technique is used to generate spread spectrum basis functions that are jointly spread in time and frequency domains for a given covariance matrix or power spectral density function. Since this is a closed form solution for orthogonal code set design, many options are possible for different code lengths. Design examples and performance simulations showed that spread spectrum KLT codes outperform or closely match with the standard codes employed in present CDMA systems.

Hybrid (Kronecker) codes are generated by taking Kronecker product of two spreading code families in a two-stage orthogonal transmultiplexer structure and are judiciously allocated to users such that their inter-code correlations are minimized. It is shown that, BER performance of hybrid codes with a code selection and allocation algorithm is better than the performance of standard Walsh or Gold code sets for asynchronous CDMA communications.

A redundant spreading code technique is proposed utilizing multiple stage orthogonal transmultiplexer structure where each user has its own pre-multiplexer. Each data bit is redundantly spread in the pre-multiplexer stage of a user with odd number of redundancy, and at the receiver, majority logic decision is employed on the detected redundant bits to obtain overall performance improvement. Simulation results showed that redundant spreading method improves BER performance significantly at low SNR channel conditions.

DESIGN AND PERFORMANCE OF CDMA CODES FOR MULTIUSER COMMUNICATIONS

by
Radharani Poluri

A Dissertation
Submitted to the Faculty of
New Jersey Institute of Technology
in Partial Fulfillment of the Requirements for the Degree of
Doctor of Philosophy in Electrical Engineering

Department of Electrical and Computer Engineering

May 2007

APPROVAL PAGE

DESIGN AND PEFORMANCE OF CDMA CODES FOR MULTIUSER COMMUNICATIONS

Radharani Poluri

Dr. Ali N. Akansu, Dissertation Advisor — Date
Professor of Electrical and Computer Engineering, NJIT

Dr. Ali Abdi, Committee Member — Date
Assistant Professor of Electrical and Computer Engineering, NJIT

Dr. Yeheskel Bar-Ness, Committee Member — Date
Distinguished Professor of Electrical and Computer Engineering, NJIT

Dr. Alexander M. Haimovich, Committee Member — Date
Professor of Electrical and Computer Engineering, NJIT

Dr. Rajiv Laroia, Committee Member — Date
Chief Technology Officer, QUALCOMM Flarion Technologies, NJ

Dr. Edip Niver, Committee Member — Date
Associate Professor of Electrical and Computer Engineering, NJIT

BIOGRAPHICAL SKETCH

Author: Radharani Poluri

Degree: Doctor of Philosophy

Date: May 2007

Undergraduate and Graduate Education:

- Doctor of Philosophy in Electrical Engineering,
  New Jersey Institute of Technology, Newark, NJ, 2007
- Master of Science in Computer Science and Engineering,
  Osmania University, Hyderabad, India, 1995
- Bachelor of Science in Electronics and Communication Engineering,
  Regional Engineering College, Warangal, India, 1983

Major: Electrical Engineering

Presentations and Publications:

A. N. Akansu and R. Poluri, "Walsh-like Nonlinear Phase Orthogonal Transforms for Direct Sequence CDMA Communications," IEEE Transactions on Signal Processing, to appear in 2007.

A. N. Akansu and R. Poluri, "New Design Methods and Multiuser CDMA Performance of Constant and Varying Power Spreading Codes," to be submitted to IEEE Transactions on Signal Processing.

A. N. Akansu and R. Poluri, "Design and Performance of Spread Spectrum Karhunen-Loeve Transform for Direct Sequence CDMA Communications," to be submitted to IEEE Signal Processing Letters.

R. Poluri and A. N. Akansu, "Data Pre-multiplexing in Multiple Stage Orthogonal Transmultiplexer for Redundancy Coding in Low-SNR Multiuser Channels," to be submitted to IEEE Signal Processing Letters.

R. Poluri and A. N. Akansu, "New Linear Phase Orthogonal Binary Codes for Spread Spectrum Multi-carrier Communications," Proc. IEEE, VTC, pp. 1-5, Sept. 2006.

R. Poluri and A. N. Akansu, "Walsh-like Nonlinear Phase Orthogonal Transforms for CDMA Communications," Asilomar Conference on Signals, Systems, and Computers, pp. 2214-2218, Nov. 2006.

R. Poluri and A. N. Akansu, "New Orthogonal Binary User Codes for Multi-user Spread Spectrum Communications," Proc. EUSIPCO, pp. 1-4, Sept. 2005.

R. Poluri and A. N. Akansu, "Short Length CDMA Codes for Wireless Sensor Networks," accepted to IEEE, Sarnoff Conference, 2007.

R. Poluri and A. N. Akansu, "Varying Power Integer Codes for CDMA Communications," submitted to IEEE, VTC, 2007.

A. N. Akansu and R. Poluri, "Spread Spectrum Karhunen-Loeve Transform for Direct Sequence CDMA Communications," submitted to IEEE, VTC, 2007.

R. Poluri and A. N. Akansu, "Multiple-Stage Orthogonal Multiplexing for Redundant Spreading in Low-SNR CDMA Systems," submitted to IEEE, GLOBECOM, 2007.

R. Poluri and A. N. Akansu, "New Orthogonal Binary User Codes for Multiuser CDMA Communication," poster presented at NJIT Graduate Research Day, November 2006.

To my parents, my husband and my son

ACKNOWLEDGMENT

First and foremost, I would like to express my sincere gratitude to my advisor Professor Ali N. Akansu for all his support, guidance and encouragement throughout my research. He taught me what is meant to be professional, meticulous and detail oriented. My special thanks are due to Dr. Yeheskel Bar-Ness, Dr. Alexander Haimovich, Dr. Edip Niver, Dr. Ali Abdi and Dr. Rajiv Laroia for their useful suggestions and sparing their invaluable time to be on my dissertation committee.

I am grateful to Professor Nirwan Ansari, Professor Durgamadhab Misra of ECE department and Dr. Ronald Kane, Dean, Graduate Studies for the critical financial support they have provided me during my study.

I also thank my friends in the lab, especially Handan, Amey, Johnsy for their help and discussions during my years at NJIT. The staff of ECE department was extremely kind and helpful to me, and my work wouldn't have been completed without their help.

I would like to thank my husband and my son for their understanding and the sacrifices they have made throughout my study. I am grateful to my parents for their encouragement and confidence in me. I am particularly indebted to my friend Anuradha for her moral support to pursue my Ph.D. studies.

TABLE OF CONTENTS

TABLE OF CONTENTS
(Continued)

TABLE OF CONTENTS
(Continued)

TABLE OF CONTENTS
(Continued)

Chapter **Page**

LIST OF TABLES

LIST OF FIGURES

LIST OF FIGURES
(Continued)

LIST OF FIGURES
(Continued)

LIST OF FIGURES
(Continued)

LIST OF FIGURES
(Continued)

LIST OF FIGURES
(Continued)

CHAPTER 1

INTRODUCTION

1.1 Communication System Design

Fundamental research on wireless communications took place more than 100 years ago. Subsequently, first commercial mobile system was installed in 1960's by Bell Labs. Further research led to the development of analog cellular mobile communication system in 1980's to increase number of users in the system. Cellular system enables reuse of spectral resources in non adjacent cell zones. More recently, digital cellular systems are introduced in 1990's to transmit digital data consisting of not only voice but also data and images at faster data rates. Apart from conventional voice communication, a number of new applications like sensor networks, mesh networks and others are using a variety of communication standards for data transfer.

Theoretical performance of wireless communication systems can be evaluated using computer simulations without the need for actual prototype development and field testing. Digital wireless communication can be categorized into three types: point-to-point communication, point-to-multipoint communication and multipoint-to-multipoint communication. Point-to-point communication corresponds to information sharing between one transmitter and one receiver, point-to-multipoint corresponds to one transmitter communicating with several receivers, and multipoint-to-multipoint means several transmitters are capable of sending information to many receivers at any time. In this dissertation point-to-point communication systems are only considered.

Point-to-point communication concept is shown in Figure 1.1. Even though, input data from a user is usually generated in continuous time domain, it is advantageous to

transmit discrete information over the digital communication channel. Accordingly, input data is first digitized and compressed in the source encoder. In addition, several input data bits can be combined together and transmitted in the form of a symbol to increase data rate. Compressed data is then fed to channel encoder which adds appropriate redundant bits to the data that help in the reduction of transmission errors at the receiver. Different error correction codes such as convolution codes, BCH codes or Reed-Solomon codes are widely used in practical systems.

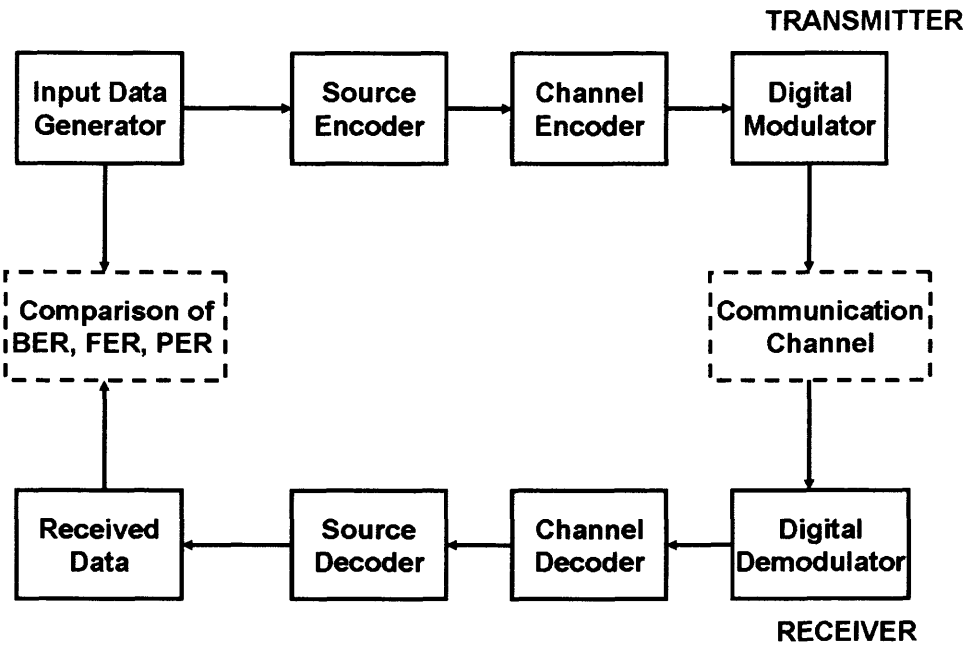

Figure 1.1 Typical point-to-point communication system block diagram.

Channel encoded data is then fed into a digital modulator which modulates the carrier signal and finally transmitted over the communication channel. Carrier signal can be mathematically represented as

$$S(t) = A(t)\exp[2\pi f_c(t) + \theta(t)] \tag{1.1}$$

where $A(t), f_c, \theta(t)$ are amplitude, frequency and phase of carrier signal, respectively. Based on the input data signal, digital modulator changes one of these characteristics of the carrier signal to achieve required modulation. In this dissertation, change of phase characteristics of the transmitted signal, so called phase modulation is only considered.

At the receiver, baseband signal is detected in the digital demodulator. Then, detected bits are fed to channel decoder, where error correction logic is applied to recover the channel compensated data bits. Finally, data is fed to source decoder in order to retrieve transmitted data bits.

Multiple access of the communication channel for different users is accomplished by allotting different time slots (TDMA), different transmission frequencies and subchannels (FDMA) or different orthogonal spreading codes (CDMA) for modulation. Channel performance is measured in terms of either bit error rate (BER), frame error rate (FER) or packet error rate (PER) depending on the data structure used for the transmission. Performance of the channel is affected by receiver noise level, level of the received signal (in turn depends on the transmitted signal), fading environment and level of interference signals, including multiuser and multipath kinds.

In this dissertation, CDMA multiple access system is studied and simulated for its BER performance under AWG noise, Rayleigh fading channel conditions and multiuser interference. Furthermore, simulation studies are performed at baseband level without RF band modulation / demodulation as lot of sampling data is required to represent signals at RF band.

1.2 Review of Previous Work

Basic building blocks of any multirate signal processing systems are decimators and interpolators, and they are well discussed in the tutorial article given in [1]. Multirate systems result in efficient processing of signals as sampling rates of the signals at various internal points of the system are kept at optimal value according to the Nyquist theorem. Multirate systems found applications in various fields such as communications, speech processing and spectral analysis. Review of multirate filter banks, polyphase networks and their applications to audio signal processing are presented in [2, 3]. Applications of transmultiplexers for frequency division multiplexing and time division multiplexing are explained in [4, 5, 6]. Digital function sets of discrete Fourier transforms (DFT) rather than continuous analog functions are used to implement filter banks in [6]. Transmultiplexers for CDMA communications, time-frequency spreads of the basis functions, various criteria for optimal basis functions are well documented in [7, 8, 9, 10]. Orthogonal transmultiplexers for DSL applications are discussed in [11].

Walsh, Gold and Kasami codes are presently used in various CDMA systems as spread spectrum codes [12, 13]. Correlation properties of these popularly used CDMA codes are presented in [14, 15, 16, 17, 18]. System analysis for performance evaluation of phase coded CDMA multiple access systems in terms of signal to noise ratios is shown in [19, 20]. Lower bounds on the cross- and auto-correlation sequences of the binary codes are analytically presented by Welch, Sidelnikov and Sarwate in [21, 22, 23] and are also reiterated in [20, 24]. It was shown that Walsh codes have the lowest total sum of square of cross-correlation values as mentioned in [25]. Variants of Gold and Walsh codes that can be used for spread spectrum applications are generated in [26, 27, 28]. Similarly,

references [29, 30, 31, 32, 33, 34] describe the methods for increasing capacity of the system in synchronous communication without considering their asynchronous performance.

Golay complementary sequences and zero correlation sequences are defined in the context of minimizing total periodic auto- and cross-correlation values and peak to mean power ratios in the case of quasi-synchronous multiuser transmission [35, 36, 37, 38]. These sets of spreading codes give good performance in the quasi-synchronous zone, but the availability of number of codes for multiuser communication is limited.

1.3 Dissertation Overview

This dissertation is a presentation of design methodology for generating different types of new spread spectrum code sets that can be used in CDMA systems for both synchronous and asynchronous communication. Few examples of such designed code sets and performance comparisons are made with presently used CDMA codes under various channel conditions.

In Chapter 2, basic digital signal processing concepts, terminologies and multirate signal processing techniques are introduced. Conditions required for perfect reconstruction of the signal are discussed in the context of a two-band perfect reconstruction quadrature mirror filter (PR-QMF) bank. Later, PR-QMF bank concepts are extended for the design of an M-band filter bank. Multirate orthogonal transmultiplexer architecture is in turn derived from M-band orthogonal filter bank which acts as a fundamental tool to implement any digital communication systems.

In Chapter 3, implementation of transmultiplexer architectures for different applications such as TDMA, FDMA and CDMA are discussed in terms of the design features of transmultiplexer's synthesis / analysis filters. The spreads of basis functions in time and frequency domains are discussed and conditions for the design of CDMA spreading codes with good performance in multiuser environment are presented.

Theoretical analysis for multiuser detection in DS-CDMA systems is presented in Chapter 4. Critical dependence of multiuser detection performance on low cross-correlation values between the code sequences is mathematically explained. Mathematical kernels for the generation of spread spectrum codes used in existing CDMA systems and their limits are discussed.

In Chapter 5, a novel design methodology for new binary spread spectrum code families is presented and new codes are generated using computer search method. New binary code families are divided into three groups- linear phase orthogonal codes, near orthogonal codes and non-linear phase orthogonal (Walsh-like) codes. With this new design, a number of independent code sets can be generated with flexible code length options compared to existing code families. BER performance characteristics of these new code sets are compared with the performance of standard code families in all types of noise channels. Then, performance characteristics are justified in terms of various correlation metrics and also in terms of their time and frequency spreads. Few sample codes are listed.

Limitations of using binary valued spread spectrum codes for CDMA applications are discussed in Chapter 6. To overcome these limitations, a new design methodology is presented for the generation of multiple sample valued, varying power, integer spread

spectrum codes. Pulse amplitude modulation (PAM) values are chosen as spread spectrum chips in this new design. Number of independent, multiple level code sets are generated by computer search method. Performance characteristics of these multiple valued spread spectrum codes are compared with binary standard codes. Performance improvements by increasing the number of chip levels for spreading input data and by keeping code length fixed are presented. Few sample codes are also listed in this chapter.

In Chapter 7, an analytical method to design multiple valued, varying power orthogonal spread spectrum codes is presented. An eigen-analysis based orthogonal block transform design methodology for the given signal statistics of spread spectrum, so called Karhunen-Loeve Transform (KLT), is extended to the design of varying power spread spectrum codes that might also be suitable for direct sequence CDMA communications. BER performance of the proposed orthogonal spreading codes is compared with the standard codes like Walsh and Gold families under AWGN channel conditions. Few design examples and sample codes are also described in the chapter.

Multiple stage orthogonal transmultiplexer structure is extended for the design of hybrid or Kronecker product codes in Chapter 8. Kronecker product codes have been generated and appropriately allocated to different users with the goal of reducing total correlation values, thus improving overall BER performance. Performance characteristics of different hybrid codes of both binary and multiple leveled codes are compared with the performance of standard code families in multiuser communication scenario.

A design method is proposed to improve the multiuser CDMA performance at low SNR conditions using multiple stage orthogonal transmultiplexer structure with fixed or varying power codes. Each user data is redundantly spread in the pre-multiplexing

stage of a user with odd number of redundancy codes and combined synchronously before transmission. Majority based decision logic is applied on the detected bits at the receiver to get an overall performance improvement.

Conclusions and future research are presented in Chapter 9.

CHAPTER 2

MULTIRATE FILTER BANKS AS SPECTRAL TRANSFORMS

Multirate signal processing tools have applications in diverse fields such as communications, speech processing, data compression and many others. They provide an efficient method for reconfiguring the signals by means of resampling of the original signal, up- and down-sampling, depending on the requirement. Multirate systems have different structures with single input-single output (SISO) multirate filter banks and multiple input-multiple output (MIMO) transmultiplexers being the most popular ones. In this chapter, discrete-time signal processing and multirate signal processing concepts will be briefly reviewed to better understand their use in communication systems.

2.1 Discrete-Time Signal Processing: Fundamentals

Discrete-time signal $\{x(n)\}$ is obtained by sampling a continuous time signal $x(t)$, where n is the time index. The discrete system of interest in this dissertation is of linear, causal and time invariant in its nature.

Let $\{h(n)\}$ be the unit sample response of a discrete-time system. Output $\{y(n)\}$ of such a system, corresponding to an input data sequence $\{x(n)\}$ can be obtained by the discrete-time convolution operation [39]

$$y(n) = \sum_k x(k)h(n-k) = x(n) * h(n) \tag{2.1}$$

where $*$ is the linear convolution operator.

Two-sided z – transform of $\{x(n)\}$ is defined as

$$X(z) = \sum_{n=-\infty}^{n=\infty} x(n)z^{-n} \tag{2.2}$$

The discrete-time Fourier transform (DTFT) of $\{x(n)\}$ is defined as

$$X(e^{j\omega}) = \sum_{n=-\infty}^{n=\infty} x(n)e^{-j\omega n} \tag{2.3}$$

and the inverse transform is defined as

$$x(n) = \frac{1}{2\pi}\int_{-\pi}^{\pi} X(e^{j\omega})e^{j\omega n}d\omega \tag{2.4}$$

When ω is evaluated at N equally spaced points on the unit circle of the z-plane, Equation (2.3) becomes the discrete Fourier transform (DFT) of $\{x(n)\}$ with size N.

$$X(k) = X(e^{j\omega})_{\downarrow \omega=\frac{2\pi k}{N}} \qquad k = 0,1,...,N-1 \tag{2.5}$$

For finite length discrete-time signals, size N DFT is defined as

$$X(k) = \sum_{n=0}^{N-1} x(n)e^{-j\frac{2\pi kn}{N}} \qquad k = 0,1,...,N-1 \tag{2.6}$$

and the corresponding inverse Fourier transform (IDFT) is defined as

$$x(n) = \frac{1}{N}\sum_{k=0}^{N-1} X(k)e^{j\frac{2\pi kn}{N}} \qquad n = 0,1,...,N-1 \tag{2.7}$$

The z-domain counterpart of time domain convolution of Equation (2.1) can be written as

$$Y(z) = H(z)X(z) \tag{2.8}$$

where $H(z)$ is the z-transform of the discrete- time system.

In the frequency domain, where $z = e^{j\omega n}$, Equation (2.8) is equal to

$$Y(e^{j\omega n}) = H(e^{j\omega n})X(e^{j\omega n}) \tag{2.9}$$

2.2 Basic Operators of Multirate Signal Processing

Basic building blocks of multirate signal processing are up- and down-samplers for changing the sampling rates of the original signal [8, 11]. In multirate systems, signals must be properly conditioned with filters of proper spectral prior to or after sampling rate conversions to avoid aliasing.

Decimation or down-sampling is the process of reducing the sampling rate of a signal by an integer number M as shown in Figure 2.1. This process involves passing input signal $\{u(n)\}$ through anti-aliasing filter $\{h(n)\}$ and then down-sampling the filtered signal. Down-sampling retains every M th sample of the input signal and relabels the time axis.

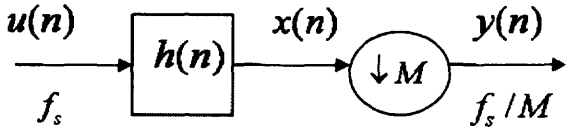

Figure 2.1 Down-sampling or decimation.

Intermediate signal $\{x'(n)\}$ can be expressed in terms of the signal $\{x(n)\}$ as

$$x'(n) = \begin{cases} x(n) & n = 0, \pm M, \pm 2M, \ldots \\ 0 & otherwise \end{cases} \tag{2.10}$$

The down-sampled signal $\{y(n)\}$ obtained from $\{x(n)\}$ can be represented as

$$y(n) = x'(n) = x(Mn) \tag{2.11}$$

In frequency domain, the down-sampled signal can be expressed as

$$Y(e^{j\omega}) = \frac{1}{M}\sum_{k=0}^{M-1} X(e^{j\frac{(\omega-2\pi k)}{M}}) \tag{2.12}$$

Time compression corresponds to stretching in frequency domain. If the original signal $X(e^{j\omega})$ is in the interval $[0,\pi]$, then down-sampled signal is in the interval $[0,\pi/M]$. An anti-aliasing filter $\{h(n)\}$ is connected before down-sampling of the signal to reduce input bandwidth to by $[0,\pi/M]$. Thus, time domain representation of decimator is equal to

$$y(n) = \sum_{k} h(Mn-k)u(k) \tag{2.13}$$

Similarly, interpolation or up-sampling refers to increasing the sampling rate of the input signal by an integer factor of M as shown in Figure 2.2. This is achieved by the combination of up-sampler followed by a low pass filter $\{g(n)\}$ to limit the high frequencies. Up-sampling inserts $M-1$ zeros between sample values and reindexes the time axis.

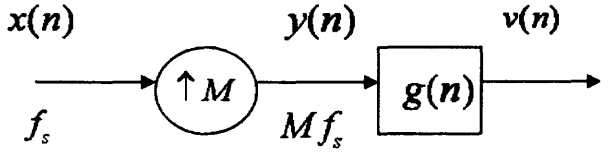

Figure 2.2 Up-sampling or interpolation.

Interpolated signal $\{y(n)\}$ can be written as

$$y(n) = \begin{Bmatrix} x(n/M) & n = 0,\pm M,\pm 2M,... \\ 0 & otherwise \end{Bmatrix} \tag{2.14}$$

Interpolation corresponds to stretching the signal in time domain or equivalently compressing in the frequency domain. In the frequency domain, the signal can be represented as

$$Y(z) = \sum_{k=-\infty}^{\infty} x(k)(z^M)^{-k}, \qquad Y(e^{j\omega}) = X(e^{j\omega M}) \tag{2.15}$$

Low pass filter $\{g(n)\}$ eliminates the high frequency signals or images that occur due to up-sampling. Time domain representation of the interpolator $\{v(n)\}$ can be expressed as

$$v(n) = \sum_{k} g(n - Mk)x(k) \tag{2.16}$$

2.3 Two-band PR-QMF Filter Bank

Purpose of subband filter bank is to decompose signal spectrum into a number of frequency bands or subbands. Multirate signal processing blocks defined in Section 2.2 are necessary tools for the perfect reconstruction (PR) of input signal at the output of analysis / synthesis filter bank. Two channel subband analysis / synthesis filter structure is displayed in Figure 2.3.

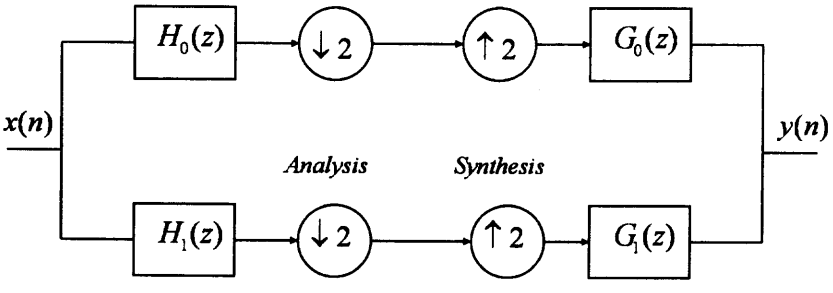

Figure 2.3 Two-band PR-QMF filter bank.

Input signal spectrum is divided into two equal subbands using low pass filter $\{h_0(n)\}$ and its quadrature mirror filter (QMF) high pass filter $\{h_1(n)\}$. Signals are then down-sampled by 2 in the analysis stage and are transmitted. At the receiver, signals are up-sampled by the rate of 2 in the synthesis section and are combined to get the input signal back. For perfect reconstruction of the input signal at the output of the synthesis section, if $\{h_0(n)\}$ is a low pass filter of FIR type, then $\{h_1(n)\}$ is a high pass filter. These two filters are related as [7, 8, 9]

$$h_1(n) = (-1)^n h_0(n), \quad H_1(e^{jw}) = H_0(e^{j(w-\pi)}) \tag{2.17}$$

If the normalization

$$\sum_{n=0}^{N-1} |h_0(n)|^2 = 1 \tag{2.18}$$

is imposed, then PR requirement in time domain can be expressed in terms of auto-correlation lags $\rho(n)$ as

$$\rho(2n) = \sum_{n=0}^{N-1} h_0(n) h_0(n+2k) = \delta(k) \tag{2.19}$$

PR-QMF conditions for 2-band filter bank can be summarized as

$$\begin{aligned} &|H_0(e^{jw})|^2 + |H_1(e^{jw})|^2 = 1 \\ &H_1(z) = z^{-(N-1)} H_0(-z^{-1}) \\ &G_0(z) = z^{-(N-1)} H_0(z^{-1}) \\ &G_1(z) = z^{-(N-1)} H_1(z^{-1}) \end{aligned} \tag{2.20}$$

If PR-QMF conditions are satisfied by all filters of two-band PR-QMF bank, then output signal $\{y(n)\}$ is a delayed version of the input signal as

$$y(n) = x(n - n_0) \tag{2.21}$$

where n_0 is a delay constant related to filter durations.

2.4 Single Input-Single Output M-band Orthogonal Filter Bank: Analysis / Synthesis Structure

Two-band filter bank analysis can be easily extended to M-band filter sections in both directions as shown in Figure 2.4. In this maximally decimated filter bank, input signal $\{x(n)\}$ is decomposed into M equal bands using analysis filters $\{h_0(n),\ h_1(n),...h_{M-1}(n)\}$. The symbol $\downarrow M$ corresponds to down-sampling of the signal by M, and the symbol $\uparrow M$ corresponds to up-sampling by a factor of M. In the synthesis section, after up-sampling, outputs of $\{g_0(n),\ g_1(n),...g_{M-1}(n)\}$ filters are combined to obtain the reconstructed signal $\{y(n)\}$.

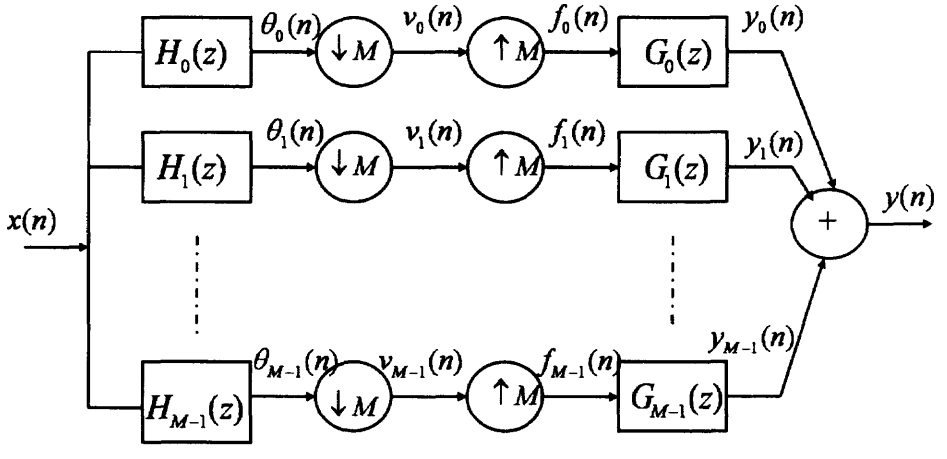

Figure 2.4 M-band PR-QMF filter bank (analysis / synthesis configuration).

Synthesis filters $\{g_r(n)\}$ are related to analysis filters $\{h_r(n)\}$ as [7, 8, 9]

$$g_r(n) = h_r^*(n_0 - n) \tag{2.22}$$

These conditions are similar to a match filter pair conditions.

PR-QMF conditions for the analysis filters in the time domain are written as [8]

$$\begin{aligned} &\sum_n h_r(n)h_r(n+Mk) = \delta(k), \quad r = 0,1,...,M-1 \\ &\sum_n h_r(n)h_s(n+Mk) = 0, \quad \mathrm{r} \neq \mathrm{s}, \forall \mathrm{n} \end{aligned} \tag{2.23}$$

The output signal of M -band filter bank will be

$$y(n) = x(n - n_0) \tag{2.24}$$

2.5 Multiple Input-Multiple Output M-band Orthogonal Transmultiplexer: Synthesis / Analysis Structure

Another popular application of multirate filter bank called transmultiplexer, which is of particular interest in this dissertation, is a structure in which synthesis filter bank is followed by analysis filter bank. This type of filter bank structures is useful for a variety of multiuser communication systems.

Figure 2.5 displays an M-band synthesis / analysis filter bank. M independent input signals $\{x_0(n), x_1(n), ..., x_{M-1}(n)\}$ are first up-sampled by a factor of M. Then these signals are interpolated using synthesis filter bank $\{g_0(n), g_1(n), ..., x_{M-1}(n)\}$. Outputs from synthesis filters (subchannel signals) are summed together to form output $\{y(n)\}$ which is transmitted over the channel. Channel noise distorts signal $\{y(n)\}$ into $\{y'(n)\}$.

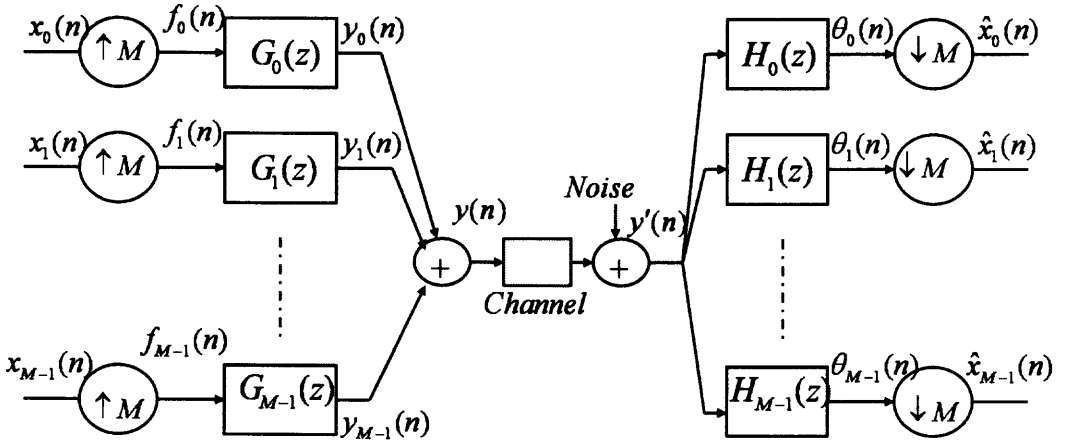

Figure 2.5 M-band transmultiplexer (synthesis / analysis configuration).

At the receiver, with the assumption of ideal channel, signal $\{y'(n)\}$ is split into M subchannels at the outputs of analysis filters $\{h_0(n), h_1(n), ..., h_{M-1}(n)\}$ and these subchannels are down-sampled by a factor of M. This operation retrieves the original signal with a constant delay if $\{g_i(n)\}$ and $\{h_i(n)\}$ are properly designed. Outputs of the analysis filters are denoted as $\{\hat{x}_0(n), \hat{x}_1(n), ..., \hat{x}_{M-1}(n)\}$. Perfect reconstruction (PR) conditions for the synthesis and analysis and filters in Figure 2.5 are the same as for the analysis / synthesis filter bank configuration described in Section 2.4.

CHAPTER 3

TRANSMULTIPLEXER APPLICATIONS

The orthogonal synthesis / analysis filter bank structure of transmultiplexer provides theoretical basis for multicarrier modulation techniques with single and multiple users in the communication system. Subchannel (multicarrier modulation) concept has been utilized for a single user in ADSL applications. The most popular application of transmultiplexer has been in multiuser communications for decades. Frequency division multiple access (FDMA), time division multiple access (TDMA) and code division multiple access (CDMA) are the three popular multiple access techniques used to share the available bandwidth in communication systems for multiple users. Synthesis / analysis filters need to be appropriately designed based on the requirements of the application in hand.

3.1 FDMA Systems

Most popular version of the orthogonal transmultiplexer configuration is of frequency division multiple access type. In FDMA, communication channel spectrum is divided into a number of non-overlapping sub-spectra (subchannel) and each user is allotted to one of them. Both synthesis and analysis filters are of frequency selective with the same subbands and ideally should have a brick wall frequency response.

3.2 TDMA Systems

In contrast to FDMA, in a TDMA communication system, each user is allocated a dedicated time slot. Each user is allowed to use full frequency spectrum during the given time slot only. Here, each synthesis filter is a simple delay of sampling interval with the Fourier transform representation as $G_k(e^{j\omega}) = e^{-jk\omega}$, $0 \le k \le M\text{-}1$. This can also be interpreted as an all-pass like user codes or synthesis filters with spectral response $|G_k(e^{j\omega})| = 1$, $0 \le \omega \le \pi$.

3.3 CDMA Systems

In CDMA systems, all users are equally allotted to all available time and frequency slots, with the aim of optimizing the overall throughput by maximizing the number of users in the system. In CDMA systems, user spreading codes (filters) cannot be unit sample functions as in TDMA or frequency selective as in FDMA. Instead, filters or orthogonal spreading codes are designed such that they are simultaneously spread in both the time and the frequency domains with minimum inter- and intra-code correlations.

3.4 Time-Frequency Localization of a Discrete-Time Function

Concentration or shaping of signal energy in the time-frequency plane is an important criterion for the detection of signals. A wide signal in the time domain has a narrow bandwidth in the frequency domain and a time domain localized signal has wide bandwidth in the frequency domain. The "uncertainty principle" describes the limits of simultaneous realization of a function in both the time and the frequency domains. These

are opposing requirements for a function to be simultaneously and maximally spread in both time and frequency domains [40].

For discrete-time signals, let $h(n) \leftrightarrow H(e^{j\omega})$ denote the discrete-time Fourier transform (DTFT) pair satisfying the relations

$$\begin{aligned} H(e^{j\omega}) &= \sum_{n=-\infty}^{n=\infty} h(n)e^{-j\omega n} \\ h(n) &= \frac{1}{2\pi}\int_{-\pi}^{\pi} H(e^{j\omega})e^{j\omega n}d\omega \end{aligned} \tag{3.1}$$

By Parseval's theorem, signal energy is the same in both time and frequency domains and is equal to [40]

$$E = \sum_{n=-\infty}^{n=\infty} |h(n)|^2 = \frac{1}{2\pi}\int_{-\pi}^{\pi} |H(e^{j\omega})|^2 d\omega \tag{3.2}$$

Time and frequency centers of a discrete sequence are calculated as [8]

$$\begin{aligned} \bar{n} &= \frac{\sum_{n=-\infty}^{n=\infty} n|h(n)|^2}{E} \\ \bar{\omega} &= \frac{\frac{1}{2\pi}\int_{-\pi}^{\pi} \omega|H(e^{j\omega})|^2 d\omega}{E} \end{aligned} \tag{3.3}$$

Time and frequency domain spreads of that sequence are defined as [8]

$$\begin{aligned} \sigma_n^2 &= \frac{\sum_{n=-\infty}^{\infty} (n-\bar{n})^2 |h(n)|^2}{E} \\ \sigma_\omega^2 &= \frac{\frac{1}{2\pi}\int_{\pi}^{\pi} (\omega-\bar{\omega})^2 |H(e^{j\omega})|^2 d\omega}{E} \end{aligned} \tag{3.4}$$

For band pass signals, σ_ω^2 needs to be defined in the range of $[0,\pi]$ rather than $[-\pi,\pi]$. In such a scenario, equations $\bar{\omega},\sigma_\omega^2$ are modified as [8]

$$\bar{\omega} = \frac{\frac{1}{\pi}\int_0^{\pi} \omega \left|H(e^{j\omega})\right|^2 d\omega}{\frac{1}{\pi}\int_0^{\pi} \left|H(e^{j\omega})\right|^2 d\omega} \tag{3.5}$$

$$\bar{\sigma}_{\omega}^2 = \frac{\frac{1}{\pi}\int_0^{\pi} (\omega - \bar{\omega})^2 \left|H(e^{j\omega})\right|^2 d\omega}{\frac{1}{\pi}\int_0^{\pi} \left|H(e^{j\omega})\right|^2 d\omega} \tag{3.6}$$

Figure 3.1 shows the time-frequency tile of a discrete-time function with σ_n^2 and σ_ω^2 defined as in Equation (3.4). Shape and location of the tile is adjusted by properly designing time and frequency centers and spreads of the user code (filter) functions. In addition to shaping the time-frequency tiles, orthogonality requirements are also imposed on the basis function design problem.

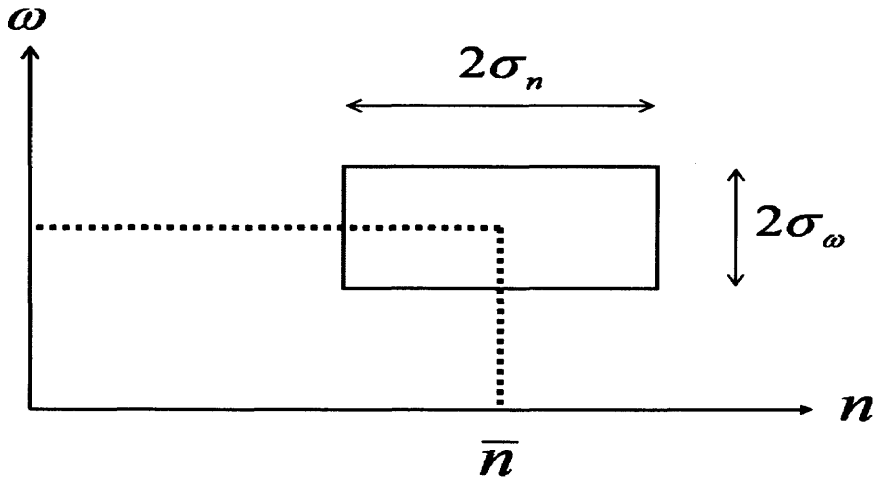

Figure 3.1 Time-frequency tile of a discrete-time function.

For designing CDMA codes, in addition to the PR-QMF conditions of Equation (2.18), inter- and intra-code correlations between the basis functions need to be minimized in order to improve detection performance.

Inter- and intra-code correlations for a two-user case are defined as

$$\begin{aligned} R_{00}(k) &= \sum_n h_r(n)h_r(n+k), \qquad k = 1,2,... \\ R_{01}(k) &= \sum_n h_r(n)h_s(n+k), \qquad \mathrm{r} \neq \mathrm{s},\ \forall \mathrm{n} \end{aligned} \tag{3.7}$$

An objective function $J_{\max}$ is set to optimize the criterion [7, 8, 9]

$$J_{\max} = \alpha\sigma_n^2 + \beta\sigma_\omega^2 - \gamma\sum_k |R_{00}(k)| - \eta\sum_k |R_{01}(k)| \tag{3.8}$$

where $\alpha, \beta, \gamma, \eta$ are constants. By optimizing the objective function, it is possible to obtain many different solutions for different values of weighting parameters $\alpha, \beta, \gamma, \eta$.

Next, chapters describe the design of spreading code basis functions based on orthogonality principles and minimization of inter- and intra-code correlation values for CDMA communication applications.

CHAPTER 4

CODE DIVISION MULTILE ACCESS SYSTEMS

In CDMA systems, multiple access capability is primarily achieved by means of coding. All users in a CDMA system are assigned different code sequences. Input data from each user is modulated with the assigned code and is transmitted. Receiver, with the knowledge of the code sequence used at the transmitter, decodes the received signal and recovers the original data bits. As the bandwidth of the code signal is much larger than the input data rate, encoding process spreads the spectrum of the information signal and hence CDMA systems are also known as spread spectrum systems. Based on the modulation method employed, CDMA protocols are divided into mainly three groups: direct sequence (DS-CDMA), frequency hopping (FH-CDMA) and time hopping (TH-CDMA). Encoded information signal modulates the transmitted carrier phase in DS-CDMA systems. It changes the transmitted carrier frequency in FH-CDMA systems. In TH-CDMA, carrier frequency is sent in bursts of time depending on the information signal. In this dissertation, only DS-CDMA systems are considered.

4.1 Direct Sequence CDMA Systems

In DS-CDMA systems, every data bit is directly multiplied (spread) with a code signal, known as spreading code. The resulting signal modulates the radio frequency (RF) carrier. Spreading signal consists of a number of code bits called chips. Ratio of the spreading signal chip rate to the original data bit rate is called the spreading gain or

processing gain. In DS-CDMA systems, all users use the same transmitting carrier frequency and can simultaneously transmit their data.

Receiver employs coherent demodulator to despread the received data using a locally generated code sequence. To be able to perform the despreading, receiver needs to know not only the code sequence that was used in the transmitted to spread the data, but also to synchronize the received signal with the locally generated code. After despreading and detection, original data bits are recovered.

Due to simultaneous transmissions of multiple users over the same channel, signal detection at the receiver for each user is limited by the interference caused by other users known as multiple access interference (MAI). MAI depends on the number of users, cross-correlation values among the user codes, delayed versions of the code of interest due to multipath, transmitted power levels of other users as well as their timing synchronization. Utilization of orthogonal codes for data spreading in a synchronized system eliminates MAI. Non-orthogonal codes or asynchronous system worsens MAI, resulting in lower system capacity. MAI in such situations can be lowered by choosing code sequences with lower cross-correlation values.

In systems with lower number of users, interested user signal coming from farther distance will be masked if other user signals are received at higher power levels. This is a classic near-far problem exists in all CDMA systems [41, 42] and typically occurs when the signal of interest is coming from cell boundaries. To combat this problem, power control is provided at the base station which ensures signals from all mobiles are received at the same power level irrespective of their distance. In this dissertation, power control

problem is avoided and all signals are assumed to be received with the same power level. Hence, their power levels are not considered in the detection process.

4.2 Mathematical Model for CDMA Communications

Received signal in a synchronized K-user CDMA system embedded in additive white Gaussian (AWGN) noise can be modeled as [19, 20, 42]

$$y(t) = \sum_{k=1}^{K} A_k b_k(t) s_k(t) + \sigma n(t) \qquad t \in [0, T] \tag{4.1}$$

where A_k is the received amplitude from k-th user, $b_k \in [-1, +1]$ is the k-th user's transmitted data bit, and $s_k(t)$ is the spreading code assigned to k-th user's data bits. A_k is assumed to be unity for all users in a power controlled system. Spreading code $s_k(t)$ is normalized to have unit energy,

$$\|s_k(t)\|^2 = \int_0^T s_k(t) dt = 1 \tag{4.2}$$

Then, performance of the receiver using a matched filter detector depends only on the cross-correlation or similarity between two spreading code waveforms defined as

$$\rho_{ki} = \langle s_k, s_i \rangle \equiv \int_0^T s_k(t) s_i(t) dt \tag{4.3}$$

Maintaining synchronization among different users is possible in the case of base station to mobile communication. In the case of mobile to base station communication, it is impossible to maintain synchronization among users since users can be switched on at random service initiation times.

The received signal of such a K-user asynchronous communication system can be mathematically modeled as

$$y(t)=\sum_{k=1}^{K}A_k b_k(t-\tau_k)s_k(t-\tau_k)+\sigma n(t) \quad t\in[0,T] \tag{4.4}$$

where τ_k are the relative time delays between different user codes received at the receiver.

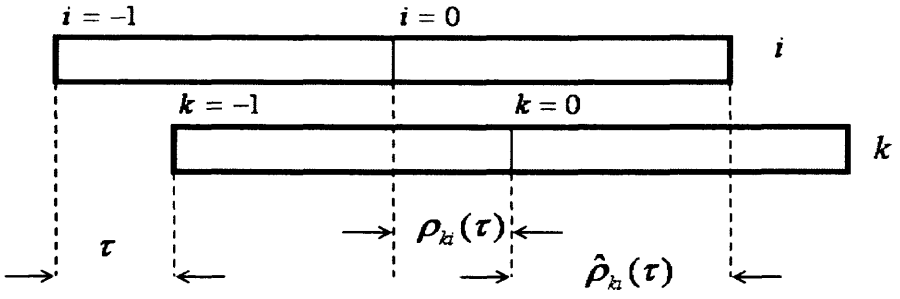

Figure 4.1 Bit durations and associated time delays, cross-correlations for a two-user asynchronous CDMA system.

Bit durations, associated relative delays and cross-correlations between the two users (k,i) are shown in Figure 4.1 for the examples of two intervals $i=0$ and $i=1$. User k is switched on after user i with a delay of τ. It might be noted that for synchronous users, $\tau_1=\tau_2=...\tau_k=0$, implying that all code sequences start at the same instant. Therefore, orthogonality of spreading codes redeems all MAI.

In asynchronous CDMA, two cross-correlation values $\rho_{ki},\hat{\rho}_{ki}$, between a pair of code sequences, depend on the timing offset between them. If $k>i$, cross-correlation values are defined as [19, 20]

$$\rho_{ki}(\tau) = \int_0^{\tau} s_i(t)s_k(t-\tau)dt$$
$$\hat{\rho}_{ki}(\tau) = \int_{\tau}^{T} s_k(t-\tau)s_i(t)dt \tag{4.5}$$

The output of the correlator, matched to the waveform $s_i(t)$, with the received signal $y(t)$ as its input, is expressed as

$$Z_i = b_i(0) + \sum_{k \neq i}^{K} [b_k(-1)\rho_{ki}(\tau_k) + b_k(0)\hat{\rho}_{ki}(\tau_k)] \tag{4.6}$$

Where $\rho_{ki}, \hat{\rho}_{ki}$ are defined in terms of aperiodic cross-correlation C_{ki} for the sequences as in [19, 20]

$$\rho_{ki}(\tau) = C_{ki}(l-N) + [C_{ki}(l+1-N) - C_{ki}(l-N)](\tau - l)$$
$$\hat{\rho}_{ki}(\tau) = C_{ki}(l) + [C_{ki}(l+1) - C_{ki}(l)](\tau - l), \quad 0 \le l \le \tau < l+1 \le N \tag{4.7}$$

C_{ki} for sequences a_k *and* a_i is defined as

$$C_{ki}(l) = \begin{cases} \sum_{j=0}^{N-1-l} a_k(j)a_i(j+l), & 0 \le l \le N-1 \\ \sum_{j=0}^{N-1-l} a_k(j-l)a_i(j), & 1-N \le l \le 0 \\ 0 & , \quad |l| \ge N \end{cases} \tag{4.8}$$

Periodic cross-correlation $\theta_{ki}(l)$ for two sequences a_k and a_l is given by [19, 20]

$$\theta_{ki}(l) = \sum_{j=0}^{N-1} a_k(j)a_i(j+l), \quad for\ \forall\ l \tag{4.9}$$

Then,

$$\theta_{ki}(l) = C_{ki}(l) + C_{ki}(l-N)\ and$$
$$\hat{\theta}_{ki}(l) = C_{ki}(l) - C_{ki}(l-N)\ for\ 0 \le l < N \tag{4.10}$$

$\theta_{ki}(l)$ is also called even correlation because $\theta_{ki}(l)=\theta_{ki}(N-l)$ and $\hat{\theta}_{ki}(l)$ is called odd correlation as $\hat{\theta}_{ki}(l)=-\hat{\theta}_{ki}(N-l)$.

If data symbols $b_k(-1)=b_k(0)$, then the matched filter output for the *i*-th receiver depends on the even correlation values and is given by

$$Z_i = b_i(0)+\sum_{k\neq i}^{K}\{b_k(0)\theta_{ki}(l_k)+[\theta_{ki}(l_k+1)-\theta_{ki}(l_k)](\tau_k-l_k)\} \tag{4.11}$$

On the other hand, if $b_k(-1)\neq b_k(0)$, then, the matched filter output depends on the odd correlation values and is equal to

$$Z_i = b_i(0)+\sum_{k\neq i}^{K}\{b_k(0)\hat{\theta}_{ki}(l_k)+[\hat{\theta}_{ki}(l_k+1)-\hat{\theta}_{ki}(l_k)](\tau_k-l_k)\} \tag{4.12}$$

Hence, it is essential to have low valued even and odd cross-correlation values among code sequences in order to have proper matched filter output.

4.3 Popular CDMA Spreading Codes

Binary valued Walsh and Gold codes are widely used as spreading codes in wireless CDMA systems [12]. Walsh codes are perfectly orthogonal codes and are ideal for synchronous CDMA communications, so called forward link or downlink transmission from base station to mobile. For asynchronous CDMA systems, where relative delays between transmitter code sequences are arbitrary, it is ideal to have spreading sequences having both impulsive auto-correlation and zero cross-correlation to reduce MAI. Mathematically, it is not possible to design such ideal spreading sequences with finite lengths for all possible delays [24]. Hence, spreading sequences with low auto- and cross-

correlation values such as m-sequences, Gold sequences and Kasami sequences are used in asynchronous reverse links or in uplink communications[12, 13].

IS-95 wireless communication standard uses orthogonal 64-length Walsh codes in the forward link transmission and m-sequence of length $(2^{15}-1)$ for reverse link. Most recent CDMA versions like Wideband CDMA (WCDMA) employ variable length orthogonal Walsh codes in the forward link and large Kasami sets or long Gold codes for the reverse link [12].

4.3.1 Orthogonal Walsh Codes

Walsh codes are generated by mapping rows of special square matrices called Hadamard matrices [14, 15, 16]. Walsh matrices are obtained from Hadamard matrices with the mapping of the elements $\{0,1\}$ onto $\{1,-1\}$, respectively. These matrices contain one row of all zeros and other rows of equal number of zeros and ones. They are recursively generated from using the following identities

$$H_1 = [0],\ H_2 = \begin{bmatrix} 0 & 0 \\ 0 & 1 \end{bmatrix}$$

$$H_4 = \begin{bmatrix} 0 & 0 & 0 & 0 \\ 0 & 1 & 0 & 1 \\ 0 & 0 & 1 & 1 \\ 0 & 1 & 1 & 0 \end{bmatrix} \quad \text{or} \quad H_{2N} = \begin{bmatrix} H_N & H_N \\ H_N & \bar{H}_N \end{bmatrix} \tag{4.13}$$

Walsh matrices of higher dimensions can also be obtained by taking Kronecker matrix product of Walsh matrices with lower lengths. Walsh functions thus generated have a size of $N = 2^n$, where n is of any integer.

Variable length orthogonal Walsh codes, also known as orthogonal variable spreading factor (OVSF) codes are recursively generated from a layered tree structure.

Here, not only the spreading sequences in the same layer but also sequences in different layers are orthogonal to each other. As bandwidth of system remains constant, due to variable length spreading codes, it is possible to have multiple data rate users in such a system [12].

Walsh code sets have unique number of zero crossings within the set. In a typical $N \times N$ size Walsh matrix, row indices (i = 0, 1, 2, ..., N-1) also indicate the number of zero crossings for the corresponding row sequences. First code in the Walsh code set of any size is a constant sequence comprising of all 1's. Remaining sequences in any Walsh code set have zero mean values. In addition, all Walsh basis functions are linear phase sequences. They are either even or odd symmetric sequences in time. While many of these features are useful for other applications, such restrictions on code sequences are not necessary for spread spectrum applications.

4.3.2 Gold Codes

Gold codes of length $(N = 2^n - 1)$ are generated from modulo-two addition of two *m*-sequences that are preferred polynomials of each other [13, 17]. From one *m*-sequence of length N (a), another sequence (a') is generated by decimating the sequence (a) with rate of q and the decimated sequence is denoted by $a' = a[q]$.

Sequence a' is of length N only if $\gcd(N, q) = 1$ where *gcd* is the greatest common divisor. Two sequences a and a' are considered preferred pair only if

$n \neq (0 \ modulo \ 4)$, implying n is *odd* or $n = (2 \ modulo \ 4)$

$a' = a[q]$ where q is *odd* and either $q = 2^k + 1$ or $q = 2^{2k} - 2^k + 1$

$$\gcd(n, k) = \begin{cases} 1 \ for \ n \ odd \\ 2 \ for \ n = 2 (\mathrm{mod}\, 4) \end{cases}$$

Auto- and cross-correlation values between two preferred pair of codes is a three-valued function with the values $[-t(n), -1, t(n)-2]$ where

$$t(n) = \begin{cases} 1+2^{\frac{n+1}{2}} \text{ for } n \text{ odd} \\ 1+2^{\frac{n+2}{2}} \text{ for } n \text{ even} \end{cases} \tag{4.14}$$

For large values of N, peak auto- and cross-correlation values of Gold codes compare with the Welch correlation bound values by a factor of $\sqrt{2}$ for n odd and by a factor of 2 for n even [19, 20].

4.3.3 Kasami Codes

Procedure for generating Kasami codes is similar to that of Gold code generation. Small Kasami set of $M = 2^n/2$ sequences and length $N = 2^n - 1$ (n is even) is obtained by decimating the first m-sequence with $2^{n/2}-1$ to get second m-sequence and then taking modulo-two addition of both m-sequences [13, 18]. Small Kasami set have three correlation values that match with Welch correlation bound values.

Large Kasami set consists of both Gold codes and small Kasami code sets as its subsets. m-sequences are generated by decimating sequence (a) by $2^{n/2}+1$ and $2^{(n+2)/2}+1$ to obtain (a') and (a'') and then modulo-adding these two sequences. Large Kasami sets have 5 valued correlation sequences $[-1, -1\pm 2^{n/2}, -1\pm 2^{n/2+1}]$.

All these types of codes are easier to generate from their mathematical kernels. But, number of such spreading sequence sets is limited in the binary sample space for any spreading length. For example, Walsh codes are available only for the lengths that are powers of 2 and Gold / Kasami codes are available for lengths equal to $2^n - 1$ for certain

(n) values. Emerging applications like sensor networks, peer-to-peer communication will have greater flexibility in their design if spreading sequences of various and shorter lengths exist. Also, at each code length, if a number of independent spreading code sets exists, then users will have the flexibility of switching from sequence set to another set. Security of such a system might be improved if receivers have the pre-determined knowledge of the code updating patterns.

This dissertation is focused on the design concepts, evaluation metrics and generation of such independent, orthogonal binary and multiple level spreading sequence sets for various lengths that can be used in both synchronous and asynchronous communication systems.

CHAPTER 5

ORTHOGONAL BINARY SPREADING CODES

In Chapter 4, widely used binary spread spectrum codes in existing CDMA systems were discussed. Popularity of these codes is due to the ease of their implementation using mathematical kernels, but the availability of such code sets is limited in number and in their length. Additional code sets might be generated if unnecessary restrictions on certain code features are waived. This chapter describes some design features, search methodology and performance of such newly generated binary code sets under different channel conditions. Designed binary code sets are broadly divided into three major groups: Orthogonal linear phase codes, Near orthogonal codes and Non-linear phase (Walsh-like) orthogonal codes.

5.1 Linear Phase Orthogonal Binary Codes

5.1.1 Design Methodology

Walsh codes are linear phase, zero mean (except the first code) and binary valued orthogonal transforms. These codes have unique number of zero crossings per sequence within the set which is not a relevant condition for spread spectrum applications. Hence, such a condition is waived in the search for new orthogonal binary code sets.

Binary representation of an n-length code requires a sample space of 2^n values. Integer numbers in the sample space are first represented in radix-2 format with [0,1] elements for a given length of the code. For example, in radix-2 format, number 45, for 8-length code is represented as $\{0,0,1,0,1,1,0,1\}$. Binary spreading codes have two possible

chip levels $[1,-1]$. Accordingly, radix elements $[0,1]$ in the n-length code are mapped into $[1,-1]$, respectively, to generate corresponding spreading code. Since mapping of $[0,1]$ elements into $[-1,1]$ generates complementary codes with equivalent but opposite polarity, any one of these two mappings can be considered. Hence, orthogonal code search in the sample space of $[0,2^{n-1}-1]$ is sufficient since numbers in the range $[2^{n-1},2^n]$ are complementary to the codes in the range $[0,2^{n-1}-1]$. Furthermore, sample space for the binary codes is restricted to only zero mean and linear phase codes. With all these restrictions, for 8, 16 and 32-length codes, eligible sample space consist of only 22, 326 and 38000 codes, respectively.

Walsh code sets have poor performance if absolute value of the normalized periodic cross-correlation between any pair of codes within the set is equal to 1 for any possible delay value between them. This condition arises if a code sequence becomes shifted version of the another code sequence or its complement for any particular delay. For example, if two 8-length Walsh code sequences $[1,1,-1,-1,1,1,-1,-1]$, $[1,-1,-1,1,1,-1,-1,1]$ are allotted to two different users in an asynchronous CDMA system, then for modulo delay of 1, both sequences become equal and result in poor detection at the receiver.

In the present design, code sequences with absolute normalized peak cross-correlation value of 1 are avoided. Also, it was observed that all Walsh sequences in n-length binary code set are multiples of either $(2^{n/2}+1)$ or $(2^{n/2}-1)$. For example in 8-length code set, all code sequences are multiples of either 15 or 17. As these code

sequences result in high cross-correlation values, multiples of $(2^{n/2}+1)$ or $(2^{n/2}-1)$ are minimized in the new code search.

Exhaustive computer search is performed on the limited binary sample space to generate desired orthogonal code sets. For n-length code, $n-1$ orthogonal code sequences are obtained with this search method. Constant sequence of either all 1's or -1's is added to the set to make it a complete orthogonal code set. Since the sample space is small for 8-length codes (22 codes), orthogonal code set with good correlation properties is not available. For code lengths of 16 or higher, and for powers of 2, (16, 32, 64 ...), a number of unique orthogonal code sets are available. It may be noted that only the constant code sequence is common in all these orthogonal code sets. Table 5.1 shows two new 16-length linear phase orthogonal code sets along with corresponding Walsh code sets represented in integer number format. It can be observed from the Table 5.1 that only the first code of constant 1's is common with Walsh code set. Appendix A shows a number of 32-length linear phase orthogonal code sets represented in integer format. More sample codes can be found in the references [43, 44, 47].

5.1.2 Bit Error Rate (BER) Performance Comparisons in AWGN Channels

BER performance of the proposed spreading code sets are simulated under additive white Gaussian noise (AWGN) conditions for 2-user case in asynchronous communication channel. For asynchronous channel performance, average BER performance is simulated for all possible pairs of code sequences within a set and for all possible delays between the code sequences. For the 16-length code set, 16*15/2=120 sequence pairs are possible with 16 possible delays between them. Figure 5.1 displays average BER performance for two users with 16-length linear phase orthogonal codes along with 16-length Walsh code

set as a function of signal to noise (SNR) ratio. Average BER performance of Walsh code set is poor due to the fact that certain code pairs have a normalized cross-correlation value of 1 for certain delays between user codes. BER performances of both proposed linear phase code sets far exceed that of Walsh codes and improve further with increase in SNR.

Table 5.1 Sample 16-Length Linear Phase Orthogonal Code Sets along with Corresponding Walsh Code Sets Represented in Integer Format

Index	16-Length Linear Phase Orthogonal Code Set1	16-Length Linear Phase Orthogonal Code Set1	16-Length Walsh Code Set
1	65535	65535	65535
2	703	4471	43690
3	3407	6120	52428
4	4080	7815	39321
5	12659	8891	61680
6	13740	11220	42405
7	14940	11595	50115
8	16003	15420	38550
9	21717	18205	65280
10	22122	18669	43605
11	22938	19890	52275
12	23333	23130	39270
13	25542	26214	61455
14	26393	29070	42330
15	26857	29905	49980
16	27702	31521	38505

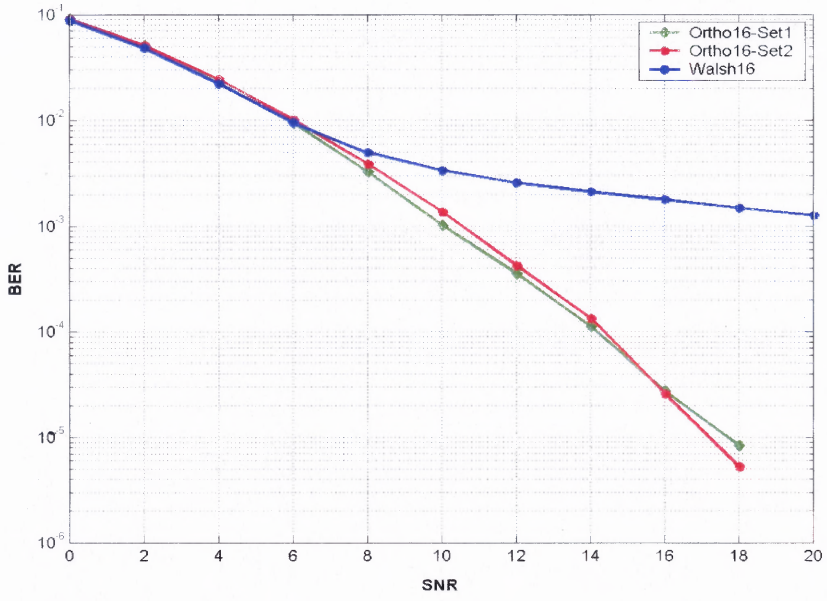

Figure 5.1 BER performances of proposed 16-length linear phase orthogonal code sets and Walsh code set for 2-users in asynchronous AWG noise channel.

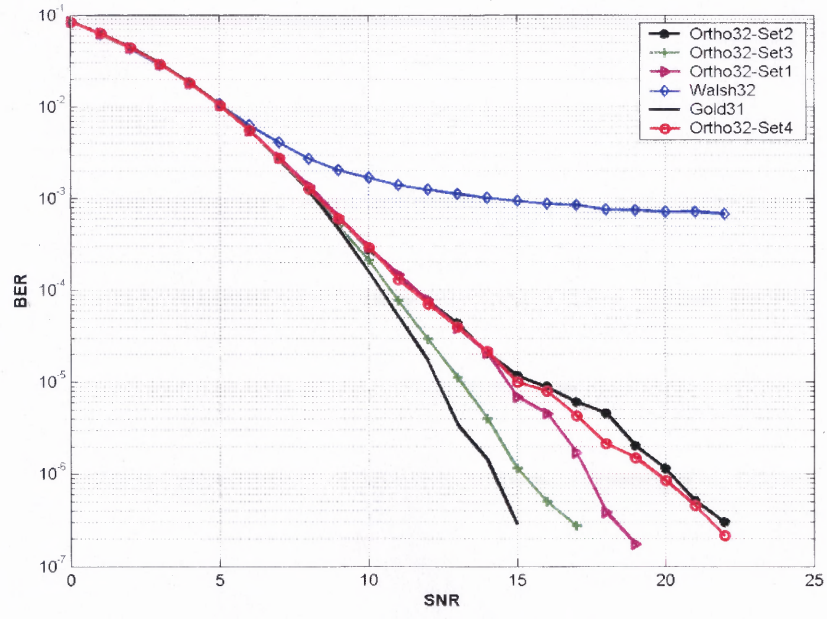

Figure 5.2 BER performances of proposed 32-length linear phase orthogonal code sets, Walsh code set and 31-length Gold code set for 2-users in asynchronous AWG noise channel.

Figure 5.2 shows the BER performance of 32-length linear phase orthogonal code sets along with 32-length Walsh code set and 31-length Gold code set. Here also, all proposed linear phase code sets outperform Walsh codes and their performances closely match with the similar length Gold codes. It is observed that there are a good number of orthogonal sets available in the sample space that gives comparable performance to standard codes used in CDMA systems at different code lengths.

5.2 Near Orthogonal Binary Codes

5.2.1 Design Methodology

Near orthogonal code sets have a cross-correlation value of -1 between any code pairs within the set for zero delay between them. Similarly, Gold codes are near orthogonal, as they have cross-correlation value of -1 between code pairs for zero delay. Gold codes exist for lengths of only $2^n - 1$, where n is not a power of 4. In addition, the number of available code sets for any given length is limited due to the restrictions of generating them from preferred polynomials.

Gold codes are widely used as spreading codes in asynchronous CDMA communication standards. Gold codes are non-zero mean as well as non-linear phase codes. Gold code sequences do not have a unique number of zero crossings per code within the set. Still, Gold codes are known for their good BER performance. Hence, sample space is searched for more near orthogonal code sets with only one condition of maximum absolute normalized correlation value being less than 1. For n-length code, sample space consists of $2^n - 1$ values.

Number of unique near orthogonal code sets for lengths of 7, 11, 15, 19, ... chips are obtained using brute force search. For n-length code, near orthogonal code set consisting of $n+1$ sequences are generated. It should be noted that for this family of sequences, constant sequence of all 1's is not part of a set. Table 5.2 shows proposed 7-length near orthogonal code sets along with 7-length Gold code and 8-length Walsh code in integer format.

Table 5.2 Sample 7-Length Near Orthogonal Code Sets, Gold Code Set and 8-Length Walsh Code Set Represented in Integer Format

Index	7-Length Near Orthogonal Code Set1	7-Length Near Orthogonal Code Set2	7-Length Gold Code Set	8-Length Walsh Code Set
1	5	7	106	255
2	18	8	30	170
3	43	49	119	204
4	60	62	36	153
5	78	82	3	240
6	89	93	77	165
7	96	100	80	195
8	119	107	57	150

5.2.2 Bit Error Rate (BER) Performance Comparisons in AWGN Channels

Two-user BER performance of proposed 7-length near orthogonal code sets given in Table 5.2 are simulated for all possible pairs of codes and for all possible delays in an asynchronous AWG noise scenario and displayed in Figure 5.3. For comparison

purposes, performances of 7-length Gold and 8-length Walsh code sets are also shown in the Figure 5.3.

Performances of near orthogonal code sets closely match with that of corresponding Gold set and outperform the 8-length Walsh set. Near orthogonal sets shown in Table 5.2 are unique sets without having any common code sequences between them or with the Gold code set. Simulation results for codes with other lengths are presented in [44, 47].

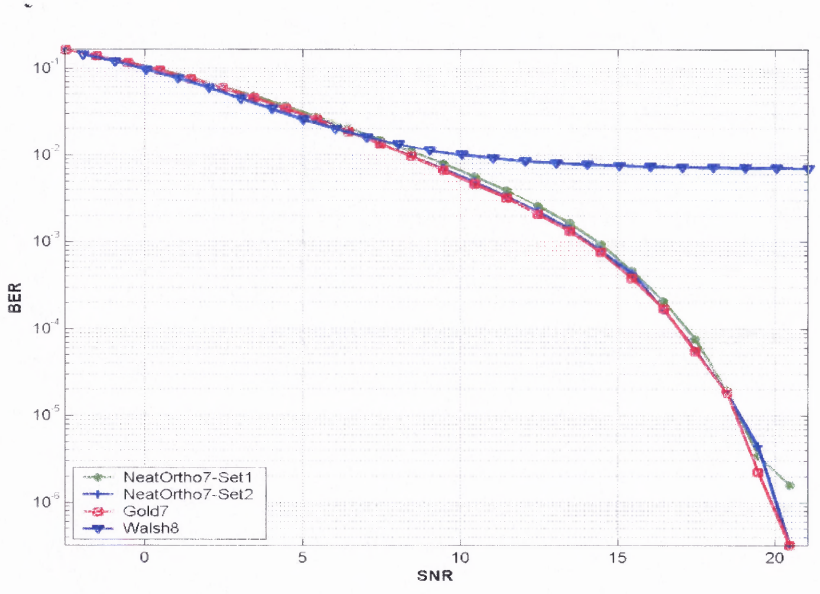

Figure 5.3 BER performances of proposed 7-length near orthogonal code sets, Gold code set and 8-length Walsh code set for 2-users in asynchronous AWG noise channel.

5.3 Non-Linear Phase (Walsh-like) Orthogonal Binary Codes

5.3.1 Design Methodology and Search Algorithm

Non-linear phase orthogonal code set features are similar to that of near orthogonal code set features. Code sequences have non-zero mean, they are non-linear in phase and without any restrictions on the number of zero crossings per code within the code set.

After all these restrictions of linear phase orthogonal code sets are waived, sample space for n-length non-linear phase orthogonal code set is of $[0, 2^n - 1]$. Sample space can be reduced to $[0, 2^{n-1} - 1]$ since code sequences in the range $[2^{n-1}, 2^n]$ are complementary to the sequences in the range of $[0, 2^{n-1} - 1]$. Orthogonal code sets are searched in the sample space using brute force search method. Search algorithm can be summarized as follows.

- Sample space consists of $[0, 2^{n-1} - 1]$ sequences for n-length code sets.
- First basis function in the orthogonal code set is selected by representing an integer number in the sample space as n-length binary code with radix-2 elements $[0,1]$. Furthermore, [0, 1] elements of this binary code are mapped into $[-1, 1]$, respectively, to generate n-length spreading code.
- Select the next basis function by checking the orthogonality with the first basis function. In addition, absolute value of the maximum normalized periodic cross-correlation value between the basis functions should be less than 1 for all possible chip delays.
- Repeat the process $n-1$ times to obtain a complete $N \times N$ orthogonal code set.
- With this search process, a number of orthogonal code sets are formed with the first basis sequence as the common basis sequence for different orthogonal code sets. By choosing a different integer as the first basis sequence of the set, a number of unique orthogonal sets can be formed.
- Finally, select orthogonal code sets that have minimum cross-correlation values among all pairs of codes as a performance metric for further analysis.
- Complexity of the search algorithm is $n(2^n - 1)$ for an n-length code set.

A number of non-linear phase (Walsh-like) orthogonal code sets are obtained for lengths that are multiples of 4 (8, 12, 16, 20, ...). As previously observed in Section 5.1, for 8-length, new orthogonal sets couldn't be obtained with linear phase properties although it is possible to obtain with non-linear phase properties. Table 5.3 displays two examples of 8-length Walsh-like code sets along with 8-length Walsh code set in integer

format. Several 32-length Walsh-like code sets are also listed in Appendix B. Design features and sample codes are also presented in [45, 46, 47].

Table 5.3 Sample 8-Length Walsh-like Code Sets and Walsh Code Set Represented in Integer Format

Index	8-Length Walsh-like Code Set1	8-Length Walsh-like Code Set2	8-Length Walsh Code Set
1	4	19	255
2	11	28	170
3	55	32	204
4	56	47	153
5	81	70	240
6	94	73	165
7	98	117	195
8	109	122	150

5.3.2 Time, Frequency and Correlation Properties of 32-length Walsh-like Codes

Time domain representations of a typical 31-length Gold code, 32-bit orthogonal Walsh code and 32-length proposed Walsh-like code are displayed in Figure 5.4. Proposed Walsh-like and Gold sequences have non-linear phase responses and non-zero mean values while Walsh sequences are linear phase functions with zero mean.

Magnitude and phase functions of these sample codes are shown in Figures 5.5 and 5.6, respectively. Note that the sample sequence of the proposed Walsh-like codes has more evenly spread frequency spectrum compared to the sample Walsh code of the same length.

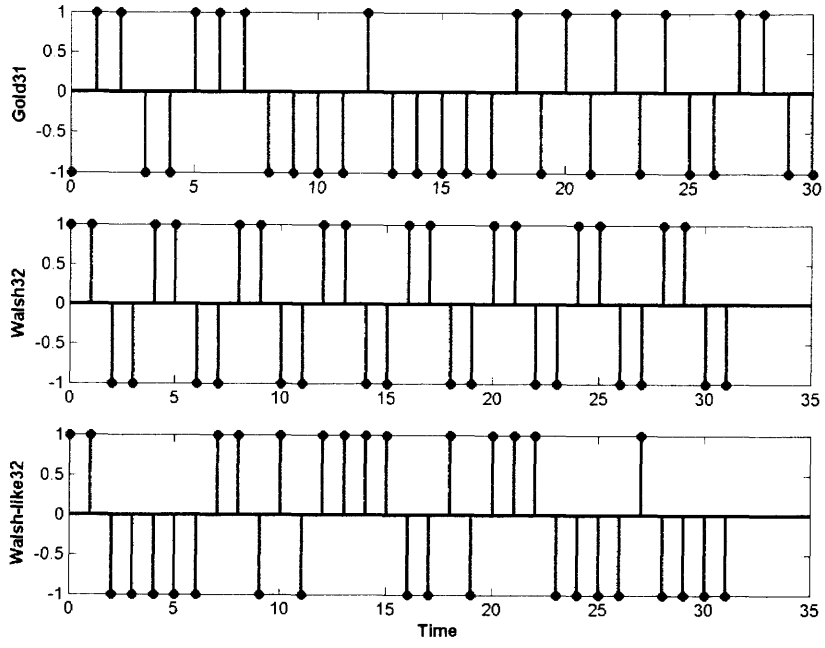

Figure 5.4 Time domain sequences of a typical 31-length Gold code, 32-length Walsh code and 32-length proposed Walsh-like code.

One sided auto-correlation sequences for the typical codes of the three families considered in Figure 5.4 are displayed in Figure 5.7. Similarly, one sided cross-correlation sequences between typical pairs of codes are displayed in Figure 5.8 for the three binary families under consideration. It is observed from the Figs. 5.7 and 5.8 that the Gold and the proposed non-linear phase Walsh-like orthogonal codes have similar auto-correlation (intra-code correlation) and cross-correlation (inter-code correlation) sequences while sample Walsh pair has worse correlation properties than the others.

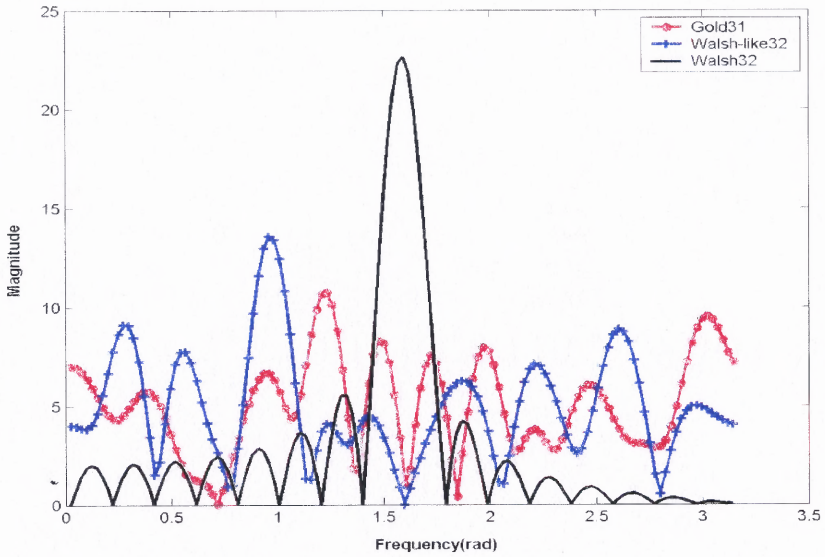

Figure 5.5 Magnitude functions of Gold, Walsh and proposed Walsh-like binary codes plotted in Figure 5.4.

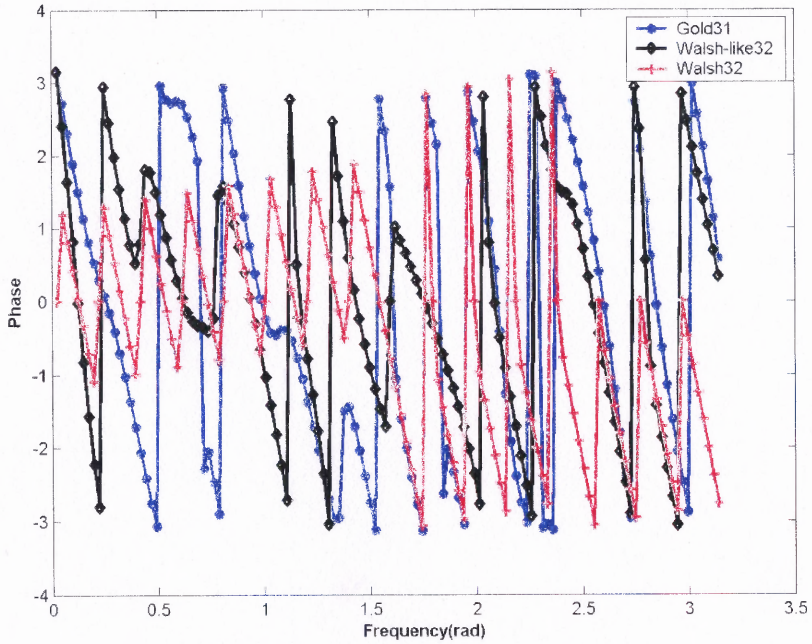

Figure 5.6 Phase functions of Gold, Walsh and proposed Walsh-like binary codes plotted in Figure 5.4.

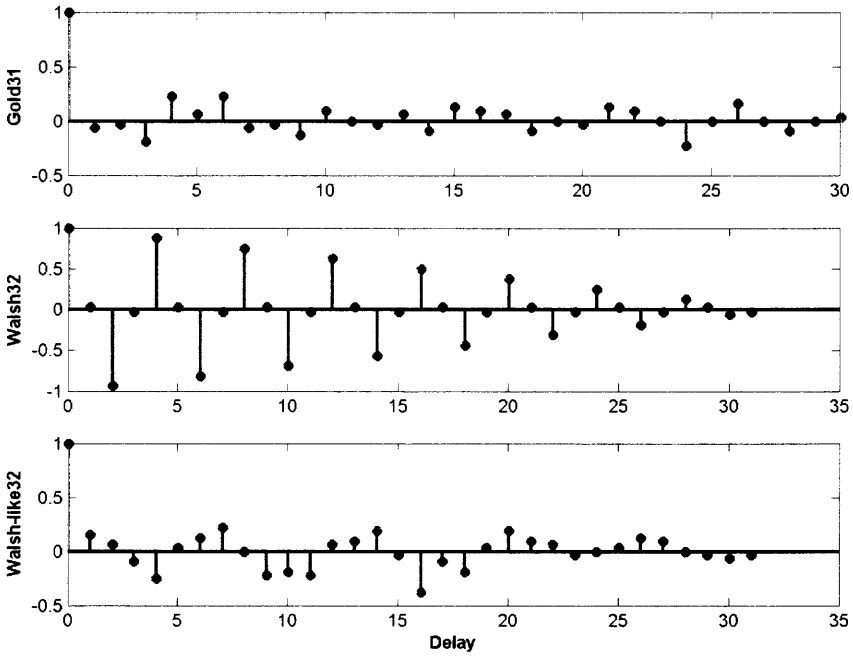

Figure 5.7 Auto-correlation functions of Gold, Walsh and proposed Walsh-like binary codes plotted in Figure 5.4.

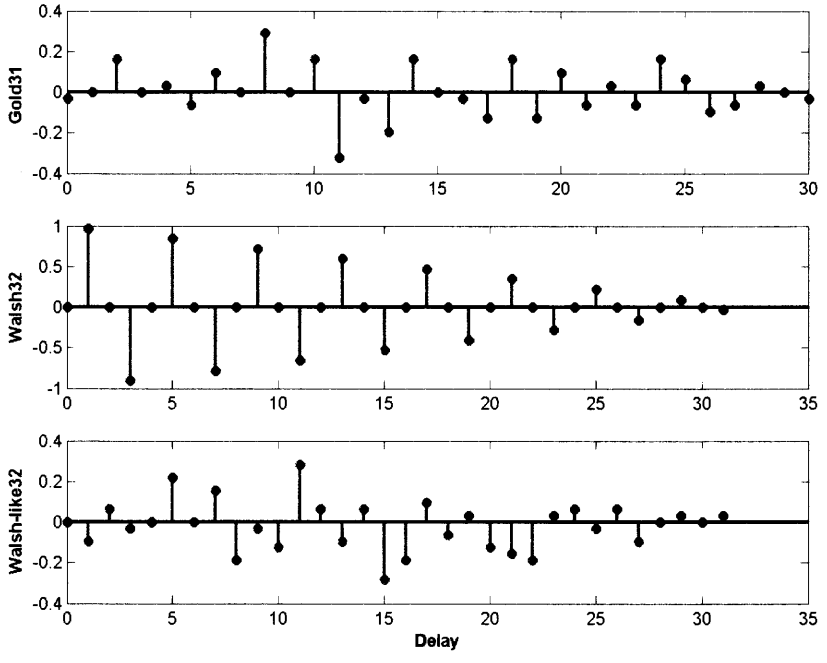

Figure 5.8 Cross-correlation functions between a typical code pair for 31-length Gold and 32-length Walsh and proposed Walsh-like binary codes.

5.3.3 Bit Error Rate (BER) Performance Comparisons for 2-Users in AWGN Channels

Figure 5.9 displays the BER performance of proposed 8-length Walsh-like code sets given in Table 5.3 averaged over all possible code pairs and for all possible delays in an asynchronous AWG noise scenario as a function of SNR. Also shown in Figure 5.9 are BER performances of 8-length Walsh code set and 7-length Gold code set. The proposed Walsh-like codes outperform Walsh codes significantly and are marginally better than comparable Gold codes at higher SNRs.

Similarly, Figure 5.10 displays BER performances of proposed 32-length Walsh-like code sets given in Appendix B along with 32-length Walsh and 31-length Gold code sets. Improved performance of Walsh-like code sets over Walsh code set is also consistent here and performances of proposed Walsh-like code sets closely match with that of Gold code set.

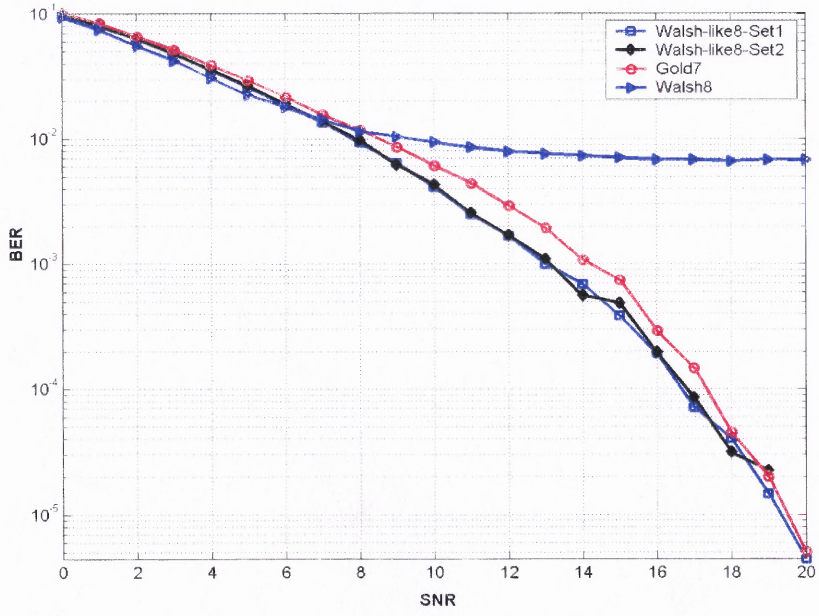

Figure 5.9 BER performances of proposed 8-length Walsh-like, Walsh and 7-length Gold code sets in asynchronous AWGN communication channel for 2-user case.

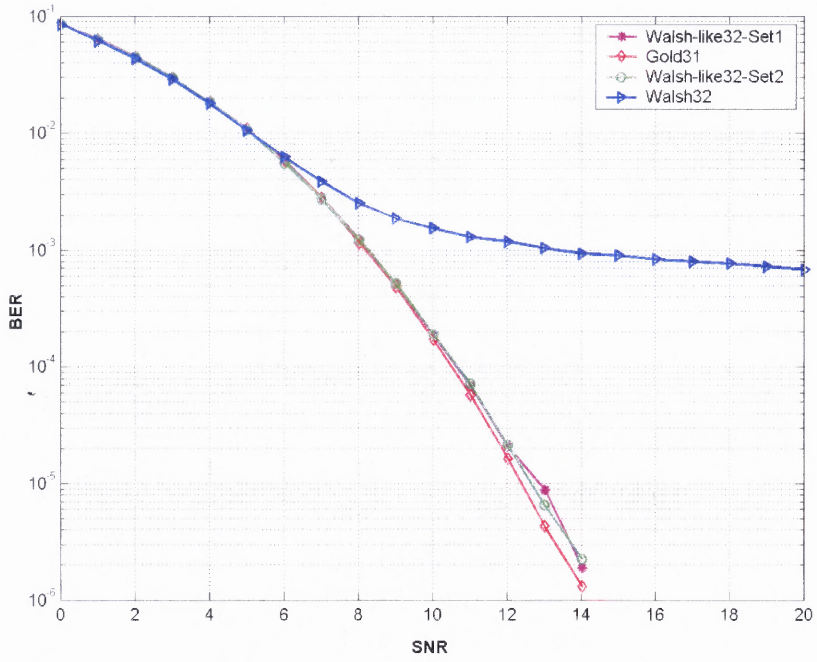

Figure 5.10 BER performances of proposed 32-length Walsh-like, Walsh and 31-length Gold code sets in asynchronous AWGN communication channel for 2-user case.

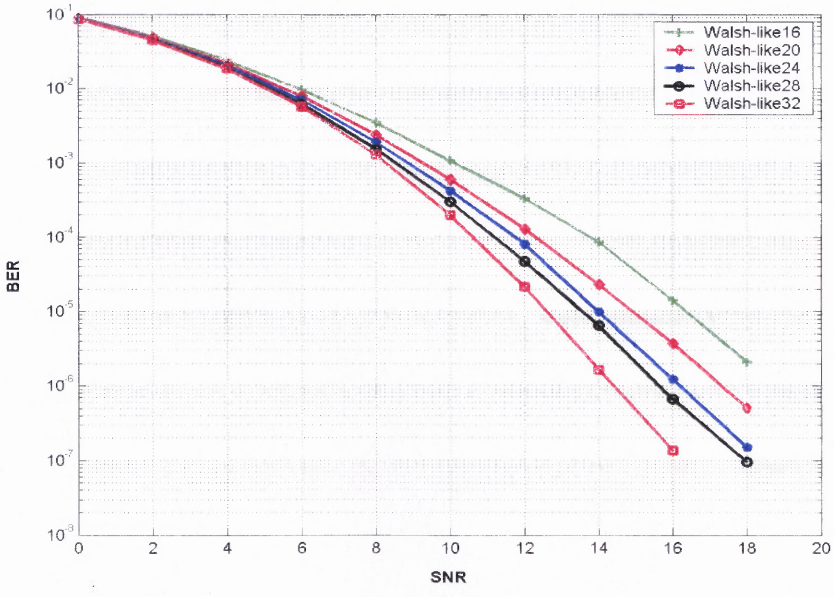

Figure 5.11 BER performances for proposed 16, 20, 24, 28 and 32-length Walsh-like code sets in asynchronous AWGN communication channel for 2-user case.

With the proposed simulation method, a number of proposed Walsh-like code sets with code lengths that are multiples of 4 (8, 12, 16, 20, 24, ...) are obtained. Figure 5.11 displays the BER performances for 16, 20, 24, 28 and 32-length Walsh-like code sets for 2-user case in asynchronous communications scenario. Performance improvement as a function of increased code length increases is observed from Figure 5.11.

Section 5.1 explained the design of linear phase orthogonal code sets and their BER performance simulations. In this section, non-linear phase (Walsh-like) orthogonal code sets are generated and BER performance characteristics are simulated. Figure 5.12 displays the relative performance of linear phase code sets and non-linear phase code sets for 16 and 32-length codes. Performance of non-linear phase code sets is better than linear phase code sets. For comparison purpose, linear phase 16 and 32-length Walsh code performances are also shown in Figure 5.12.

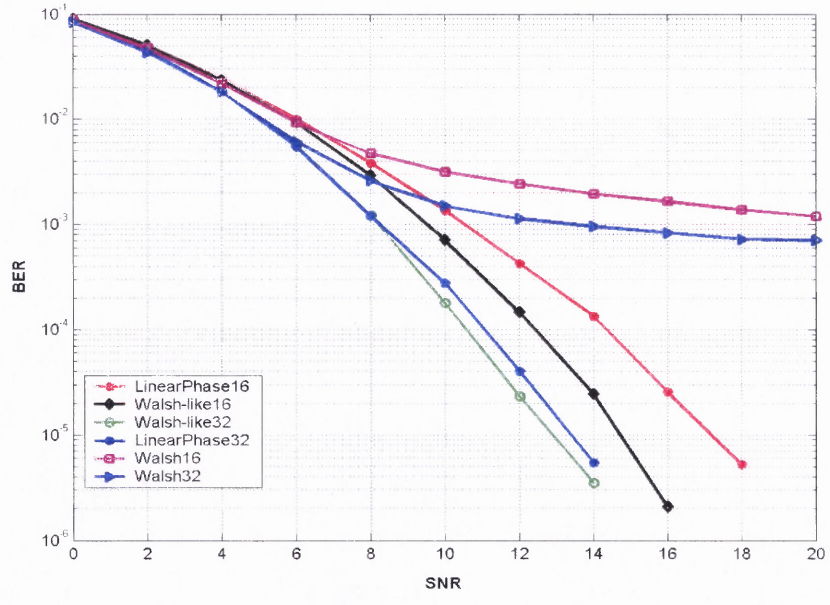

Figure 5.12 BER performances of proposed 16, 32-length linear phase and non-linear phase (Walsh-like) code sets along with 16, 32-length Walsh code sets in asynchronous AWGN channel for 2-user case.

5.3.4 Multiuser Bit Error Rate (BER) Performance Comparisons in AWGN Channels

BER performance for multiuser scenario is simulated by allotting unique spreading sequences to different users with random delays between them and taking average BER performance over a large number of independent simulation runs.

Figure 5.13 displays the multiuser performance comparisons of 8-length Walsh-like orthogonal code sets along with 8-length Walsh and 7-length Gold code sets for SNR=20 dB as a function of number of users. Similarly, Figure 5.14 displays the multiuser performance of 32-length Walsh-like code sets, Walsh code and 31-length Gold code families evaluated at SNR=20 dB.

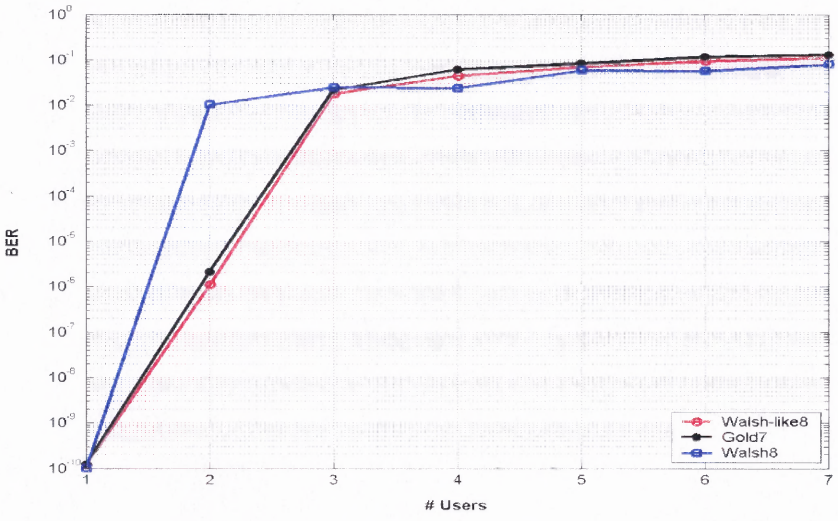

Figure 5.13 Multiuser BER performances of proposed 8-length Walsh-like, Walsh code sets along with 7-length Gold code set in asynchronous AWGN channel at SNR=20 dB as a function of number of users in the channel.

As the number of simultaneous users in the communications system increases, inter-code (multiuser interference) and intra-code correlations (self-induced multipath interference) dominate the BER performance. Therefore, BER performances of the three

types of code sets merge together at higher number of users in a multiuser communication system as observed in Figs. 5.13 and 5.14. In order to improve detection of such a scenario, multiuser detection techniques such as decorrelator or MMSE type of receivers need to be used in the system [48, 49].

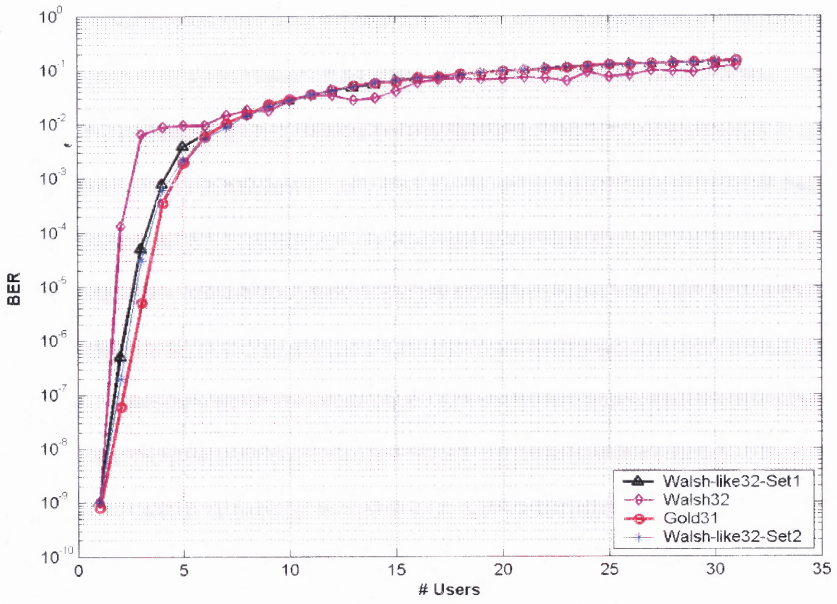

Figure 5.14 Multiuser BER performances of proposed 32-length Walsh-like, Walsh code sets along with 31-length Gold code set in asynchronous AWGN channel at SNR=20 dB as a function of number of users in the channel.

5.3.5 Bit Error Rate (BER) Performance Comparisons in Rayleigh Flat, Slow Fading Channel

Rayleigh fading occurs in a wireless communication system when there are multiple reflective paths between the transmitter and receiver without any line of sight component. This is usually the scenario when the receiver is in motion. Under Rayleigh flat fading conditions, multipath components of a symbol arrive at the receiver within the symbol duration. Hence, such components are not resolvable. Channel is assumed to have a

constant gain over a bandwidth which is greater than the transmitted signal bandwidth [50, 51, 52].

For slow fading conditions, Doppler signal spread due to receiver motion is much smaller than the transmitted symbol bandwidth. Therefore, fading characteristics are such that, channel conditions are assumed to remain the same during a symbol interval. Spectral characteristics of the transmitted signal are preserved at the receiver where as the amplitude of the received signal changes in time. There will be performance degradation due to fading since unresolved received components can add up destructively during the symbol interval. Fading channel for each user is modeled independently of the other users in the uplink scenario.

Rayleigh fading is a multiplicative distortion and received signal $y(t)$ is modeled as $y(t) = h(t)\, s(t) + n(t)$, where $h(t)$ is the impulse response of the channel waveform, $s(t)$ is the transmitted signal, $n(t)$ is the AWG noise. For flat fading channel, $h(t)$ consists of a single tap with zero delay. $h(t)$ is a wide-sense stationary (WSS) complex Gaussian process, with zero mean and unity variance, uniform phase distribution and Rayleigh probability density function (pdf) amplitude distribution. Clark's model is used to define the spectral characteristics of the channel that are controlled by the Doppler frequency of the mobile [54]. Smith's simulation model is employed for generating the fading model [54].

Auto-correlation sequence of the random process $h(t)$ is controlled by the Doppler frequency f_d and it is equal to

$$R(\tau) = E\left\{h(t)h^*(t-\tau)\right\} \square J_0(2\pi f_d \tau) \tag{5.1}$$

where J_0 is the zero-order Bessel function of the first kind [53].

Hence, complex Gaussian samples generated for $h(t)$ are masked with a filter whose power spectral density (PSD) function is given by

$$S_{hh}(f) = \frac{1}{\pi f_d} \sqrt{1-(f/f_d)^2} \quad |f| < f_d \tag{5.2}$$

where f_d is the Doppler frequency [50, 54].

Inverse FFT followed by a square root operation is applied on the resulting samples to generate Rayleigh distributed amplitude pdf.

Figure 5.15 displays the BER performances of the proposed 32-length Walsh-like code sets, Walsh code set and 31-length Gold code set for both synchronous and asynchronous Rayleigh flat, slow fading channel conditions for 2-user case.

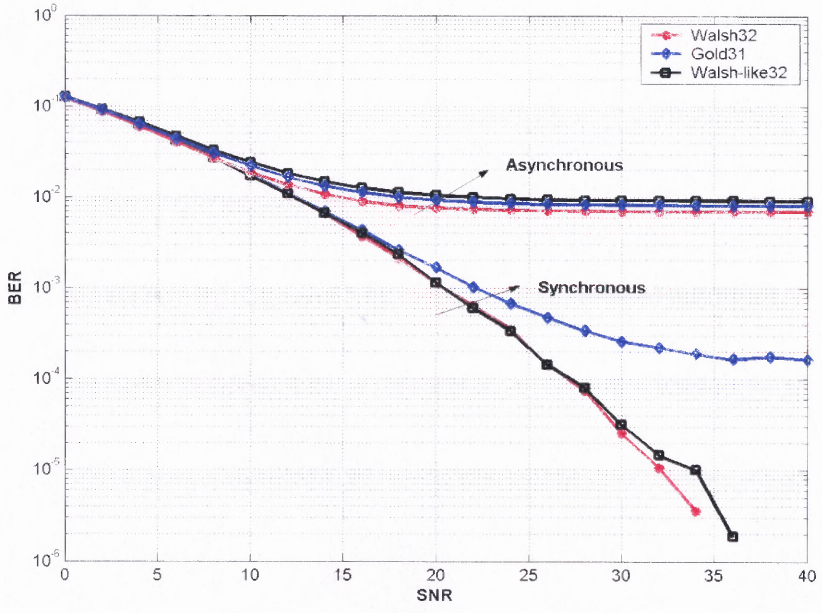

Figure 5.15 BER performances of proposed 32-length Walsh-like, Walsh code sets along with 31-length Gold code set in synchronous and asynchronous Rayleigh flat, slow fading channel for 2-user case.

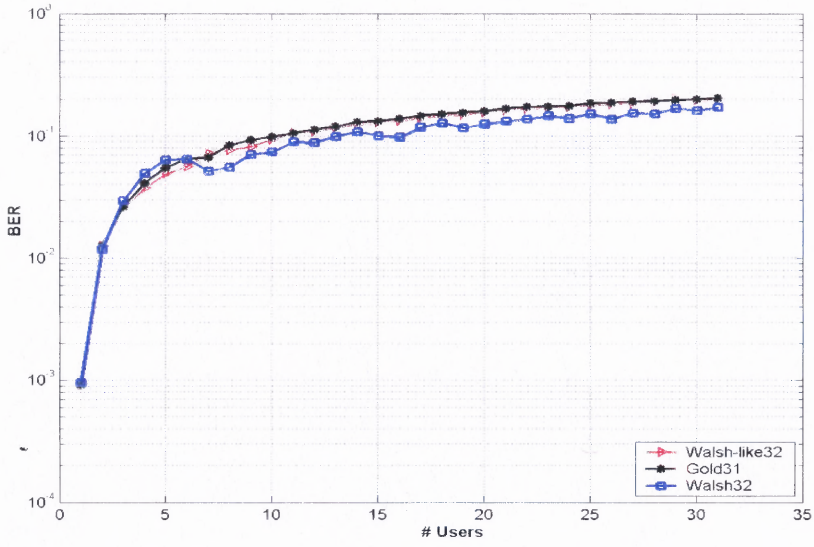

Figure 5.16 Multiuser BER performances of proposed 32-length Walsh-like, Walsh code sets along with 31-length Gold code set in asynchronous Rayleigh flat, slow fading channel at SNR=20 dB as a function of number of users in the channel.

The figure displays that the performance of the proposed Walsh-like code sets closely matches with the standard code sets performance in asynchronous channel conditions and in synchronous conditions, and Walsh-like codes perform better than Gold code set. Performance for all types of code sets is poor in asynchronous channel scenario. Figure 5.16 displays the asynchronous multiuser BER performance of the same codes as a function of the number of users in the channel at SNR = 20 dB. It is observed from these curves that all code sets perform similarly in Rayleigh flat fading channels.

5.3.6 Correlation Performance Metrics

Performance of different code families can also be analyzed by numerically evaluating their cross-correlation parameters such as aperiodic, even and odd correlation values.

Signal to noise ratio (SNR) which is the most important performance characteristic of any CDMA system can be calculated as [19, 20],

$$SNR = \left\{ \frac{N_0}{2E} + \frac{1}{6N^3} \sum_{\substack{k=1 \\ k \neq i}}^{K} \gamma_{k,i} \right\}^{-\frac{1}{2}} \tag{5.3}$$

where $2E/N_0$ is energy/bit ratio , N is the length of the code sequence, K is the number of users and $\gamma_{k,i}$ is the interference power generated due to multiple access defined by the cross-correlation parameters. To obtain the worst case performance of the system, it is essential to get the highest bound values for $\gamma_{k,i}$.

$\gamma_{k,i}$ is defined as [19, 20],

$$\gamma_{k,i} = 2\mu_{k,i}(0) + \mu_{k,i}(1) \tag{5.4}$$

where

$$\begin{aligned} 2\mu_{k,i}(0) &= \sum_{m=0}^{N-1} \theta_{k,i}^2(m) + \sum_{m=0}^{N-1} \hat{\theta}_{k,i}^2(m) \\ \mu_{k,i}(1) &= \sum_{m=1-N}^{N-1} C_{k,i}(m) C_{k,i}(m+1) \end{aligned} \tag{5.5}$$

Here, $\theta_{k,i}, \hat{\theta}_{k,i}, C_{k,i}$ are even, odd, aperiodic cross-correlation values as defined in Equation (4.6). From these three basic correlation values, their maximum, mean, deviation, sum of square of correlation values are calculated [55]. Here, the deviation is defined as the ratio of standard variance to the mean.

Table 5.4 lists the absolute values of the normalized maximum, mean, deviation, sum of square of three types of correlation values for 8-length Walsh, the proposed Walsh-like codes (a typical one), and 7-length Gold code sets. It is observed from the table that the normalized maximum cross-correlation value for Walsh set is 1, resulting in its poor asynchronous BER performance while Walsh-like code set has the lowest maximum cross-correlation value, explaining its superior performance compared to other

code sets. Deviation value for the proposed Walsh-like codes is comparable to Gold codes where as it is much higher for Walsh codes. Walsh code family has the lowest sums of square of correlation values compared to code sets of other two families. But, some Walsh code pairs have maximum correlation values, resulting in poorer average performance. Hence, sum of square of correlation values can not be considered in evaluating the average performance of the entire code set.

Similarly, Table 5.5 lists the absolute values of the normalized maximum, mean, deviation, sum of square of three types of correlation values for 32-length Walsh, proposed Walsh-like codes (a typical one) and 31-length Gold code sets. Here also, normalized maximum cross-correlation value for Walsh code set is 1. For both Walsh-like and Gold sets, correlation value is less than 1. Walsh-like parameters match closely with that of Gold parameters in all metrics considered in Table 5.5, explaining their similarity in BER performance curves.

These inter-code and intra-code correlation properties (multiuser interference) along with the channel noise conditions imposed on them dictate the performance of a multiuser communication system at the receiver. Therefore, choosing the best possible user codes with minimum intra-code and inter-code correlation properties will significantly improve the performance of a DS-CDMA communication system particularly when the number of users in the system is low.

Table 5.4 Cross-correlation Metrics for Proposed 8-Length Walsh-like, Walsh and 7-Length Gold Codes

Parameter	Walsh 8	Gold 7	Walsh-like 8
Maximum Even Correlation $(\theta_{k,i})$	1	0.7143	0.5
Maximum Odd Correlation $(\hat{\theta}_{k,i})$	1	0.7143	0.7500
Maximum Aperiodic Correlation $(C_{k,i})$	0.8750	0.7143	0.6250
Mean Even Correlation $\frac{1}{2N-1}\sum_{l=0}^{N-1}\lvert\theta_{k,i}(l)\rvert$	0.0893	0.2959	0.2143
Mean Odd Correlation $\frac{1}{2N-1}\sum_{l=0}^{N-1}\lvert\hat{\theta}_{k,i}(l)\rvert$	0.2232	0.2959	0.2545
Mean Aperiodic Correlation $\frac{1}{2N-1}\sum_{l=1-N}^{N-1}\lvert C_{k,i}(l)\rvert$	0.1417	0.2033	0.2545
Deviation – Even Correlation Standard Variance $(\theta_{k,i})$ / Mean $(\theta_{k,i})$	0.6135	0.1284	0.2870
Deviation – Odd Correlation Standard Variance $(\hat{\theta}_{k,i})$ / Mean $(\hat{\theta}_{k,i})$	0.2378	0.1284	0.1850
Deviation – Aperiodic Correlation Standard Variance $(C_{k,i})$ / Mean $(C_{k,i})$	0.1697	0.1291	0.1850
Sum of square of even correlation $\sum_{l=0}^{N-1}\theta_{k,i}^2(l)$	14	24.5	25
Sum of square of odd correlation $\sum_{l=0}^{N-1}\hat{\theta}_{k,i}^2(l)$	23	24.5	25
Sum of square of aperiodic correlation $\sum_{l=1-N}^{N-1}C_{k,i}^2(l)$	18.5	24.5	24.5

Table 5.5 Cross-correlation Metrics for Proposed 32-Length Walsh-like, Walsh and 31-Length Gold Codes

Parameter	Walsh32	Gold31	Walsh-like32
Maximum Even Correlation $(\theta_{k,i})$	1	0.2903	0.625
Maximum Odd Correlation $(\hat{\theta}_{k,i})$	1	0.5484	0.6875
Maximum Aperiodic Correlation $(C_{k,i})$	0.9687	0.3871	0.5625
Mean Even Correlation $\frac{1}{2N-1}\sum_{l=0}^{N-1}\lvert\theta_{k,i}(l)\rvert$	0.0536	0.1374	0.1321
Mean Odd Correlation $\frac{1}{2N-1}\sum_{l=0}^{N-1}\lvert\hat{\theta}_{k,i}(l)\rvert$	0.0981	0.1415	0.1361
Mean Aperiodic Correlation $\frac{1}{2N-1}\sum_{l=1-N}^{N-1}\lvert C_{k,i}(l)\rvert$	0.0624	0.0946	0.0935
Deviation – Even Correlation Standard Variance $(\theta_{k,i})$ / Mean $(\theta_{k,i})$	0.3582	0.0896	0.0979
Deviation – Odd Correlation Standard Variance $(\hat{\theta}_{k,i})$ / Mean $(\hat{\theta}_{k,i})$	0.1786	0.0790	0.0862
Deviation – Aperiodic Correlation Standard Variance $(C_{k,i})$ / Mean $(C_{k,i})$	0.1378	0.0729	0.0711
Sum of square of even correlation $\sum_{l=0}^{N-1}\theta_{k,i}^2(l)$	350	449	482
Sum of square of odd correlation $\sum_{l=0}^{N-1}\hat{\theta}_{k,i}^2(l)$	431	449	480
Sum of square of aperiodic correlation $\sum_{l=1-N}^{N-1}C_{k,i}^2(l)$	390	449	481

5.3.7 Time-Frequency Localization

Time domain center and spread values, frequency domain center and spread values ($\bar{n}, \sigma_n^2$, $\bar{\omega}$ *and* σ_ω^2) are calculated as discussed in Section 3.4 [7, 8] for proposed 32-length Walsh-like, Walsh and 31-length Gold code sets and are plotted in Figure 5.17. From the figure, it is observed that all the three code families considered have constant time spread σ_n^2 as they are binary in nature with the same fixed power level. Walsh code sequences have less frequency domain spread values (σ_ω^2) compared to Gold code sequence values. Walsh-like codes and Gold codes have similar σ_ω^2 values. These spread values justify their BER performance characteristics in all types of channel noise conditions.

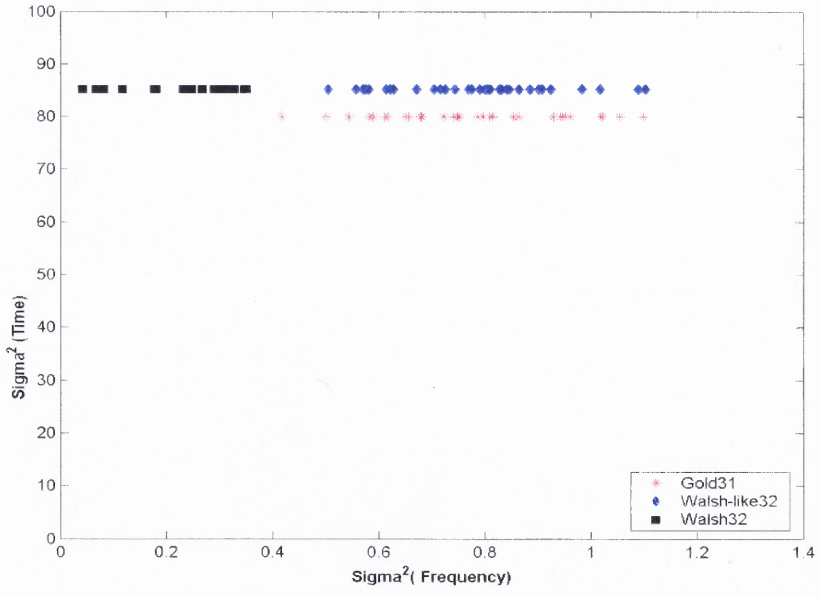

Figure 5.17 Time-frequency localizations for proposed 32-length Walsh-like, Walsh and 31-length Gold code sets.

CHAPTER 6

MULTIPLE LEVEL INTEGER VALUED ORTHOGONAL SPREADING CODES

Binary valued Walsh and Gold codes are widely used as spreading codes in existing CDMA systems. In Chapter 4, limitations of these code families in terms of available code lengths and in numbers are discussed. In Chapter 5, design issues and sample codes for various types of binary orthogonal code sets are presented. It was shown that the proposed new set of codes either exceed or closely match standard families in performance. In this chapter, limitations of binary level codes, design issues of multiple level codes and their performance characteristics are discussed.

Multiple level polyphase sequences and their applications to CDMA systems are explained in references [56, 57]. Polyphase codes generate fixed power envelope creating similar kind of problems as binary leveled code sets. Synthesis of multiple level complementary sequences and construction of multiple level Hadamard matrices are described in [58, 59]. Availability of these code sets is limited and these sequences are not useful for asynchronous communication with random delays.

6.1 Limitations of Binary Codes

Binary code sets have the chip values (+1, -1) and generate constant envelope or fixed power modulating signal at the RF power amplifier. Amplifiers usually operate as a linear device under small signal conditions and become more non-linear and distorted with increase in input drive level. Amplifier distortion increases inter modulation components and adjacent channel interference [60, 61].

On the other hand, amplifiers are less efficient in their linear range of operation. Power efficiency, $P_{ae}(t)$ of the amplifier is defined as [60]

$$P_{ae}(t) = (P_{rf}(t) - P_{in}(t)) / P_{dc}(t) \tag{6.1}$$

where $P_{in}(t)$ and $P_{rf}(t)$ are the input and the output RF signal power at the amplifier and $P_{dc}(t)$ is the dc power supplied.

Average total power consumed by the amplifier is [60]

$$\begin{aligned} \overline{P}_t &= \overline{P}_{dc} + P_{in} \\ &= \overline{P}_{rf}(1 + (1 - \overline{P}_{ae})\overline{P}_{dc} / \overline{P}_{rf}) \\ &= \overline{P}_{rf}(1 + w) \end{aligned} \tag{6.2}$$

where $\overline{X}$ is the average value of X and w is the fractional average power not converted into the RF power. Increasing the input drive signal in turn increases the efficiency of the RF amplifier and thus increases the total transmitted power. Lower efficiency results in power loss at the RF amplifier, thus limiting the battery life of the communication system. Higher efficiency amplifier increases the distortion in the system. Hence, an optimum operating point has to be arrived which results in better efficiency and lower distortion.

Current research on RF amplifier design is aimed at increasing the linear range of RF amplifiers with lower distortion levels and higher efficiency. With such technological advances, implementation of varying power codes is becoming feasible for wireless and radio communications.

6.2 Design Methods for Multiple Level (Varying Power) Spreading Codes

6.2.1 Multiple Level Integer Codes

In multiple level integer coding, discrete amplitude levels, similar to the pulse amplitude modulation (PAM) levels, are used as chip signals for spread spectrum codes. Chip amplitudes are chosen such that they are zero mean. For example, for a 4-level coding, chip amplitudes are of $\{-3,-1,1,3\}$ and for 8-level coding, chip amplitudes are of $\{-7,-5,-3,-1,1,3,5,7\}$.

An n-length code with 4-level chip values requires a sample space of 4^n integer numbers. This is equivalent to 2^{2n} numbers in binary sample space. It is known that for representing integer numbers in binary level coding requires radix-2 elements $\{0,1\}$. Similarly, 4-level coding requires radix-4 elements $\{0,1,2,3\}$ and 8-level coding requires radix-8 elements $\{0,1,2,3,4,5,6,7\}$ and so on. Higher level coding representation requires more radix elements.

Weights of the coding elements in radix-4 for n-length code are $\{4^{n-1},4^{n-2},.....,4^1,4^0\}$ and similarly in radix-8, element weights are $\{8^{n-1},8^{n-2},.....,8^1,8^0\}$. For example, number 125 in radix-4 format for 8-length code is represented as $\{0,0,0,0,1,3,3,1\}$ as this is equivalent to $\{4^3.1+4^2.3+4^1.3+4^0.1\}$. Furthermore, these radix numbers are mapped into corresponding PAM chip levels with the mapping as $\{0\rightarrow -3,1\rightarrow -1,2\rightarrow 1,3\rightarrow 3\}$ for radix-4 and $\{0\rightarrow -7,1\rightarrow -5,2\rightarrow -3,3\rightarrow -1,$ $4\rightarrow 1,5\rightarrow 3,6\rightarrow 5,7\rightarrow 7\}$ for radix-8.

Exhaustive computer search is performed within the sample space in order to obtain orthogonal code sets in an iterative manner. The procedure to generate n-length, m-level orthogonal code sets is summarized as follows.

- Sample space consists of $[0, m^{n-1}-1]$ sequences for m-level, n-length code sets.
- As the first step, select any number in the sample space as the first basis function and convert the number into corresponding m-level radix format for n-length code. Map these radix elements into corresponding chip levels.
- Convert all numbers within the sample space into m-level, n-length code. Check for the orthogonality with the first basis function. In addition, maximum absolute normalized cross-correlation value should be less than 1. If both of these conditions are met, select that code as the next basis function.
- Repeat the process to get N basis sequences of the orthogonal set.
- Conditions for selecting orthogonal codes are similar to the binary Walsh-like codes described in Section 5.3.1. Basis sequences are non-linear phase and non-zero mean codes. No restrictions are imposed on the number of zero crossings within code set.
- By selecting a different integer as the first basis function, an entirely independent orthogonal set can be obtained.
- For multiple chip level codes, in addition to these constraints, norm of the basis function is also considered as another design parameter. All the basis sequences in the orthogonal set are designed to have the same norm. Table 6.1 lists different possible norms for 4-level, 8-length codes.

Sample space is searched with these constraints and a number of multiple level orthogonal sample codes are obtained.

Table 6.1 Possible 4-Level, 8-Length Code Elements and Their Norms

Code Elements	$Norm^2$
±1,±1,±1,±1,±1,±1,±1,±1	8
±3,±1,±1,±1,±1,±1,±1,±1	16
±3,±3,±1,±1,±1,±1,±1,±1	24
±3,±3,±3,±1,±1,±1,±1,±1	32
±3,±3,±3,±3,±1,±1,±1,±1	40
±3,±3,±3,±3,±3,±1,±1,±1	48
±3,±3,±3,±3,±3,±3,±1,±1	56
±3,±3,±3,±3,±3,±3,±3,±1	64
±3,±3,±3,±3,±3,±3,±3,±3	72

As an example, a typical 4-length, 4-level orthogonal code set obtained through computer search is given below

$$\begin{bmatrix} -3 & -1 & 1 & 3 \\ -1 & 3 & -3 & 1 \\ -1 & 3 & 3 & -1 \\ 3 & 1 & 1 & 3 \end{bmatrix}$$

4-length orthogonal set with good correlation properties are not available with binary level coding. However, it is possible to obtain good orthogonal set with 4-level coding. Table 6.2 lists the integer representation of 8-length, 4-level and 8-level orthogonal sets. Integer representations of few other multiple level codes are also shown in the reference [62].

Table 6.2 Integer Representation of 8-Length, 4-Level and 8-Level Orthogonal Code Sets

Decimal Values	4-Level Integer Codes								Decimal Values	8-Level Integer Codes							
329	-3	-3	-3	-1	-1	-3	1	-1	275689	-7	-5	-7	-1	-3	-1	3	-5
7038	-3	-1	1	3	-1	3	3	1	2340109	-5	-7	7	-1	-3	1	-5	3
11364	-3	1	3	-3	-1	1	-1	-3	4065418	-5	7	1	-7	1	-3	-5	-3
13907	-3	3	-1	1	-1	-1	-3	3	5025695	-3	-1	-5	-3	7	5	-1	7
19927	-1	-3	3	-1	3	-1	-1	3	5434840	-3	1	3	5	5	7	-1	-7
22496	-1	-1	-1	3	3	1	-3	-3	7024251	-1	-3	5	-3	7	-5	7	-1
24826	-1	1	-3	-3	3	3	1	1	7771132	-1	3	3	-5	-5	7	7	1
31437	-1	3	1	1	3	-3	3	-1	15042897	7	-5	-1	-7	1	3	-3	-5

6.2.2 Multiple Level Short Length Codes

Short length codes are more useful for applications like wireless sensor networks or mesh networks where communication nodes are placed at close proximity and system complexity is of great concern. Zigbee protocols are defined for such short range and low cost applications. Typical communication ranges in sensor nodes are of the order of 10-75 meters with an output power of 0 dBm and their data rates vary from 20 Kbps to 250 Kbps. CDMA techniques are used in this standard for multiple access of the radio channel [63].

Longer ranges in traditional wireless communication require higher processing gain for the receivers, thus requiring longer spreading codes in CDMA. Operational conditions are different in sensor networks as they operate at shorter ranges with less

available power. Shorter code lengths can be generated off-hand and stored as in look up tables. This process reduces the expensive power requirements at each sensor node.

Multiple level code searches are also extended to find near orthogonal code sets for odd code lengths. For some code lengths, minimum basis elements required for finding orthogonal / near orthogonal code sets are ternary chip values $\{-1,0,1\}$. All basis sequences within the code set are designed to have the same norm.

Table 6.3 Basis Elements for Representing Short Length Spreading Codes and Their Norms

Length	Basis Elements	$Norm^2$	Orthogonal / Near Orthogonal
4	$\{-3,-1,1,3\}$	20	Orthogonal
5	$\{-1,0,1\}$	4	Near Orthogonal
6	$\{-1,0,1\}$	4	Orthogonal
7	$\{-1,1\}$	7	Near Orthogonal
8	$\{-1,1\}$	8	Orthogonal
9	$\{-1,0,1\}$	8	Near Orthogonal
10	$\{-1,0,1\}$	8	Orthogonal
11	$\{-1,1\}$	11	Near Orthogonal
12	$\{-1,1\}$	12	Orthogonal
13	$\{-1,0,1\}$	12	Near Orthogonal
14	$\{-1,0,1\}$	10	Orthogonal
15	$\{-1,1\}$	15	Near Orthogonal
16	$\{-1,1\}$	16	Orthogonal

Table 6.3 lists the minimum basis elements required for generating code sets with good correlation properties for short length codes of lengths up to 16 and their corresponding norms. For example, 4-length codes require minimum basis elements $\{-3,-1,1,3\}$ for good orthogonal code set representation with square of norm as 20. In Table 6.3, near orthogonal code set refers to a cross-correlation value of -1 between any pair of codes for zero delay between them.

It is well known that communication performance improves as the spreading code length increases, by keeping the number of basis elements the same. From Table 6.3, it can be inferred that among the 2-level code families, performance of 16-length code set will be better than 12-length code set which in turn will be better than 8- length code set.

Basis elements shown in Table 6.3 for representing orthogonal / near orthogonal code sets are the minimum chip levels needed for a given length of the code. Communication performance significantly improves by keeping the length of the code same and increasing the number of chip levels. For example, for 6-length, orthogonal code sets are obtained with chip levels of 3, 5, 7, 9, 11, and 13. Orthogonal code sets with 2, 4, 6, 8, 10 chip levels are not available for 6-length codes.

Table 6.4 lists the absolute values of normalized maximum and sum of square of even, odd and aperiodic cross-correlation values discussed in Section 5.3.5 for different 6-length multiple level codes. As the number of levels increases, maximum cross-correlation values decrease. As the maximum cross-correlation values are lowest for 11-level code sets, these code sets should give best performance for all the types of code sets. As the number of levels is increased further, cross-correlation values increase,

resulting in performance deterioration. Table 6.5 lists the integer representation of different multiple level 6-length codes.

BER performances of different multiple level codes are discussed in the next section.

Table 6.4 Cross-correlation Metrics for Different Multiple Level, 6-Length Codes

Parameter	3 Level	5 Level	7 Level	9 Level	11 Level	13 Level
Maximum Even Correlation $(\theta_{k,i})$	.75	.7	0.8	.73	.64	.72
Maximum Odd Correlation $(\hat{\theta}_{k,i})$	.75	.8	.65	.73	.64	.70
Maximum Aperiodic Correlation $(C_{k,i})$	.75	.7	0.7	.73	.64	.70
Sum of square of even correlation $\sum_{l=0}^{N-1}\theta_{k,i}^2(l)$	11	13.1	10	13	14	13
Sum of square of odd correlation $\sum_{l=0}^{N-1}\hat{\theta}_{k,i}^2(l)$	12	13.5	13	13	13	14
Sum of square of aperiodic correlation $\sum_{l=1-N}^{N-1}C_{k,i}^2(l)$	12	13.3	11	13	14	13

Table 6.5 Integer Representation of Different Multiple Level, 6-Length Codes

3-Level Codes Basis Elements $\{-1, 0, 1\}$ Norm^2 - 4	5-Level Codes Basis Elements $\{-2, -1, 0, 1, 2\}$ Norm^2 - 10	7-Level Codes Basis Elements $\{-3, -2, -1, 0, 1, 2, 3\}$ Norm^2- 20	9-Level Codes Basis Elements $\{-4, -3, -2, -1, 0, 1, 2, 3, 4\}$ Norm^2- 26	11-Level Codes Basis Elements $\{-5, -4, -3, -2, -1, 0, 1, 2, 3, 4, 5\}$ Norm^2- 50	13-Level Codes Basis Elements $\{-6, -5, -4, -3, -2, -1, 0, 1, 2, 3, 4, 5, 6\}$ Norm^2- 50
22	182	2858	9832	17968	95570
396	8378	51974	163032	143082	2433484
404	8476	60218	218158	847144	2469152
524	10660	73438	272578	847218	2779564
528	10714	77530	310372	885134	3144890
670	12932	103798	372786	885216	3356242

6.2.3 Bit Error Rate (BER) Performance Comparisons in AWGN Channels

Mathematically speaking, BER performance of multiple level codes will be better than binary level codes since inter-code correlations become smaller with the increase in spreading code chip levels. BER performances for different multiple level codes are simulated for 2-user and multiuser scenarios in AWG noise environment. BER performance is averaged over all the possible combinations of user codes and for all possible code delays.

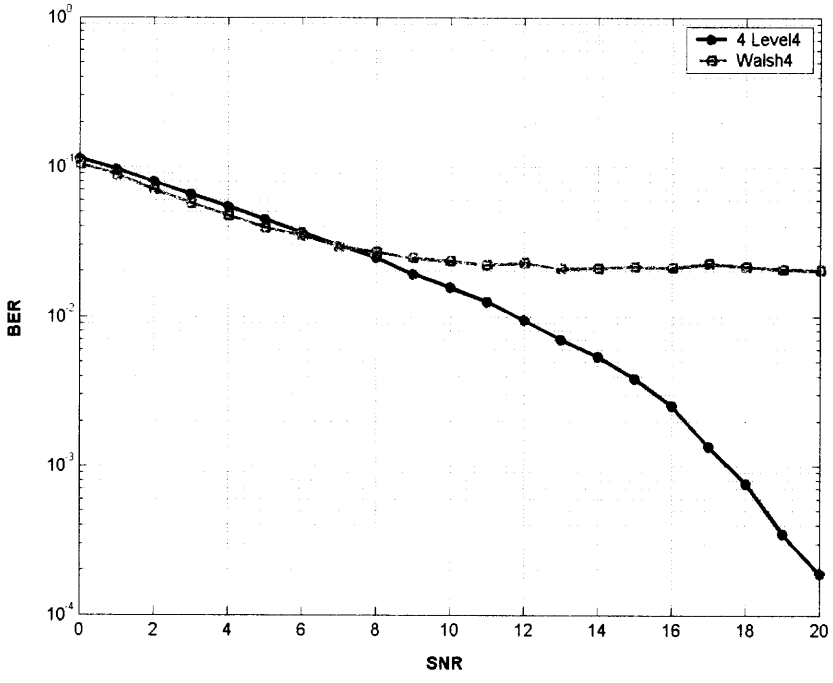

Figure 6.1 BER performances for proposed 4-level, 4-length code set and 4-length binary Walsh code set in asynchronous AWGN channel for 2-user case.

Figure 6.1 displays the BER performance of proposed 4-level, 4-length multiple valued code set and standard 4-length Walsh code set. As some Walsh code pairs have poor cross-correlation properties for certain delays, average performance for the set is poor. The proposed 4-length, 4-level code set does not have such cross-correlation

limitations, thus providing significantly better performance than Walsh code set under the same test conditions. During simulations, all binary and multiple level codes are normalized to unity for uniform performance comparison.

Figure 6.2 displays the BER performance of 8-length, 4-level and 8-level codes along with 8-length Walsh-like and Walsh codes, and 7-length Gold codes for 2-user scenario. It is observed from this figure that the performance of 4-level codes is better than 2-level Walsh-like codes and performance of 8-level codes is better than 4-level codes.

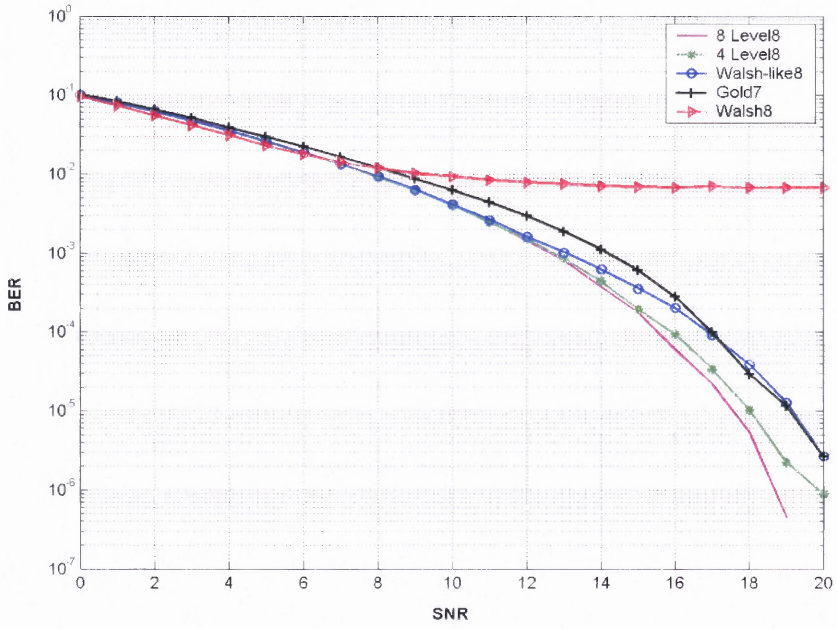

Figure 6.2 BER performances for proposed 8-length, 4-level and 8-level code sets, binary 8-length Walsh-like and Walsh code sets, and 7-length Gold code set in asynchronous AWGN channel for 2-user case.

Similarly, Figure 6.3 displays the 2-user performance of proposed 16-length, 4 and 8-level varying power code sets along with binary Walsh-like and Walsh code sets. Here also, performance of multiple level code sets is better than 2-level code sets.

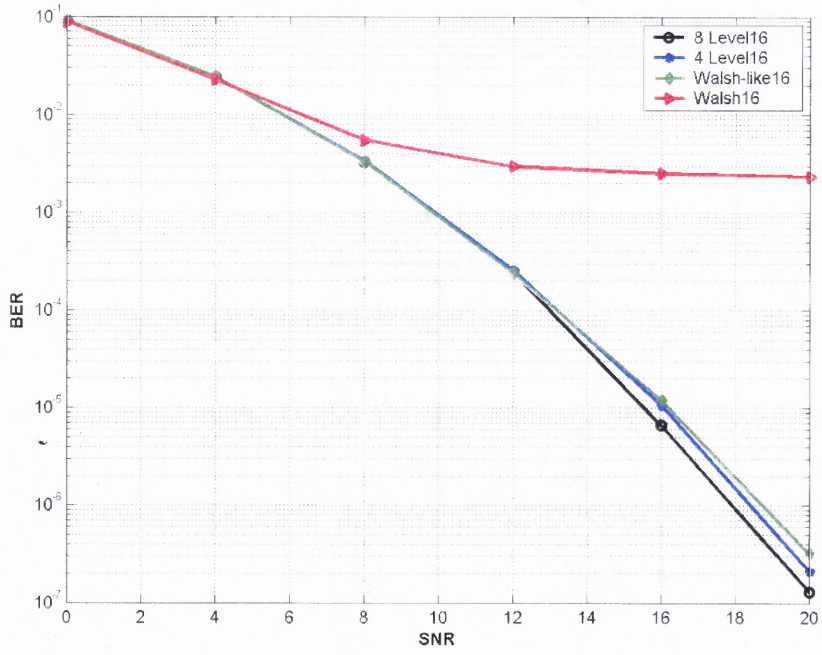

Figure 6.3 BER performances for proposed 16-length, 4-level and 8-level code sets, binary Walsh-like and Walsh code sets in asynchronous AWGN channel for 2-user case.

At short code lengths, BER performance improvement with increasing the chip levels and keeping the code length fixed is observed more clearly. Figure 6.4 displays the BER performance of different multiple level code sets given in Table 6.5 for 6-length codes in a 2-user scenario. From Figure 6.4, it can be observed that BER performance improves as the number of chip values is increased up to a certain level and there after no significant improvement is observed. 11-level code set provides an improvement factor of about 3 dB at 10^{-4} BER. BER performance deteriorates beyond 11-level coding. Similar conclusions have been drawn while analyzing the maximum correlation values of Table 6.5 for multiple level 6-length code sets.

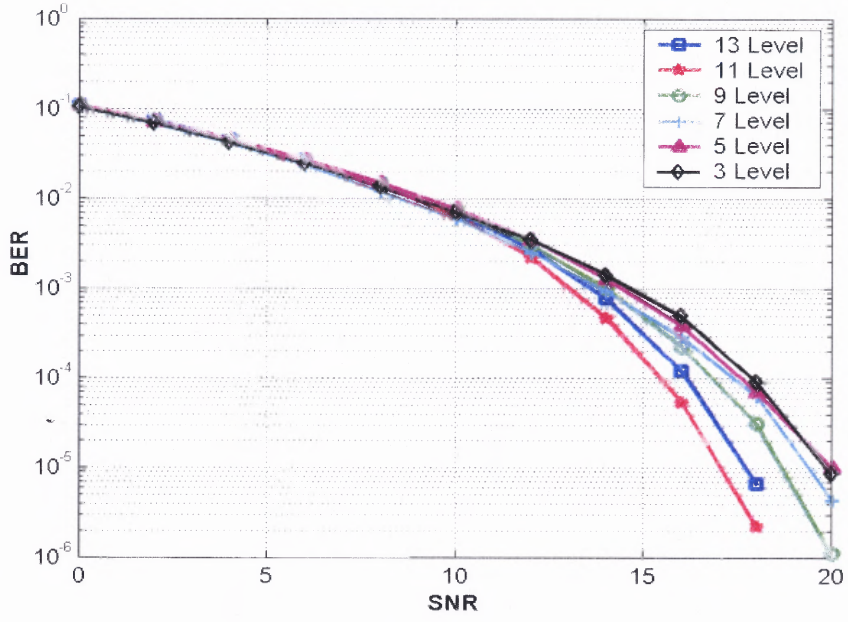

Figure 6.4 BER performances for proposed 6-length 3, 5, 7, 9, 11 and 13-level code sets in asynchronous AWGN channel for 2-user case.

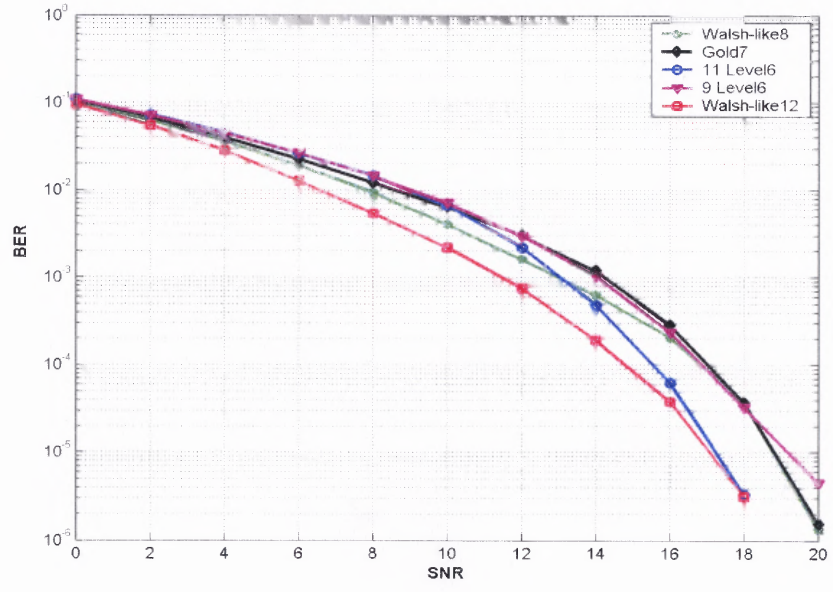

Figure 6.5 BER performances for proposed 6-length 9 and 11-level code sets along with binary 7-length Gold and 8 and 12-length Walsh-like code sets in asynchronous AWGN channel with 2-users.

Shorter length codes with higher number of chip values may perform as good as longer spreading codes with binary chip values. As a case in point, Figure 6.5 shows that BER performance of 9-level, 6-length codes closely matches with 2-level, 7-length Gold codes and performance of 11-level, 6-length codes matches with the performance of 2-level, 12-length binary Walsh-like codes at high SNRs.

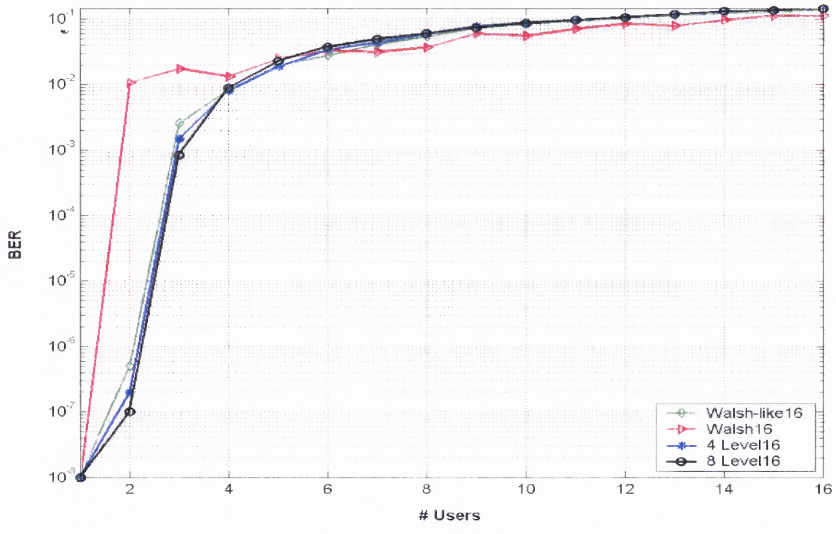

Figure 6.6 Multiuser BER performances for 16-length code sets with 4, 8 levels of coding along with binary Walsh-like and Walsh code sets in asynchronous AWGN channel evaluated at SNR=20 dB.

Figure 6.6 displays the multiuser performance of 16-length, 4 and 8-level varying power code sets along with 16-length Walsh-like and Walsh code sets in asynchronous environment as a function of number of users simulated at SNR=20 dB. As number of users increases, performances of all types of codes deteriorate due to increase in inter-code correlations and advantages of multiple level codes diminish. System performance can be improved by using decorrelator or MMSE type of receiver instead of a matched filter detector.

CHAPTER 7

VARYING POWER SPREAD SPECTRUM KLT CODES

The design and performance of binary and multiple valued orthogonal integer code sets are discussed in the previous chapters. All of those code sets were generated using exhaustive computer search method within the predefined sample space. In this chapter, an analytical method to generate multiple and real valued orthogonal code sets with varying power property and their performance characteristics are presented.

7.1 Karhunen-Loeve Transform (KLT) Basics

Let $\{s(n)\}$ be the n-length discrete-time signal satisfying the DTFT pair relation $s(n) \leftrightarrow S(e^{j\omega})$.

Input covariance matrix for signal $\{s(n)\}$ is expressed as

$$\mathbf{R}_s = E\{\mathbf{s}\mathbf{s}^T\} \tag{7.1}$$

where $E[\ ]$ is the expectation operator.

KLT which is the optimal block transform for the given input covariance matrix $\mathbf{R}_s$ has the unique property [8, 64, 65],

$$R_s A^T = A^T \Lambda \tag{7.2}$$

where $\Lambda = diag(\sigma_0^2, \sigma_1^2, \cdots\cdots, \sigma_{N-1}^2)$ and A is orthonormal transform satisfying

$$A^T A = \delta(n) \tag{7.3}$$

With this transformation, covariance matrix for the spectral coefficient vector is diagonal and is defined as

$$R_\theta = AR_s A^T = AA^T \Lambda \tag{7.4}$$

The maximum possible energy compaction of a $N \times N$ unitary transform, so called gain of transform coding over pulse code modulation (G_{TC}), is defined as [8]

$$G_{TC}^N = \frac{\frac{1}{N}\sum_{k=0}^{N-1}\sigma_k^2}{\left(\prod_{k=0}^{N-1}\sigma_k^2\right)^{1/N}} \tag{7.5}$$

where $\{\sigma_k^2\}$ are the diagonal elements of Λ.

G_{TC} value goes down to one whenever the input power spectrum is of white. At small values of G_{TC}, transform domain processing and coding of the input signal does not bring any improvements over the time domain pulse code modulation (PCM) coding. In contrast, G_{TC} value is higher than 1 whenever the input spectrum has uneven energy distribution. In such cases, transform domain coding brings performance improvements over PCM coding. This metric has been widely used in the source coding field to rank and compare the energy repacking performance of orthogonal transforms for the given input signal spectrum.

Design examples for generating orthogonal spread spectrum *KLT* code sets with varying power basis functions that are eigen-vectors for a known covariance matrix R_s or power spectral density function are explained in the next section. Variety of power spectrum signal models like auto-regressive *(AR)* and auto-regressive moving average *(ARMA)* can be used as input signal statistics in the design of spread spectrum *KLT* code sets.

7.2 Spread Spectrum KLT Design Examples

7.2.1 *AR(1)* Source Model

As a first example to highlight the proposed design method, auto-regressive order one $AR(1)$ source model is considered and is defined as [8, 66]

$$s(n) = \rho s(n-1) + \eta(n) \tag{7.6}$$

where $\eta(n)$ is a zero mean, unit variance white noise, and the correlation coefficient is in the range of $-1 < \rho < 1$.

For the white noise,

$$E\{\eta(n)\eta(n+k)\} = (1-\rho^2)\delta(k) \tag{7.7}$$

where $\delta(k) = \begin{cases} 1 & k = 0 \\ 0 & otherwise \end{cases}$

Auto-correlation sequence for this discrete-time random signal is expressed as

$$R_s(k) = \rho^{|k|} \text{ for } k = 0, \pm 1, \pm 2, \ldots \tag{7.8}$$

and its covariance matrix is defined as

$$R_s = \begin{bmatrix} 1 & \rho & \rho^2 & \cdots & \rho^{N-1} \\ \rho & 1 & \rho & \cdots & \rho^{N-2} \\ \rho^2 & \rho & 1 & \cdots & \rho^{N-3} \\ \vdots & \vdots & \vdots & \cdots & \vdots \\ \rho^{N-1} & \rho^{N-2} & \rho^{N-3} & \cdots & 1 \end{bmatrix} \tag{7.9}$$

Eigen-values for this covariance matrix, for N even, are given by [8]

$$\sigma_k^2 = \lambda_k = \frac{1-\rho^2}{1-2\rho Cos\omega_k + \rho^2}, \quad 0 \le k \le N\text{-}1 \tag{7.10}$$

where $\{\omega_k\}$ values are the positive roots of the polynomial

$$tan(N\omega_k) = \frac{(1-\rho^2)Sin\omega_k}{Cos\omega_k - 2\rho + \rho Cos\omega_k} \tag{7.11}$$

and the resulting KLT matrix of size $N \times N$ is calculated as

$$\mathbf{A}(k,n) = \frac{2}{N+\sigma_k^2} Sin\left[\omega_k (n - \frac{N-1}{2}) + \frac{(k+1)\pi}{2}\right], 0 \le k, n \le N-1 \tag{7.12}$$

Therefore, maximum energy compaction measure for this input signal model can be expressed as [8]

$$G_{KLT}^{N} = \frac{1}{\prod_{k=0}^{N-1}\left(\frac{1-\rho^2}{1-2\rho Cos\omega_k + \rho^2}\right)^{1/N}} \tag{7.13}$$

with the upper bound value, as $N \to \infty$,will be

$$G_{KLT}^{\infty} = \frac{\frac{1}{2\pi}\int_{-\pi}^{\pi} S_s(e^{j\omega})d\omega}{\exp\left\{\frac{1}{2\pi}\int_{-\pi}^{\pi} \ln[S_s(e^{j\omega})]d\omega\right\}} \tag{7.14}$$

where

$$S_s(e^{j\omega}) = \sum_{k=-\infty}^{\infty} R_s(k)e^{-j\omega k} \tag{7.15}$$

For white noise, $\rho = 0$ *and* $G_{KLT}^{\infty} = 1$ and coding gain is not achieved with transform coding over the signal domain coding.

Figure 7.1 displays energy compaction (G_{TC}^{8}) performance of 8-length KLT codes designed for $AR(1)$ source model as a function of correlation coefficient ρ. Figure 7.2 shows corresponding power spectral density function for $AR(1)$ source model with different ρ values. It is well known that several source coding applications like speech and image require $\rho > 0.8$. In this correlation region, the discrete cosine transform (DCT), a fixed transform successfully used in image and video compression standards

matches very closely with that of the optimum performance achieved using KLT. From Figure 7.2, it is observed that in the region where $\rho < 0.5$, power spectral density is more uniformly spread.

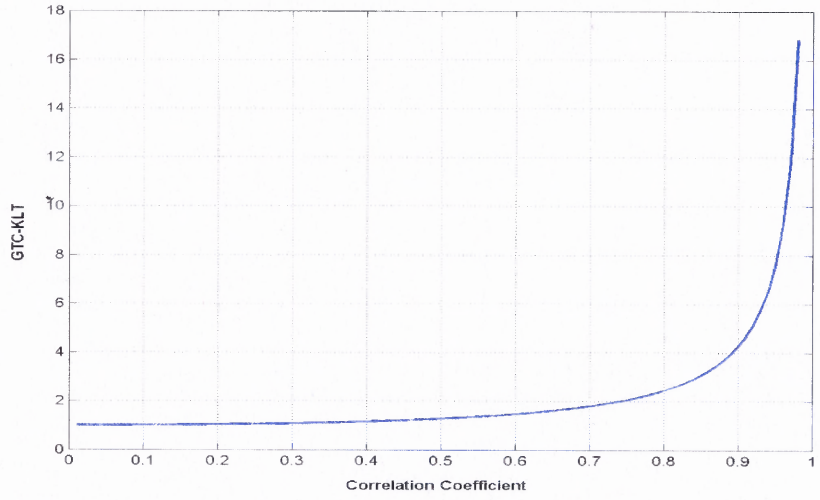

Figure 7.1 Energy compaction (G_{TC}^{8}) performance of 8-length KLT designed with $AR(1)$ source model as a function of its correlation coefficient.

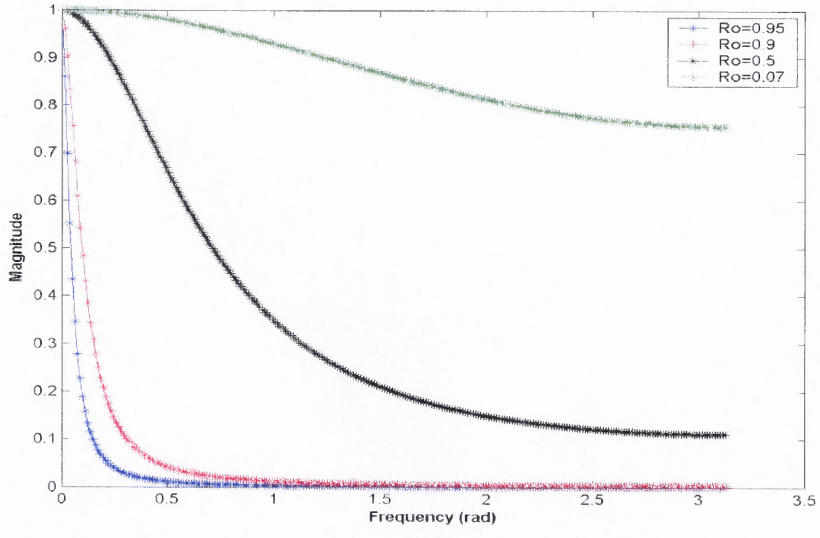

Figure 7.2 Power spectral density function for various $AR(1)$ source models.

7.2.2 Modeling from Power Spectral Density

As second example, a known spread spectrum power spectral density (PSD) function is considered and modeled as *AR* process [66]. Normalized auto-correlation sequence is generated from the power spectral density function using inverse Fourier transform (IFT). Furthermore, covariance matrix and the corresponding eigen-values and vectors are generated. Figure 7.3 shows the sample power spectral density function used and Figure 7.4 displays the corresponding auto-correlation sequence.

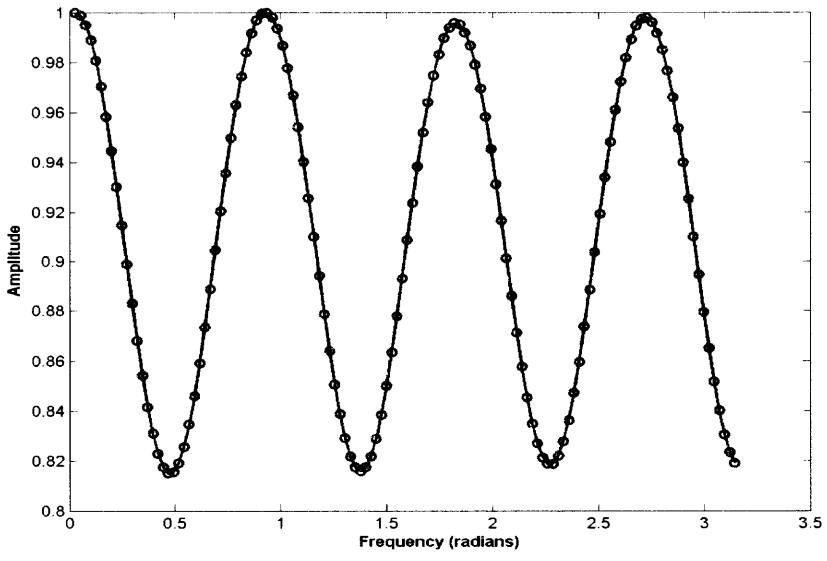

Figure 7.3 Power spectral density (PSD) function used for the generation of 8×8 spread spectrum *KLT* codes.

For higher code lengths, auto-correlation sequences and power spectral density (PSD) functions are generated in a reverse manner. Normalized auto-correlation sequence is obtained from any of the sequences of standard Gold or Walsh-like code sets and subsequently covariance matrix is formed. PSD function is generated from the auto-correlation sequence. This PSD function in turn can also be modeled as an *ARMA* sequence for generating other spread spectrum *KLT* codes.

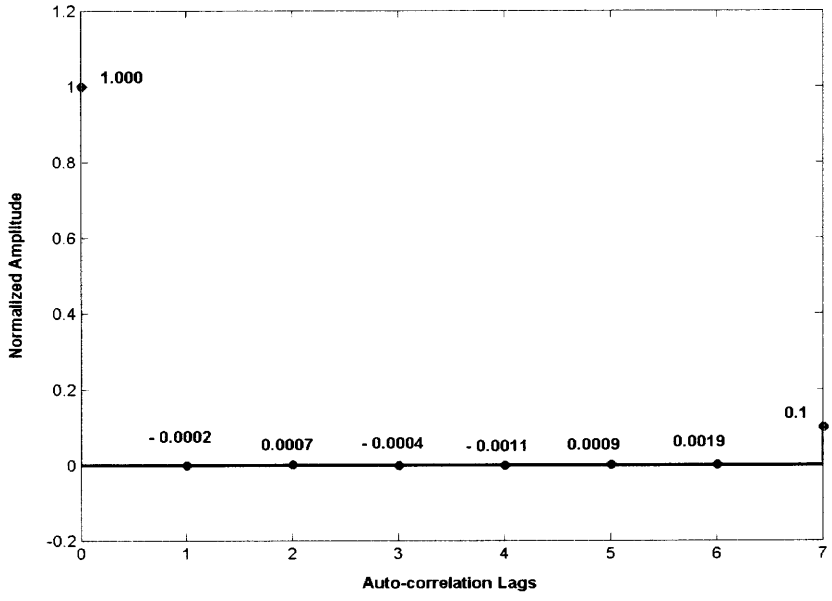

Figure 7.4 Auto-correlation sequence generated from the PSD plotted in Figure 7.3.

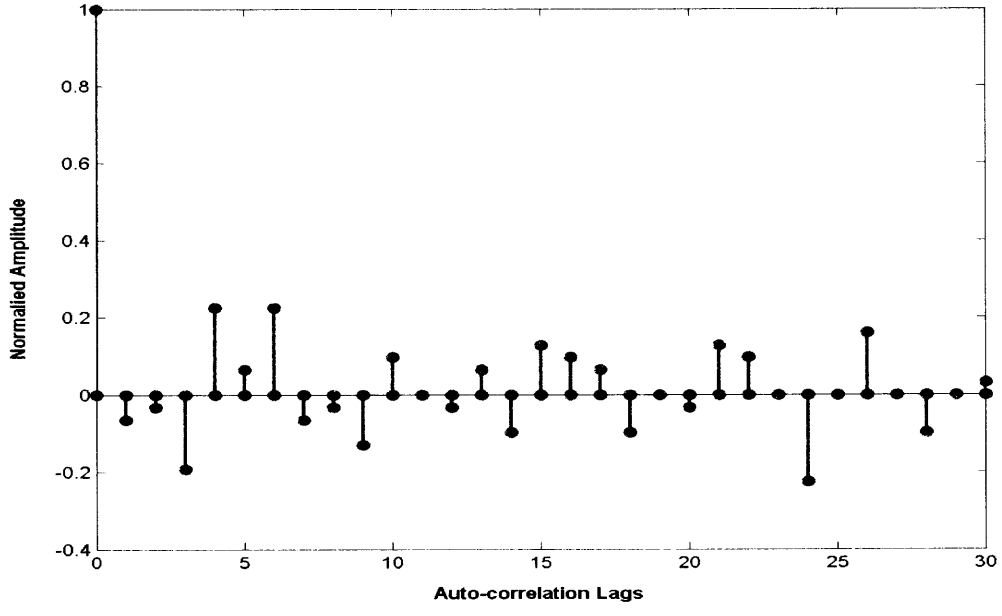

Figure 7.5 A typical auto-correlation sequence obtained from a 31-length Gold code sequence.

For example, typical 31-length Gold code is given in Equation (7.16) and its normalized auto-correlation sequence is shown in Equation (7.17). Auto-correlation sequence is plotted in Figure 7.5 and the corresponding power spectral density function is plotted in Figure 7.6.

$$\begin{bmatrix} -1 & 1 & 1 & -1 & -1 & 1 & 1 & 1 & -1 & -1 & -1 & -1 & 1 & -1 & -1 & -1 \\ -1 & -1 & 1 & -1 & 1 & -1 & 1 & -1 & 1 & -1 & -1 & 1 & 1 & -1 & -1 & \end{bmatrix} \tag{7.16}$$

$$\begin{bmatrix} 1.0000 & -0.0645 & -0.0323 & -0.1935 & 0.2258 & 0.0645 & 0.2258 & -0.0645 \\ -0.0323 & -0.1290 & 0.0968 & 0.0000 & -0.0323 & 0.0645 & -0.0968 & 0.1290 \\ 0.0968 & 0.0645 & -0.0968 & 0.0000 & -0.0323 & 0.1290 & 0.0968 & 0 \\ -0.2258 & 0 & 0.1613 & 0 & -0.0968 & 0.0000 & 0.0323 & \end{bmatrix} \tag{7.17}$$

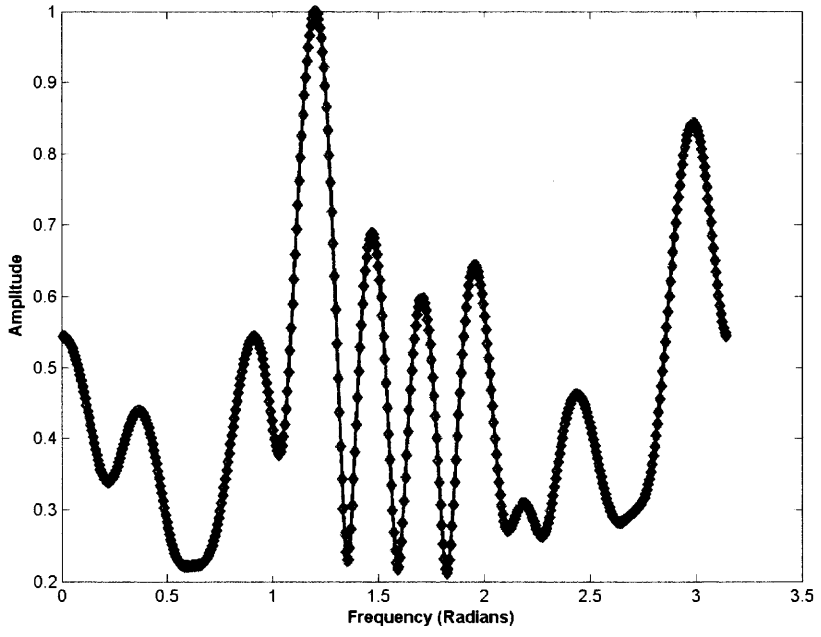

Figure 7.6 Power spectral density function for the auto-correlation sequence plotted in Figure 7.5.

Covariance matrix and eigen-vectors are generated from this auto-correlation sequence. Normalized correlation sequences can also be obtained from taking cross-correlation sequence of two code sequences and substituting the value 1 at zero delay position. An important criterion is that the resulting correlation sequence should be well spread in time and frequency domains to give good BER performance.

Similarly, Equations (7.18) and (7.19) are two typical 31-length Gold code sequences considered for generating the correlation sequence and Equation (7.20) is their corresponding correlation sequence.

$$\text{Code1}=\begin{bmatrix} -1 & 1 & 1 & -1 & -1 & 1 & 1 & 1 & -1 & -1 & -1 & -1 & 1 & -1 & -1 & -1 \\ -1 & -1 & 1 & -1 & 1 & -1 & 1 & -1 & 1 & -1 & -1 & 1 & 1 & -1 & -1 & \end{bmatrix} \quad (7.18)$$

$$\text{Code2}=\begin{bmatrix} 1 & -1 & 1 & 1 & 1 & -1 & -1 & -1 & -1 & -1 & 1 & -1 & 1 & 1 & 1 & -1 \\ -1 & -1 & 1 & 1 & 1 & 1 & -1 & -1 & -1 & -1 & 1 & 1 & 1 & -1 & 1 & \end{bmatrix} \quad (7.19)$$

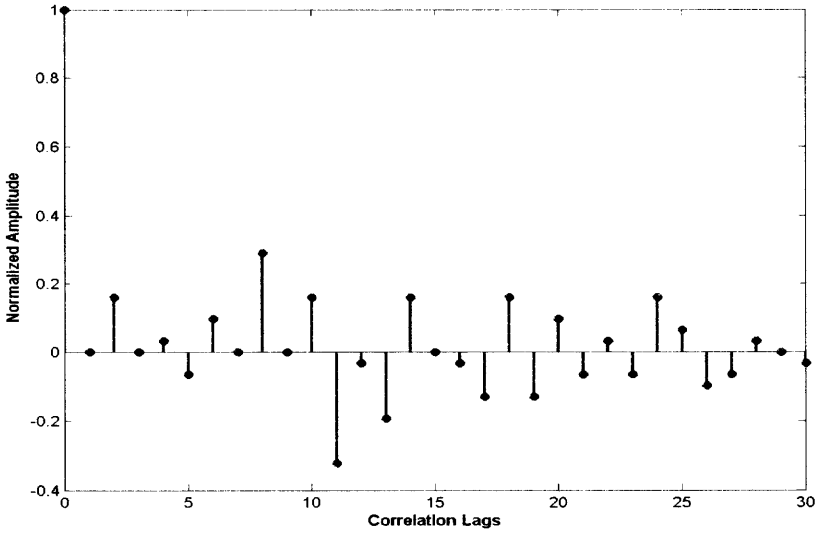

Figure 7.7 A typical correlation sequence obtained from the cross-correlation of two 31-length Gold code sequences.

Figure 7.7 displays the correlation sequence obtained from cross-correlation of these two Gold sequences and Figure 7.8 shows the corresponding power spectral density.

$$\begin{bmatrix} 1.0000 & -0.0000 & 0.1613 & 0.0000 & 0.0323 & -0.0645 & 0.0968 & -0.0000 \\ 0.2903 & -0.0000 & 0.1613 & -0.3226 & -0.0323 & -0.1935 & 0.1613 & 0 \\ -0.0323 & -0.1290 & 0.1613 & -0.1290 & 0.0968 & -0.0645 & 0.0323 & -0.0645 \\ 0.1613 & 0.0645 & -0.0968 & -0.0645 & 0.0323 & 0.0000 & -0.0323 & \end{bmatrix} \quad (7.20)$$

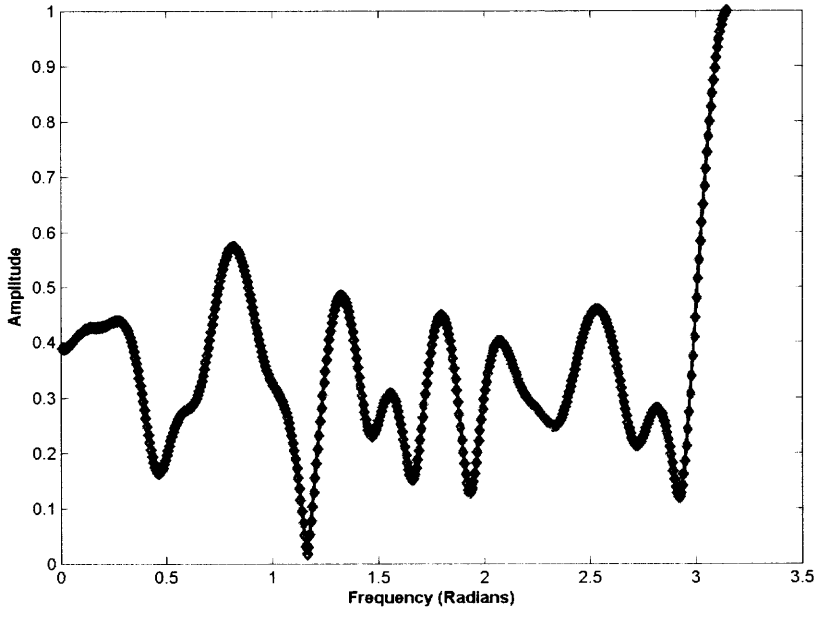

Figure 7.8 Power spectral density function for the correlation sequence plotted in Figure 7.7.

Different covariance matrices and in turn different eigen-vectors can be obtained by utilizing correlation sequences of different Gold / Walsh-like sequences. Similar procedure can be applied for generating spread spectrum *KLT* codes of any desired length. In the next section, performance characteristics of different types of *KLT* codes are discussed.

7.3 Performance Characteristics of Varying Power Spread Spectrum KLT Codes

7.3.1 Bit Error Rate (BER) Performance Comparisons in AWGN Channels

BER performance of 8-length spread spectrum *KLT* code sets designed by using $AR(1)$ model discussed in Section 7.2 is simulated for 2-user case in asynchronous communication channel under AWG noise environment. BER performance is averaged over all possible pairs of codes and for all possible delays and compared with the industry standard spreading codes.

Simulations have shown that spread spectrum *KLT* row vectors rather than column vectors give better BER performance. This is due to the fact that row functions are more spread in frequency domain than column functions. Figure 7.9 and 7.10 display the magnitude response functions of the column and row vectors of 8×8 spread spectrum *KLT* codes generated using $AR(1)$ method. This is a valid observation for all the types of *KLT* codes considered in this dissertation.

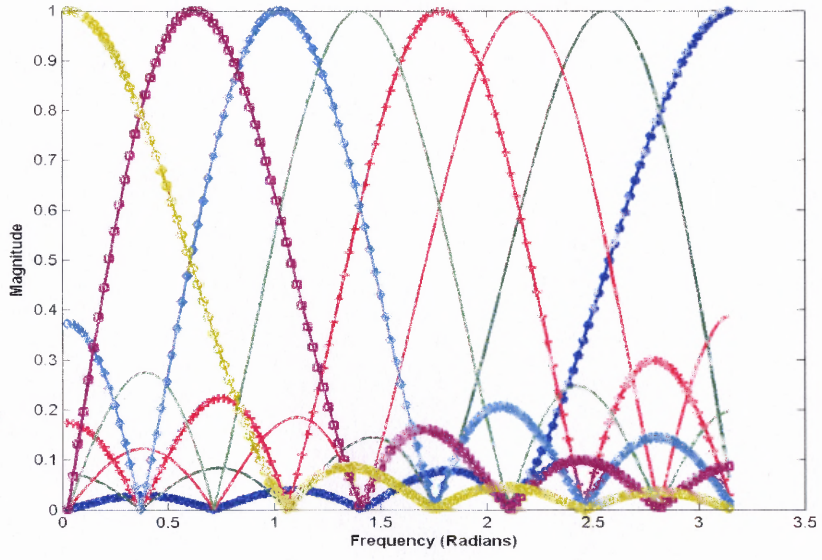

Figure 7.9 Magnitude response functions of the column vectors of 8×8 spread spectrum *KLT* codes generated using AR (1) model with $\rho = 0.07$.

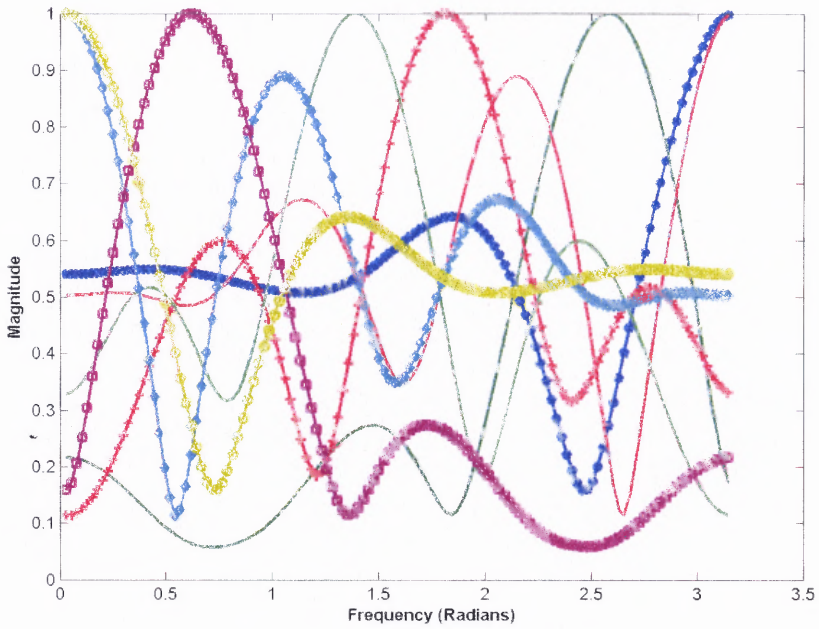

Figure 7.10 Magnitude response functions of the row vectors of 8×8 spread spectrum *KLT* codes generated using *AR* (1) model with $\rho = 0.07$.

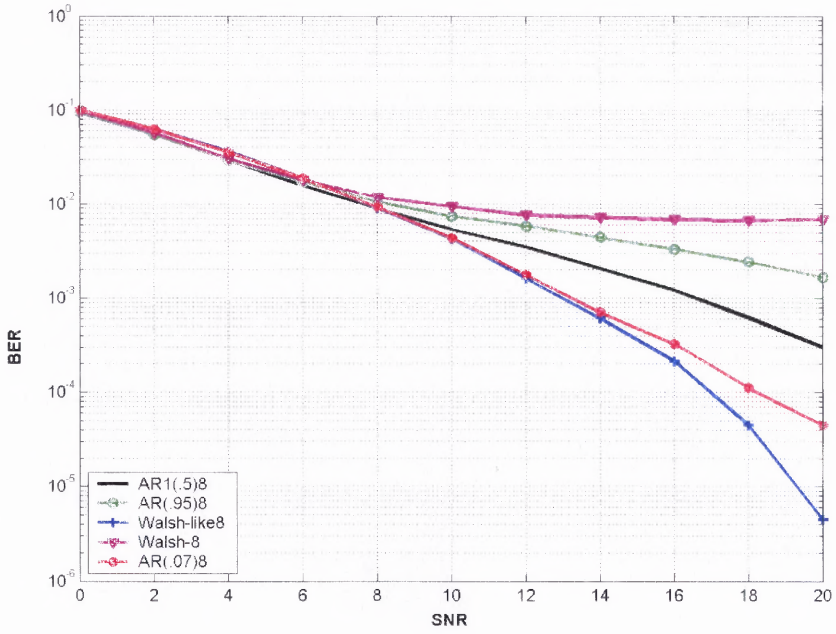

Figure 7.11 BER performances of 8-length Walsh, Walsh-like and different *AR*(1) model spread spectrum *KLT* code sets for asynchronous AWGN channel with two users.

Figure 7.11 displays the BER cures of 8-length orthogonal *KLT* code sets generated with $AR(1)$ model with auto-correlation coefficients of $\rho = 0.07$, 0.5 and 0.9 along with 8-length Walsh-like and Walsh code sets. It is observed from Figure 7.11 that, BER performances of $AR(1)$ source model based *KLT* code sets improve as the auto-correlation value decreases. This is due to the fact that at lower values of auto-correlation, power spectrum is whiter resulting in better spread basis functions. On the other hand, BER performances of all $AR(1)$ model based spread spectrum *KLT* codes considered are inferior to binary Walsh-like codes, implying that higher order AR models are needed for better performance.

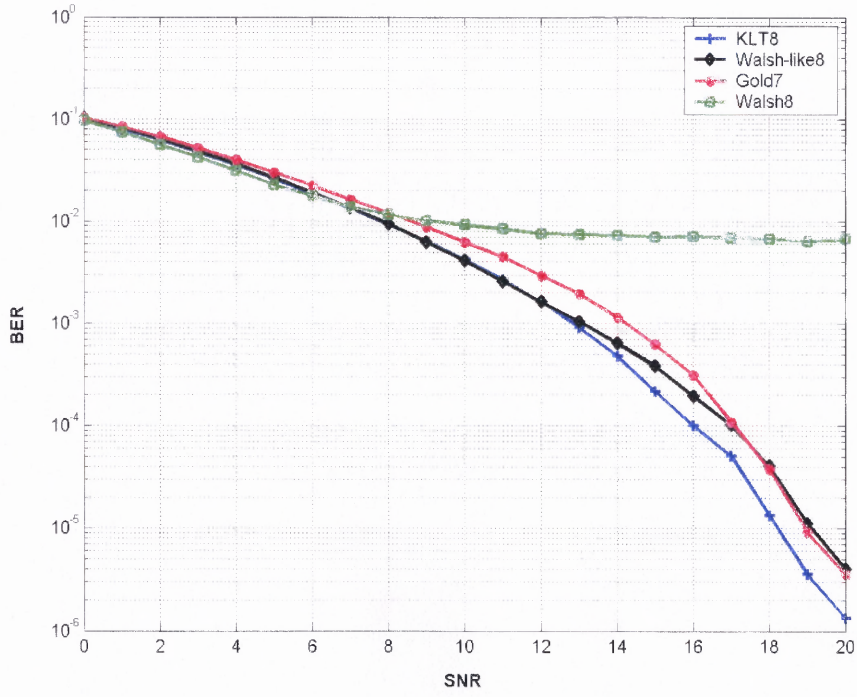

Figure 7.12 BER performances of 8-length spread spectrum *KLT*, Walsh, Walsh-like and 7-length Gold code sets for asynchronous AWGN channel with two users.

BER performance of 8-length spread spectrum *KLT* code set derived from the auto-correlation sequence plotted in Figure 7.4 is displayed in Figure 7.12. For comparison purposes, BER performances of 8-length Walsh-like and Walsh code sets along with 7-length Gold code sets are also displayed. Performance of multiple level 8-length KLT codes is better than Walsh-like and other binary codes. Table 7.1 lists typical 8-length spread spectrum *KLT* basis vectors. *KLT* basis elements shown in the Table 7.1 are real and have a minimum of 4 decimal positions. It is not practically feasible to choose basis elements with such accuracy. Even by rounding the basis elements to only two decimal digits, negligible performance degradation is observed.

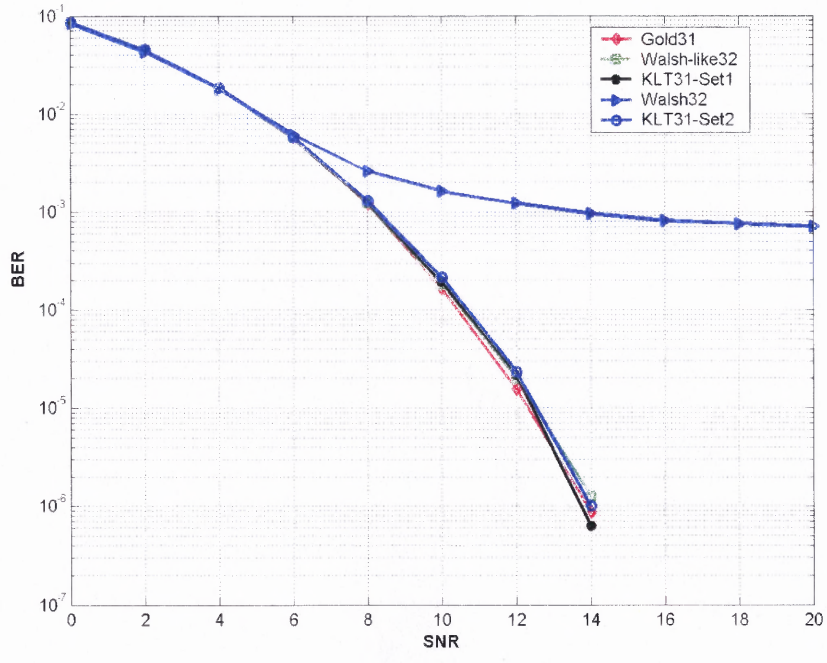

Figure 7.13 BER curves of two 31-length spread spectrum *KLT*, Gold and 32-length Walsh, Walsh-like code sets for asynchronous AWGN channel with two users.

Table 7.1 Typical 8-Length Spread Spectrum *KLT* Values

Spreading Codes	Eigen Vector 1	Eigen Vector 2	Eigen Vector 3	Eigen Vector 4	Eigen Vector 5	Eigen Vector 6	Eigen Vector 7	Eigen Vector 8
1	0.7071	0.0026	0.0038	0.0006	-0.0016	0.0007	0.0009	-0.7071
2	0.0030	-0.5245	-0.3377	0.1579	0.4722	0.0432	-0.6009	-0.0024
3	0.0003	0.3093	-0.5463	0.2501	0.3894	-0.5027	0.3727	-0.0023
4	-0.0010	0.3595	0.2958	0.6423	0.3540	0.4954	0.0025	0.0021
5	0.0010	-0.3595	0.2958	0.6423	-0.3540	-0.4954	0.0025	0.0021
6	-0.0003	-0.3093	-0.5463	0.2501	-0.3894	0.5027	0.3727	-0.0023
7	-0.0030	0.5245	-0.3377	0.1579	-0.4722	-0.0432	-0.6009	-0.0024
8	-0.7071	-0.0026	0.0038	0.0006	0.0016	-0.0007	0.0009	-0.7071

Figure 7.13 displays the BER performances of both 31-length *KLT* codes discussed in Section 7.2.2 along with standard 31-length Gold, 32-length Walsh-like and Walsh code sets. Performances of both spread spectrum *KLT* codes far exceed that of Walsh codes and closely match with Gold codes and Walsh-like codes performance at all SNRs. Advantage of *KLT* codes is that number of such independent code sets can be generated using eigen value methods. By extending the design method to *ARMA* methods, innumerable design solutions are available and this is a topic of future studies.

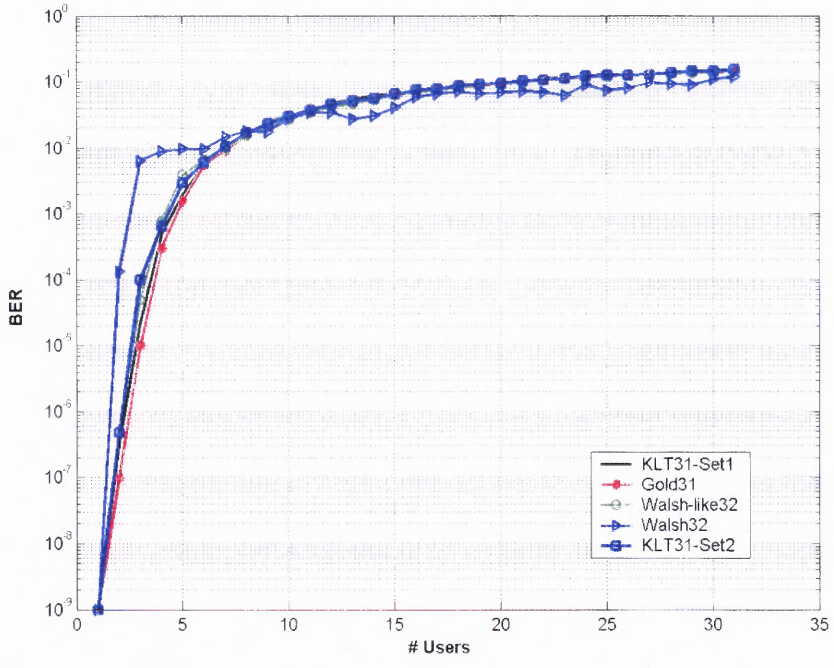

Figure 7.14 Multiuser BER performance curves of two 31-length spread spectrum *KLT*, Gold and 32-length Walsh, Walsh-like code sets for asynchronous AWGN channel evaluated at SNR=20 dB.

Multiuser BER performances are simulated for the two 31-length spread spectrum *KLT* codes at SNR=20 dB in AWG noise and is displayed in Figure 7.14 as a function of the number of users. For comparison purposes, multiuser performances of comparable length Gold, Walsh-like and Walsh code sets are also displayed.

From Figure 7.14, it is observed that at higher number of users, performances of all types of codes considered are the same and they are poor. Other processing methods like decorrelator or MMSE receiver need to be incorporated at the receiver in order to improve the BER performance in a multiuser scenario.

7.3.2 Time-Frequency Localization

Time and frequency spreads (σ_n^2) and (σ_ω^2) for the basis functions are calculated for both 31-length spread spectrum *KLT* codes, Gold codes and 32-length Walsh-like, Walsh code sets according to Equations (3.4) and (3.5) and they are plotted in Figure 7.15. It is observed that Gold, Walsh-like and *KLT* codes have similar (σ_ω^2) values, explaining their similarity in BER performance. Walsh codes have smaller (σ_ω^2) value, indicating their poor performance in asynchronous communication channel. Binary level codes have constant time spread (σ_n^2) as they have fixed power level where as multiple valued spread spectrum *KLT* codes have variable (σ_n^2) values.

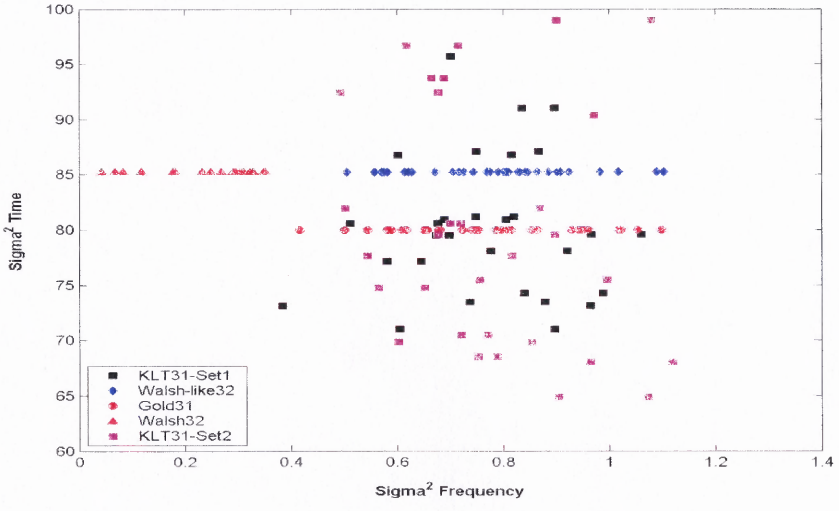

Figure 7.15 Time-frequency localizations for two 31-length spread spectrum *KLT*, Gold and 32-length Walsh-like, Walsh code sequences.

CHAPTER 8

KRONECKER PRODUCT (HYBRID) INTEGER CODES IN MULTIPLE STAGE ORTHOGONAL TRANSMULTIPLEXERS

Different types of orthogonal code sets proposed in the previous chapters, namely, fixed power binary, varying power multiple level integer codes and spread spectrum *KLT* codes with real values are all of fixed length. Multiple stage orthogonal transmultiplexer structures help to better understand the mathematical foundations for generating Kronecker product or hybrid codes by taking product of two or more code families.

In this chapter, two unique applications employing multiple stage orthogonal transmultiplexers are proposed. First application is, to generate Kronecker product codes for two or higher number of code families of any type or any length. These Kronecker product code sequences are judiciously allotted to users based on their correlation properties to improve overall BER performance in a multiuser system. Second application is to allot a number of hybrid codes to each user as redundant spreading codes in a CDMA environment in order to improve the detection performance particularly at low SNR channels. Design concepts and performance improvements with these proposed applications are discussed in the following sections,

8.1 Multiple Stage Orthogonal Transmultiplexer Theory

8.1.1 Kronecker Product Codes

Let $A=\left[a_{ij}\right]$ be an $n\times n$ matrix and let B be an $m\times m$ matrix. Then, the Kronecker matrix product of A and B is an $mn\times mn$ block matrix equal to [16, 67]

$$Hybrid\ Code = A \otimes B = \begin{bmatrix} a_{11}B & a_{12}B & \dots & a_{1n}B \\ a_{21}B & a_{22}B & \dots & a_{2n}B \\ \dots & \dots & \dots & \dots \\ a_{n1}B & a_{n2}B & \dots & a_{nn}B \end{bmatrix} \tag{8.1}$$

where the notation $\otimes$ indicates the Kronecker matrix product operator.

Note that the Walsh transform of size $N = 2^m$ is obtained by applying Kronecker product operation on the 2×2 kernel matrix, m times as [16]

$$H_1 = \frac{1}{\sqrt{2}}\begin{bmatrix} 1 & 1 \\ 1 & -1 \end{bmatrix} \quad , H_N = \frac{1}{\sqrt{2}}\begin{bmatrix} H_{N-1} & H_{N-1} \\ H_{N-1} & -H_{N-1} \end{bmatrix} = H_1 \otimes H_{N-1} \tag{8.2}$$

For Walsh code generation, both matrices A and B are of binary in nature and resulting in hybrid code of binary type.

8.1.2 Relationship between Multiple Stage Transmultiplexer and Kronecker Product Codes

The mathematical relationship between multiple stage orthogonal transmultiplexer and Kronecker product code operation can be easily shown by taking an example and deriving the resulting codes from both methods.

Kronecker product of 4-length Walsh sequence $A_{4\times4}$ and 2-length Walsh sequence $B_{2\times2}$ is calculated as follows.

$$A = \begin{bmatrix} 1 & 1 & 1 & 1 \\ 1 & 1 & -1 & -1 \\ 1 & -1 & -1 & 1 \\ 1 & -1 & 1 & -1 \end{bmatrix}, \quad B = \begin{bmatrix} 1 & 1 \\ 1 & -1 \end{bmatrix}$$

$$A \otimes B = \begin{bmatrix} 1 & 1 & 1 & 1 & 1 & 1 & 1 & 1 \\ 1 & -1 & 1 & -1 & 1 & -1 & 1 & -1 \\ 1 & 1 & 1 & 1 & -1 & -1 & -1 & -1 \\ 1 & -1 & 1 & -1 & -1 & 1 & -1 & 1 \\ 1 & 1 & -1 & -1 & -1 & -1 & 1 & 1 \\ 1 & -1 & -1 & 1 & -1 & 1 & 1 & -1 \\ 1 & 1 & -1 & -1 & 1 & 1 & -1 & -1 \\ 1 & -1 & -1 & 1 & 1 & -1 & -1 & 1 \end{bmatrix} \tag{8.3}$$

For a two-stage orthogonal transmultiplexer, equivalent diagrams are shown in Figure 8.1 with 4-length Walsh sequence $A_{4\times4}$ as $H_0(z)$ matrix and 2-length Walsh sequence $B_{2\times2}$ as $H_1(z)$ matrix [8].

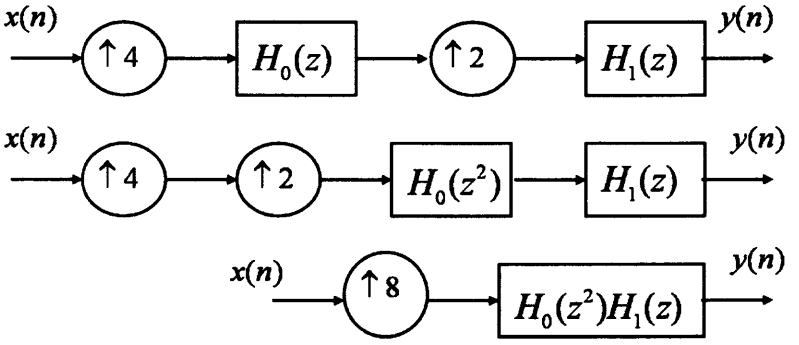

Figure 8.1 Equivalent structures for two-stage orthogonal transmultiplexer.

First row of $H_0(z)$ matrix is $1+z^{-1}+z^{-2}+z^{-3}$ and first row of $H_1(z)$ is $1+z^{-1}$. $H_0(z^2)$ in the 3rd equivalent structure is represented by the polynomial $1+z^{-2}+z^{-4}+z^{-6}$. Product $H_0(z^2)$ and first row of $H_1(z)$ gives $1+z^{-1}+z^{-2}+z^{-3}+z^{-4}+z^{-5}+z^{-6}+z^{-7}$ which is same

polynomial as the first row of Kronecker product in Equation (8.2). Product of $H_0(z^2)$ and second row of $H_1(z)$, which is $1-z^{-1}$, gives $1-z^{-1}+z^{-2}-z^{-3}+z^{-4}-z^{-5}+z^{-6}-z^{-7}$ polynomial same as second row of Kronecker product in Equation (8.2). Similarly, other rows of Kronecker product are obtained by the multiplication of other rows of $H_0(z)$ matrix with $H_1(z)$ matrix.

Hence, mathematical operations of either multiple stage orthogonal transmultiplexer structure or Kronecker product operation can be used for generating hybrid codes.

8.2 Hybrid Spreading Codes

8.2.1 Generation of Hybrid Spreading Codes

Hybrid integer code sets are generated by taking Kronecker matrix product of two orthogonal code matrices A and B of any type (binary or multiple level), without any restriction on their code lengths. In addition, these code matrices need not belong to the same code family. For example, code matrix A can be a Walsh code set and B can be Walsh-like code set. In this section, binary Walsh-like and multiple level orthogonal code families designed in the previous chapters are used as matrix A and Walsh code set is used as matrix B. Values in Table 5.4 and 5.5 indicate that Walsh code sets have low sum of square of cross-correlation values where as Walsh-like code sets have lower maximum cross-correlation values. Kronecker product codes generated using such codes families give better performance results than the standard single family codes.

8.2.2 Hybrid Spreading Codes Assignment to Users

Spreading codes generated with Kronecker product method have to be judiciously allocated to different users in order to take advantage of resulting low cross-correlation values among certain code pairs.

Figure 8.2 displays block diagram of a two-stage orthogonal transmultiplexer for the 32-length hybrid codes generated using 4-level, 4-length integer codes as stage 1 codes ($A_{4\times4}$) and binary 8-length Walsh codes as stage 2 codes ($B_{8\times8}$). Input data is up-sampled first by four and convolved with the first stage spreading code. Then the data is further up- sampled by eight and convolved with the second stage spreading code to generate the final hybrid code set.

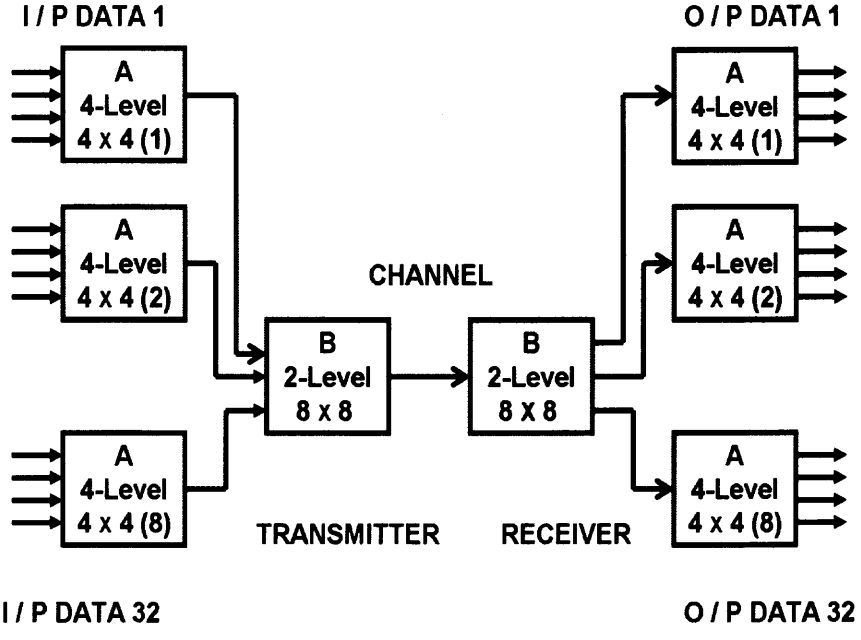

Figure 8.2 A two-stage orthogonal transmultiplexer for the generation of 32-length hybrid spreading codes.

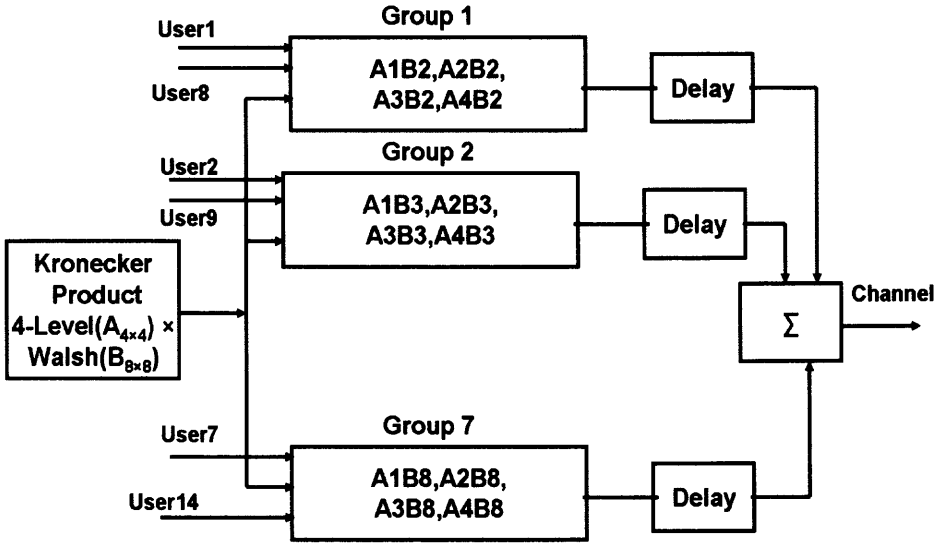

Figure 8.3 Block diagram for generating 32-length Kronecker product (hybrid) code set by using 4-level, 4-length varying power code set and binary, 8-length Walsh code sets along with their groupings.

Figure 8.3 displays the block diagram for the generation and rearrangement of 32-length hybrid codes for spread spectrum application. The first Walsh code, constant sequence in the set, is not considered for hybrid code set generation. Hybrid product codes obtained from the Kronecker product of 2^{nd} Walsh code in the set with the 4-level code family are formed in *Group1*. Similarly, spreading codes obtained from the Kronecker product of 3^{rd} Walsh code with 4-level code family are stored in *Group2* and so on. Spreading code for *User1* is selected from *Group1*, spreading code for *User2* is selected from *Group2* and spreading code for *User7* is selected from *Group7*. For *User8*, code is selected once again from *Group1*, for *User9* from *Group2* and the process repeats.

After allocating these spreading codes to different users, data is spread and asynchronously combined over the multiuser communication channel. At the receiver, reverse operation is performed on the received data to recover the transmitted bits.

The reason for such a grouping is that codes in different groups have less cross-correlation values among themselves than the codes within the same group. Identifying the inter- and intra-code correlations of user codes in a library of codes will improve the overall performance of a multiuser communication system. This particular way of generation of hybrid spreading codes and allocating these codes to different users can be easily extended to any number of multiple stages of orthogonal transmultiplexers with dynamic spreading code allocation algorithm in a system. BER performance of hybrid code sets along with the performance of existing single code families are presented in the next section.

8.2.3 Bit Error Rate (BER) Performance Comparisons in AWGN Channels

Average BER performance for hybrid spreading codes of different lengths are simulated for multiuser environment under asynchronous AWG noise conditions.

Figure 8.4 displays BER performances of 32-length hybrid code set discussed in the previous section for the two cases of 7 and 14 users along with comparable 31-length Gold code set performance. Performance of hybrid codes with proper code assignment to different users is better than Gold codes performance for both 7 and 14 users in the system.

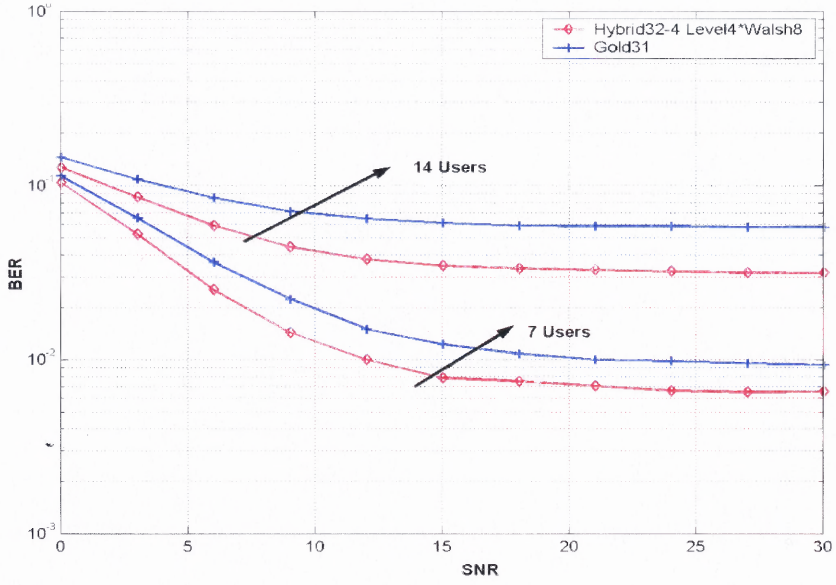

Figure 8.4 BER performance curves for 32-length Kronecker product (hybrid) and 31-length Gold code sets in asynchronous AWGN channel with 7 and 14 users.

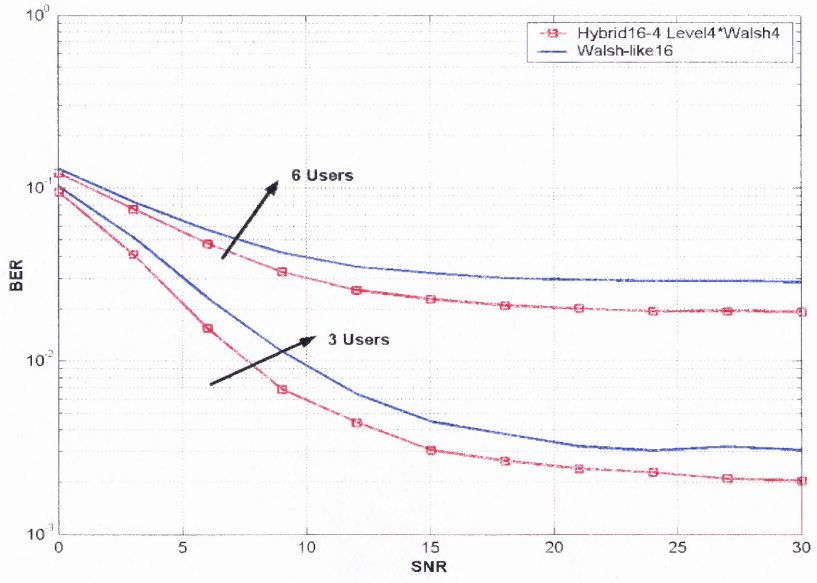

Figure 8.5 BER performance curves for 16-length Kronecker product (hybrid) and 16-length Walsh-like code sets in asynchronous AWGN channel with 3 and 6 users.

Similarly, Figure 8.5 displays BER performance of 16-length hybrid code set generated with the Kronecker product of 4-length, 4-level code and 4-length, binary Walsh code set for 3 and 6 users in asynchronous channel scenario. It is seen from Figure 8.5 that performance of the hybrid codes is much better than Walsh-like codes which in turn perform comparable to Gold codes and significantly outperform Walsh codes. In general, it can be concluded that the proposed hybrid codes clearly outperform Gold, Walsh and Walsh-like spreading code families for all lengths. This is another aspect that deserves further studies in the future.

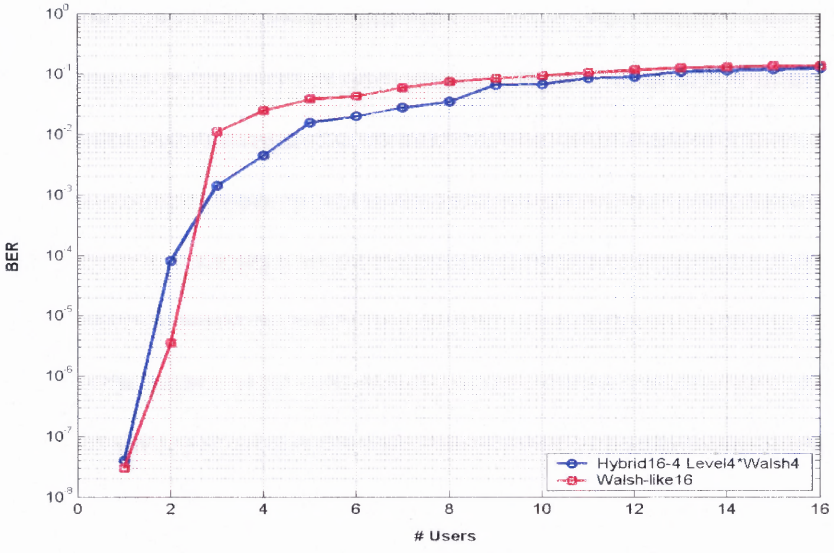

Figure 8.6 BER performance curves for 16-length Kronecker product (hybrid) and Walsh-like families at SNR=20 dB as a function of the number of users for asynchronous AWGN channel scenario.

Figure 8.6 displays the multiuser performance of 16-length hybrid codes and Walsh-like codes as a function of the number of users in the channel simulated at SNR=20 dB. Similarly, Figure 8.7 shows multiuser performance of 32-length hybrid and 31-length Gold codes at 20 dB SNR.

It is observed from these figures that existing code families perform marginally better than hybrid codes at smaller number of users in the system, but at higher number of users, hybrid codes outperform. Hence, the multiuser communication system performance might be improved by judiciously selecting orthogonal spreading codes based on number of users in the system. Moreover, dynamically changing user spreading codes will offer additional layer of system security and data integrity.

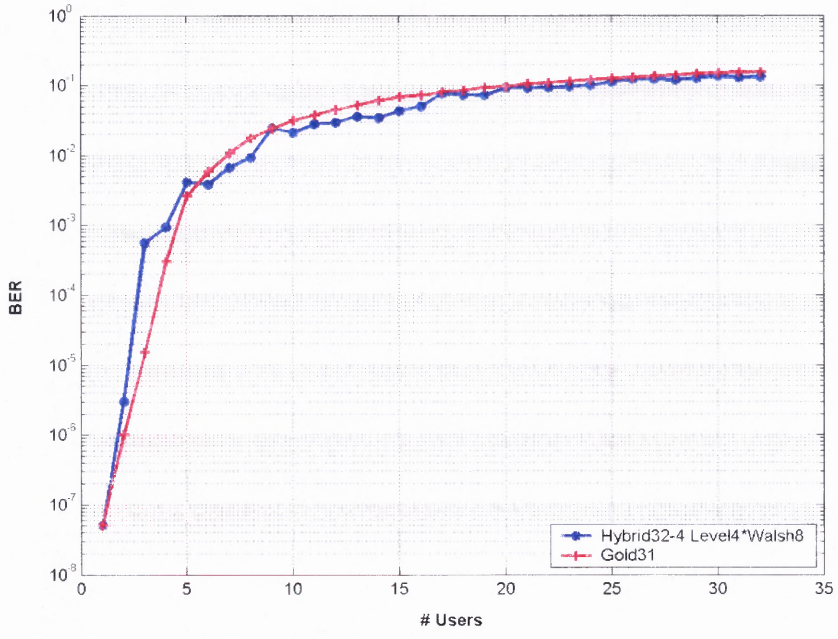

Figure 8.7 Multiuser BER performance curves for 32-length Kronecker product (hybrid) and 31-length Gold code sets at SNR=20 dB for asynchronous AWGN channel scenario.

8.3 Redundancy Codes in a Multiple Stage Orthogonal Transmultiplexer

8.3.1 Introduction

In CDMA communication, it is a common practice, to allot each user a unique code for spreading input data before its transmission. Data from different users is combined asynchronously over the channel. At the receiver of interest, corresponding spread

spectrum code is used for despreading and detection of data. As the number of users increases in the system, multiuser interference increases. Detectors at the receiver typically operate at a signal to noise plus interference ratios of the order of 5-10 dB. At lower signal to noise ratios, reliable detection is not possible.

Redundant (or repetition) coding has been used with different modulation techniques for improving channel performance under Rayleigh fading conditions. Data transmission is repeated over number of independent diversity channels and a combined decision is made at the receiver. One of the simplest methods of redundant coding used is time diversity method where transmitted data streams are repeated at different time intervals, hence independent channel states are maintained. In another method, independent channels are realized through data transmission with a number of transmitting frequencies as in frequency division keying (FDK), orthogonal frequency division multiplexing (OFDM) or multicarrier CDMA [68, 69, 70]. Recently, multiple input-multiple output (MIMO) techniques have been developed to use independent transmitting antennas as a space time diversity technique [71]. More recent versions of CDMA implementations employ multicode [72] techniques (MCCDMA) where each user is allotted number of spreading codes to increase data rate for that user. User data is split into a number of parallel data streams and different spreading codes are used to simultaneously transmit these data bit streams.

In this dissertation, redundant codes or repetition coding is proposed in order to improve detection performance particularly at lower signal to noise ratios. Each user is allotted an odd number of codes for data spreading in the first stage of orthogonal transmultiplexer. Input data is spread using these codes and the spread data is

synchronously combined, resulting in varying power input data at the user's RF power amplifier in the transmitter. Data bits from different users are asynchronously combined with random delay over the channel. At the receiver, simple majority logic decision (reason for odd number of spreading codes for each user) is employed on the detected bits to get overall bit error performance.

Users can be allocated either standard single family codes or hybrid codes generated with the transmultiplexer structure.

8.3.2 Redundant Code Generation

Figure 8.8 displays the block diagram for allocation and processing of 3 redundant codes for each user at the transmitter and receiver in asynchronous CDMA system.

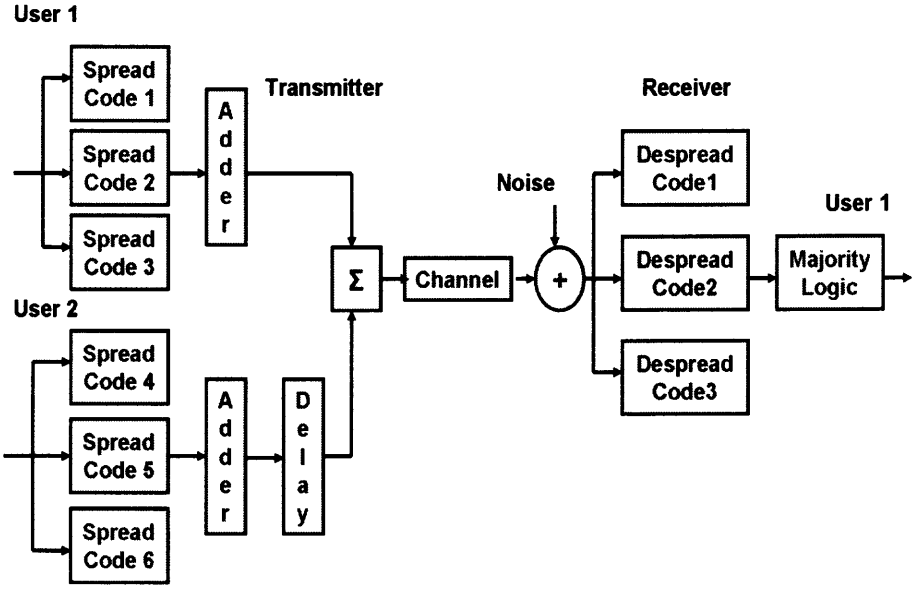

Figure 8.8 Block diagram for 2-user, 3-channel redundancy coding with single family of spreading codes.

Data from *user1* is spread simultaneously with three codes *code1*, *code2* and *code3* and is combined, resulting in having a variable power data at the RF power

amplifier in *user1* transmitter. *user2* data is similarly spread with three other spreading codes *code4*, *code5* and *code6* and is combined. Data from both users is asynchronously combined over the channel. At *user1* receiver, received data bits are despread using *code1*, *code2* and *code3* and are detected. Majority logic decision of at least 2 out of 3 detections is applied on the individually detected code channels to get overall detection performance.

Let N be an odd number of spreading codes using which each user data is simultaneously spread, combined and transmitted. Majority logic decision is the probability of finding detections in at least $(N+1)/2$ spreading channels out of a total of N channels.

As these N spreading code channels are independent, Bernoulli trials can be used to analytically express the bit error rate performance (P_n) [68]

$$P_n = 1 - \sum_{i=(N+1)/2}^{N} (1-P_e)^i P_e^{N-i} \tag{8.4}$$

where P_e is the bit error probability with single spreading code.

This expression is equivalent to

$$\begin{aligned} P_3 &= 1-(1-P_e)^2[1+2P_e] \\ P_5 &= 1-(1-P_e)^3[1+3P_e+6P_e^2] \\ P_7 &= 1-(1-P_e)^4[1+4P_e+10P_e^2+20P_e^3] \\ P_9 &= 1-(1-P_e)^5[1+5P_e+15P_e^2+35P_e^3+70P_e^4] \end{aligned} \tag{8.5}$$

for 3, 5, 7 and 9 redundancy codes per user.

As P_e is less than 1, P_n value will become smaller as the number of spreading codes keeps increasing.

Redundant code generation method using a two-stage orthogonal transmultiplexer for 2-users with three spreading codes for each user is displayed in Figure 8.9. Input data bit is first up-sampled by eight and convolved using three spreading codes in first stage transmultiplexer and the combined data is further up-sampled by eight and convolved with spreading codes in second stage transmultiplexer. Spreading codes for different users can be the same in the first stage transmultiplexer but 2nd stage spreading codes have to be unique for each user. Reverse operation of down-sampling and despreading is performed on the received bits using two stages of orthogonal transmultiplexer in order to obtain detected bits. This design can be extended to any number of users or stages of orthogonal transmultiplexers with the same number of redundancy codes for each user.

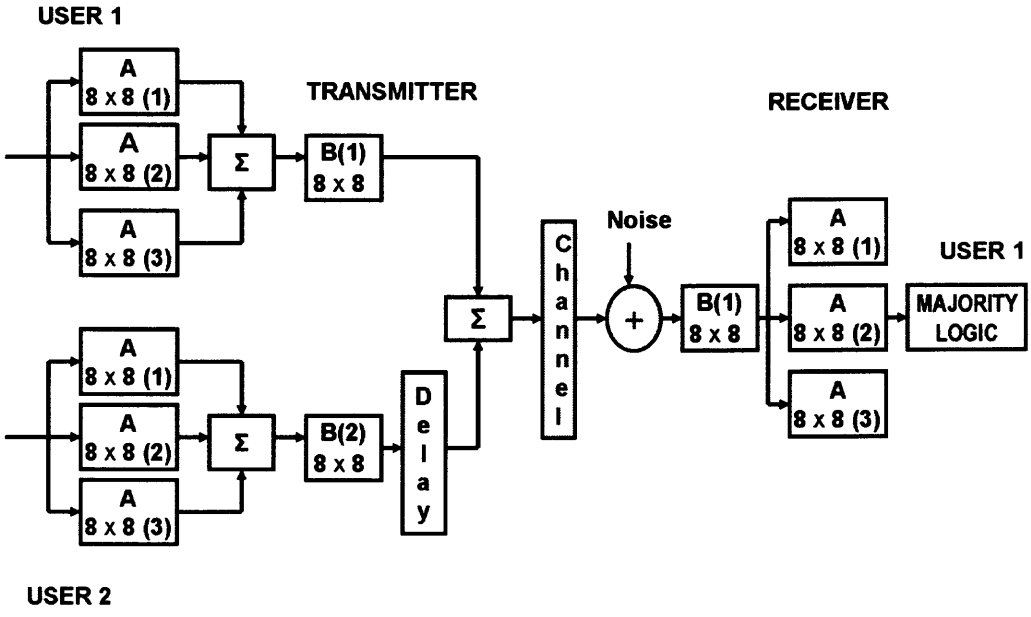

Figure 8.9 Block diagram for 2-user, 3-channel redundancy coding with two-stage orthogonal transmultiplexer.

This method of allocating number of spreading codes for each user decreases the number of available users compared to a single code per user system. On the other hand,

it is preferable to have fewer numbers of users with good BER performance than having more number of users with poorer performance in a low SNR channel.

8.3.3 Bit Error Rate (BER) Performance Comparisons

Two-user BER performance is simulated and displayed in Figure 8.10 for 16-length Walsh-like codes in asynchronous channel by allocating 1, 3, 5 and 7 numbers of unique spreading sequences to each user. It is noted that allocating one spreading code to each user corresponds to regular CDMA channel. BER performance improves with increase in number of spreading codes allocated to each user at low SNRs. At higher SNR, BER performance with higher number of spreading codes for each user is poorer than single spreading code performance. This phenomenon is due to the fact that multiuser cross-correlations or multiuser interference rather than noise dominates at higher SNRs.

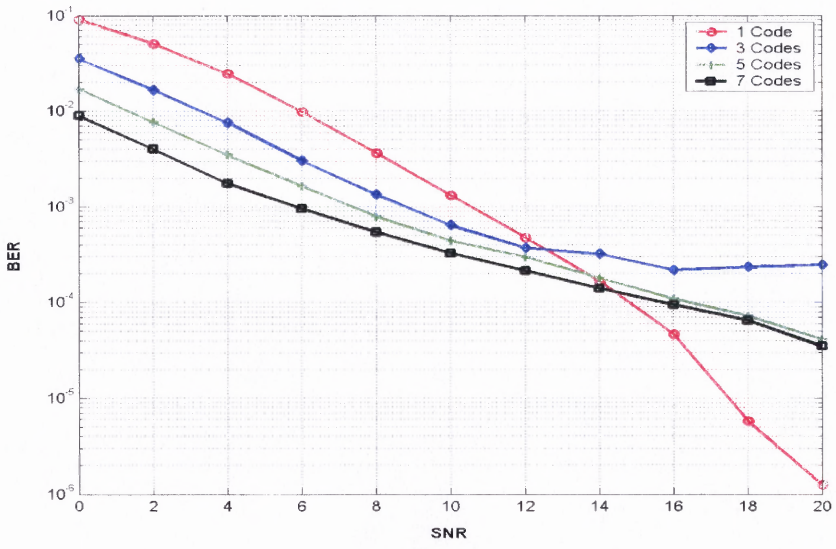

Figure 8.10 BER performances of 16-length Walsh-like code set with 1, 3, 5 and 7 redundant spreading codes for 2-users in AWG noise.

Similarly, Figure 8.11 displays the BER performance of 31-length Gold codes for 2-users with 1, 3, 5 and 7 unique spreading codes allocated to each user. Here also, communications performance improves at lower SNRs with increase in the number of spreading codes for each user.

Figure 8.12 displays asynchronous BER performance variation of 31-length Gold codes for 2-users with the increase in the number of spreading channel codes per user at different SNRs. BER performance is improved at low SNRs (up to 10 dB) as the number of spreading codes per user is increased from 1 to 7. If spreading codes are increased further, performance rather deteriorates. Single code performance is better than having more number of codes per user at high SNRs. Hence, based on the channel conditions, number of spreading codes should be judiciously allocated to each user.

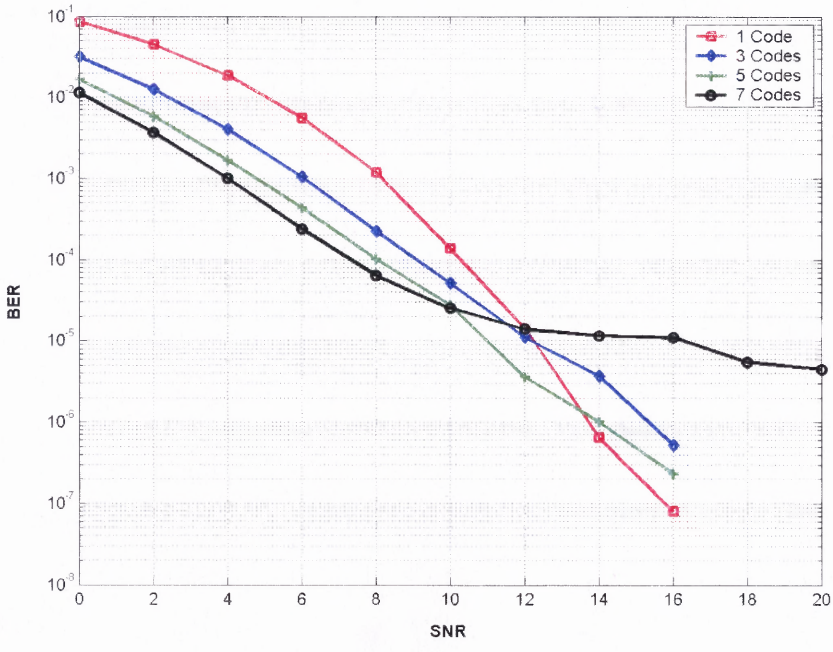

Figure 8.11 BER performances of 31-length Gold code set with 1, 3, 5 and 7 redundant spreading codes for 2-users in AWG noise.

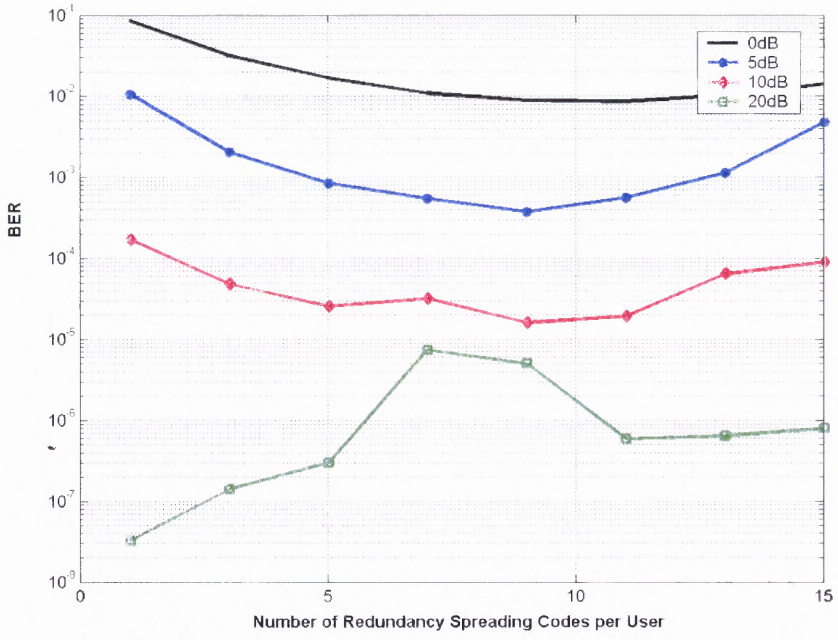

Figure 8.12 BER performance variations with number of spreading codes for 31-length Gold code set at different SNRs in AWG noise for 2-user case.

Performance improvements with redundancy coding are also observed using hybrid or Kronecker product codes. As an example, 64-length product codes are generated using two unique Walsh-like code sets in a 2-stage orthogonal transmultiplexer and redundant spreading code performance is simulated by allocating three codes to each user. User1 data is spread with any three codes in 1st stage and 1st code in 2nd stage. User2 data is spread with any three codes in 1st stage and 2nd code in 2nd stage. This process is repeated for up to eight users. For 9th user, 1st stage spreading codes different from user1's codes are used with the same 1st code in 2nd stage. Similar code assignment is repeated up to 16 number of users.

Figures 8.13, 8.14 and 8.15 display the multiuser performance of hybrid codes by allocating three spreading codes for each user evaluated at SNR = 5 dB, 10 dB and 20 dB, respectively.

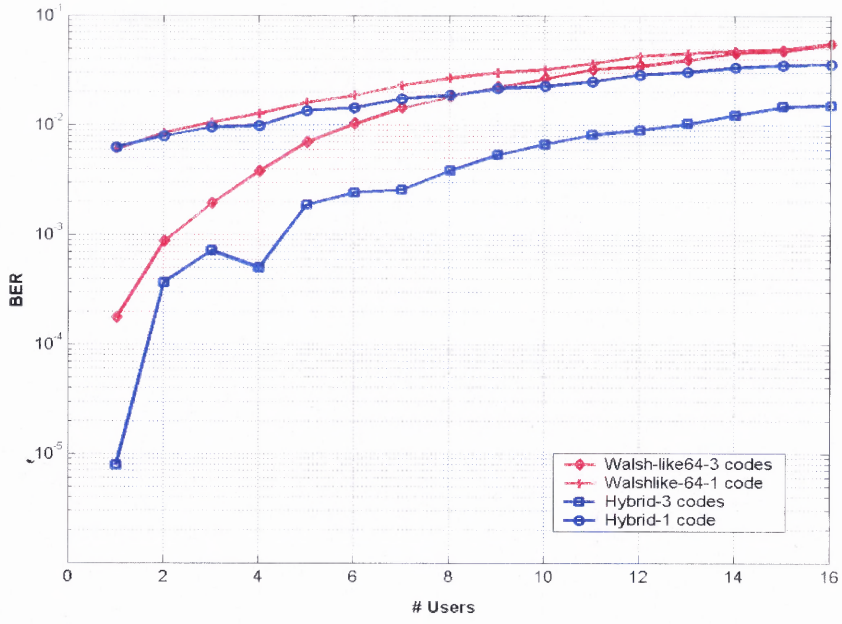

Figure 8.13 Multiuser BER performances of 64-length hybrid and Walsh-like code sets with 1, 3 redundancy spreading codes in AWG noise at SNR=5 dB.

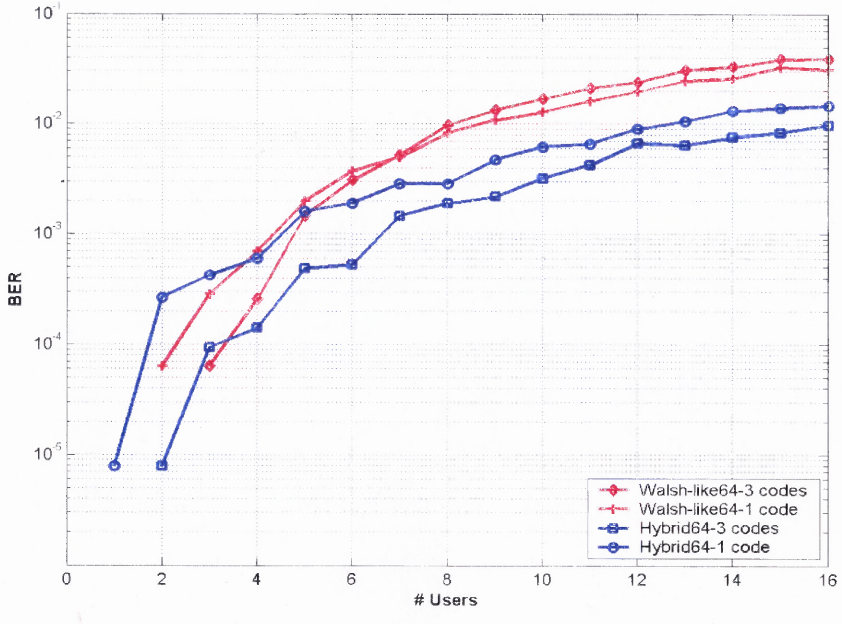

Figure 8.14 Multiuser BER performances of 64-length hybrid and Walsh-like code sets with 1, 3 redundancy spreading codes in AWG noise at SNR=10 dB.

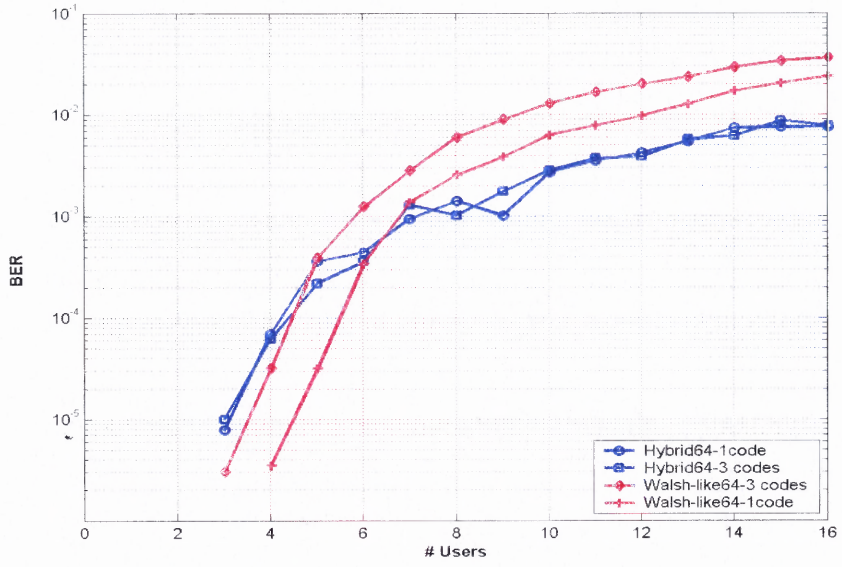

Figure 8.15 Multiuser BER performances of 64-length hybrid and Walsh-like code sets with 1, 3 redundancy spreading codes in AWG noise at SNR=20 dB.

These figures indicate that BER performance improvement is significant with redundant spreading channels at low SNRs and for smaller number of users in the system. As the number of users in the system increases, performance of all types of codes becomes poor. Also, at low SNRs, hybrid codes tend to give better BER results compared to standard single family codes like Walsh-like and Gold codes. At higher SNRs, performance improvement with redundant coding is marginal and performance advantage of hybrid codes compared to standard codes is minimal.

Figure 8.16 displays synchronous and asynchronous BER performance of 64-length hybrid codes with 1, 3, 5 and 7 codes for 2-users in Rayleigh flat fading conditions. Performance improves in the case of synchronous channel with the increase in the number of spreading codes for each user, where as improvement is negligible in the case of asynchronous channel.

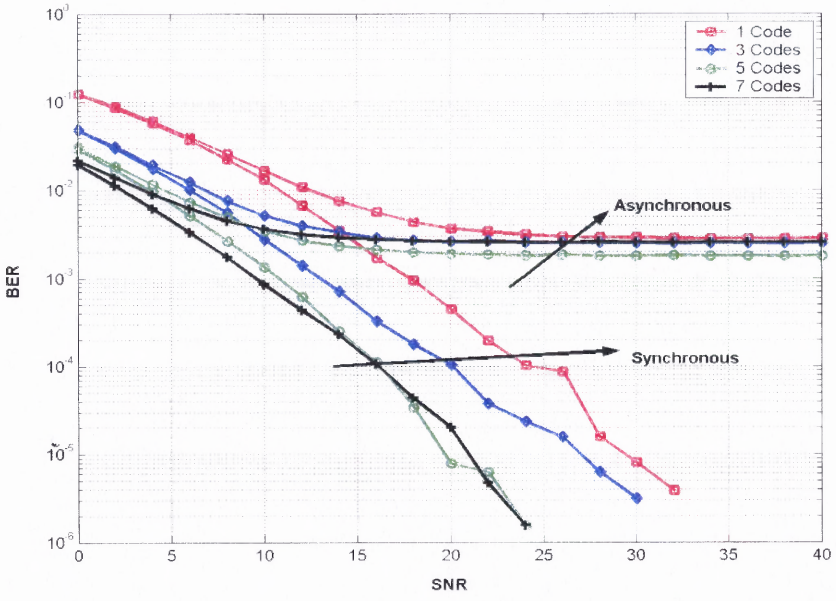

Figure 8.16 BER performances of 64-length hybrid code set for synchronous and asynchronous Rayleigh flat fading channel with 1,3,5,7 spreading codes for 2-user scenario.

Figure 8.17 displays multiuser performance of 64-length hybrid and Walsh-like codes with 1, 3, 5 and 7 redundancy codes in Rayleigh flat fading channel evaluated at SNR = 5 dB. This figure also indicates that performance improvement is negligible for asynchronous channels in Rayleigh flat fading channel.

It is noted that in the case of AWGN noise, performance improvement with channel coding at 5 dB SNR is substantial, as shown in Figure 8.12, where as in case of Rayleigh channel, improvement is minimal. This is due to the fact that as each user data is simultaneously spread with different codes, same channel conditions are applied for all code sequences. There is no significant improvement in Rayleigh flat fading conditions as channel diversity is not available for user data bits. To improve performance in Rayleigh flat fading conditions, diversity techniques like frequency hopping, space code or time diversity techniques need to be incorporated in the system.

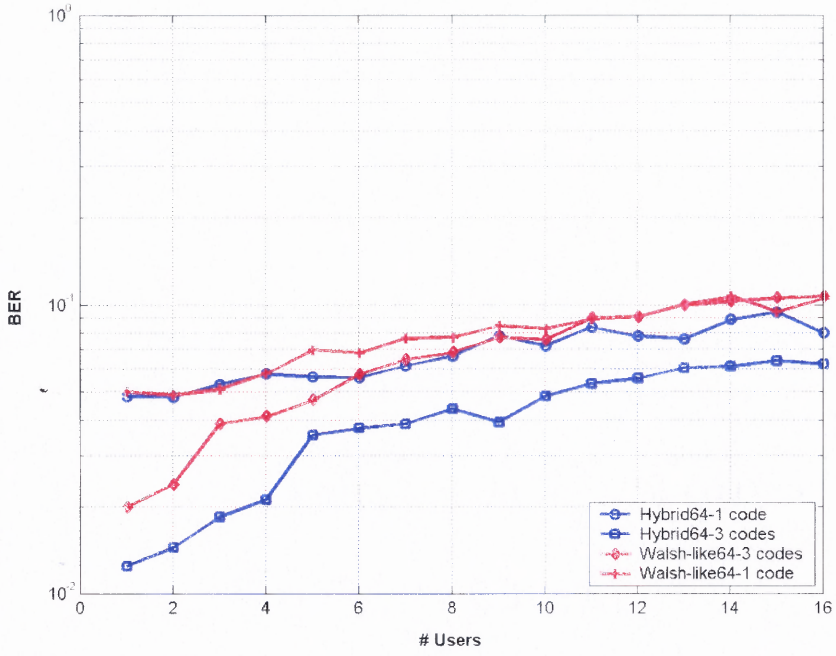

Figure 8.17 Multiuser BER performances of 64-length hybrid and Walsh-like code sets with 1 & 3 redundancy spreading codes in asynchronous Rayleigh flat fading channel at SNR=5 dB.

CHAPTER 9

CONCLUSIONS AND FUTURE RESEARCH

Orthogonal transmultiplexer configuration suitable for CDMA communications scenario is chosen as the theoretical frame work for this dissertation. Transmultiplexer basis functions are designed based on the orthogonality principle as well as minimization of inter- and intra-code correlation values among the basis functions.

Growing demand for new spread spectrum communication applications necessitates the design of additional orthogonal code sets with flexible code lengths and power requirements. New linear phase, near orthogonal and non-linear phase (Walsh-like) code families are proposed and designed for different code lengths by relaxing the constraints on the code design not pertinent for spread spectrum applications. Performance characteristics of these proposed new sets of codes are closely matching with the widely used CDMA codes in all channel conditions.

With recent advances in RF amplifier design, varying power codes are becoming feasible for an efficient CDMA system. In this dissertation, design methodology for multiple valued integer spread spectrum codes is proposed. BER performance of multiple level orthogonal code sets is better than corresponding binary valued codes. It is shown that system performance improves as the number of spreading code levels increases with fixed code length. Short length codes with multiple level spreading codes are particularly useful for short distance communication scenarios like sensor node networks. Sample short length codes have been given in the dissertation. More research is required for the design of optimal short length codes suitable for Zigbee applications.

KLT technique is extended for designing multiple valued, varying power orthogonal spreading codes suitable for DS-CDMA communications. It is shown that spread spectrum *KLT* code sets outperform Walsh codes and are comparable to or marginally better than the widely used Gold codes in all channel conditions and examples considered. An important advantage of the proposed technique is its analytical nature that provides infinitely many orthogonal spreading code solutions with flexible code lengths and good BER performance for given input signal statistics. In the dissertation, spread spectrum PSD function has been modeled as an AR process. Further study is needed in modeling PSD function with accurate ARMA models. As spread spectrum *KLT* code generation requires lot of mathematical computations, an efficient algorithm for practically implementing *KLT* codes needs to be developed.

Hybrid codes are generated by taking Kronecker product of two or more orthogonal spreading code matrices in a multiple stage transmultiplexer structure. Code families considered can be of any size, any family and can be of binary or multiple level chip values with the aim of minimizing total cross-correlation values. BER performance improves by optimally allotting hybrid spreading codes to different users compared to single family code assignment.

In this dissertation, a design method is proposed to improve system performance by means of redundant spreading codes. Each user data bit is simultaneously spread with odd number of spreading codes and is synchronously combined prior to transmission in the first stage of a multiple stage orthogonal transmultiplexer. With redundant spreading codes, significant improvements in BER performance are observed particularly at the low SNR conditions. As the number of spreading codes is increased for each user,

performance improves in asynchronous channel as long as cross-correlation values are lower than noise level. Hence, an optimum choice for redundant codes needs to be defined based on the channel conditions. An efficient switching algorithm for dynamically changing the spreading codes based on the channel conditions needs to be investigated.

In the dissertation, BER performance characteristics improvements with different multiple level, varying power spreading codes compared to the corresponding binary spreading codes have been shown at the code level. Effect of varying power codes on RF power amplifier in terms of its peak to average power ratio (PAPR) or crest factor needs to be studied. Furthermore, entire CDMA system needs to be simulated using multiple level spreading codes with RF band modulation / demodulation.

APPENDIX A

32-LENGTH LINEAR PHASE ORTHOGONAL CODE SETS

Table A.1 Four Sets of 32-Length Linear Phase Orthogonal Code Sets Represented in Integer Format

Index No	Orthogonal Set 1	Orthogonal Set 2	Orthogonal Set 3	Orthogonal Set 4
1	4294967295	4294967295	4294967295	4294967295
2	98303	180223	5973503	319487
3	16679167	16597247	116291424	16457983
4	41942592	31456128	199813167	25165440
5	231461808	246836592	304520119	244314480
6	252612367	252530447	429217383	252391183
7	267481103	258578160	446421336	267702287
8	364277160	267563023	477474360	384929640
9	731228628	858878771	593345220	733105620
10	858960691	859155660	629325403	859247411
11	869092403	869174323	699821460	868805683
12	870848460	880434732	774992779	899430828
13	1009628220	998920668	902022060	980170332
14	1010648003	1010729923	939458579	1010361283
15	1019395267	1019313347	1011666371	1019681987
16	1045580412	1019585340	1059591420	1027850940
17	1320689010	1390659402	1193068317	1306798002
18	1431622997	1431770453	1202818530	1405768650
19	1437280853	1437133397	1286539981	1431401813
20	1455793002	1437349290	1292890290	1437502037
21	1499216538	1515775397	1366974090	1516144037
22	1515922853	1515993690	1455520917	1520532133
23	1520753317	1520900773	1539580890	1528146138
24	1529070810	1561577658	1567797573	1547328570
25	1701940902	1712320614	1634031993	1716939366
26	1718032793	1717885337	1760139030	1717746073
27	1721296537	1721443993	1792447657	1721583257
28	1728999654	1741687782	1850886774	1730778342
29	1759930134	1756994838	1891164913	1759091478
30	1768483177	1768318614	1915216974	1768769897
31	1771509353	1768630633	1956395310	1771222633
32	1889261838	1771361897	2064330529	1890051342

APPENDIX B

32-LENGTH NON-LINEAR PHASE (WALSH-LIKE) ORTHOGONAL CODE SETS

Table B.1 Two sets of 32-Length Walsh-like and Walsh Code Sets Represented in Integer Format

Index No	Walsh-like32 Set1	Walsh-like32 Set2	Walsh-32
1	58392308	58386676	4294967295
2	136970343	136975975	2863311530
3	366559442	366565074	3435973836
4	512343617	512337985	2576980377
5	627959339	627958315	4042322160
6	775755960	775756984	2779096485
7	869160973	869161997	3284386755
8	949921438	949920414	2526451350
9	1141297881	1141299929	4278255360
10	1331047498	1331045450	2857740885
11	1386573055	1386571007	3425946675
12	1509266028	1509268076	2573637990
13	1645310470	1645312518	4027576335
14	1765903509	1765901461	2774181210
15	1957874720	1957872672	3275539260
16	2145530547	2145532595	2523502185
17	2262016061	2262021693	4294901760
18	2374196910	2374191278	2863289685
19	2423266843	2423261211	3435934515
20	2602623112	2602628744	2576967270
21	2697246946	2697247970	4042264335
22	2878621297	2878620273	2779077210
23	3060205252	3060204228	3284352060
24	3174561879	3174562903	2526439785
25	3249482256	3249483280	4278190335
26	3405763715	3405762691	2857719210
27	3607925814	3607924790	3425907660
28	3697044133	3697045157	2573624985
29	3887631055	3887632079	4027518960
30	3974657116	3974656092	2774162085
31	4045092073	4045091049	3275504835
32	4199271034	4199272058	2523490710

REFERENCES

[1] R. E. Crochiere and L. R. Rabiner, "Interpolation and Decimation of Digital Signals: A Tutorial Review," Proceedings of IEEE, Vol. 69, pp. 300-331, March 1981.

[2] P. P. Vaidyanathan, "A Tutorial on Multirate Digital Filter Banks," Proceedings of IEEE International Symposium on Circuits and Systems, Espoo, Finland, pp. 2241-2248, June 1988.

[3] P. P. Vaidyanathan, "Multirate Digital Filters, Filter Banks, Polyphase Networks, and Applications: A Tutorial," Proceedings of IEEE, Vol. 78, pp. 56-93, Jan. 1990.

[4] H. Scheuermann and H. Gockler, "A Comprehensive Survey of Digital Transmultiplexing Methods," Proceedings of IEEE, Vol. 69, pp. 1419-1450, Nov. 1981.

[5] M. Vetterli, "Perfect Transmultiplexers," Proceedings of IEEE ICASSP, pp. 2567-2570, April 1986.

[6] M. Vetterli, "A Theory of Multirate Filter Banks," IEEE Transactions ASSP, Vol. 35, pp. 356-372, March 1987.

[7] A. N. Akansu, P. Duhamel, X. Lin and M. D. Courville, "Orthogonal Transmultiplexers in Communication: A Review," IEEE Transactions on Signal Processing, Vol. 46, pp. 979-995, April 1998.

[8] A. N. Akansu and R.A. Haddad, Multiresolution Signal Decomposition: Transforms, Subbands, Wavelets, 2nd Edition, Academic Press, 2001.

[9] A. N. Akansu, M. V. Tazebay and R. A. Haddad, "A New Look at Digital Orthogonal Transmultiplexers for CDMA Communications," IEEE Trans. on Signal Processing (Special Issue on Advanced Signal Processing for Communications), Vol. 45, pp. 263-267, Jan. 1997.

[10] M. K. Tsatsamis and G. B. Ginnakis, "Multirate Filter Banks for Code Division Multiple Access Systems," Proceedings of IEEE ICASSP, Vol. 2, pp. 1484-1487, May 1995.

[11] X. Lin, "Orthogonal Transmultiplexers: Extensions to Digital Subscriber Line (DSL) Communications," Ph.D. Dissertation, Jan. 1998.

[12] Website for CDMA2000, WCDMA standards : http://www.3gpp.org

[13] E. Dinan and B. Jabbari, "Spreading Codes for Direct Sequence CDMA and Wideband CDMA Cellular Networks," IEEE Communications Magazine, pp. 48-54, 1998.

[14] J. L. Walsh, "A Closed Set of Normal Orthogonal Functions," Americ. Journal of Mathematics, Vol. 55, pp. 5-24, 1923.

[15] J. J. Sylvester, "Thoughts on Inverse Orthogonal Matrices, Simultaneous Sign Successions, and Tessellated Pavements in Two or More Contours," Phil. Mag., Vol. 34, pp. 461-475, 1867.

[16] K. G. Beauchamp, Applications of Walsh and Related Functions, Academic Press, 1984.

[17] R. Gold, "Maximal Recursive Sequences with 3-Valued Recursive Cross correlation Functions," IEEE Transactions on Information Theory, Vol. IT-14, pp.154-156, 1968.

[18] T. Kasami, "Weight Distribution Formula for Some Class of Cyclic Codes," Coordinated Science Lab., Univ. Illinois, Urbana. Tech. Rep R-285 (AD632574), 1966.

[19] M. Pursely, "Performance Evaluation for Phase-Coded Spread Spectrum Multiple-Access Communication- Part I & II: System Analysis," IEEE Transactions on Communications, Vol. Com-25, No. 8, pp. 795-803, Aug.1977.

[20] D. V. Sarwate and M. B. Pursely, "Cross Correlation Properties of Pseudorandom and Related Sequences," Proceedings of IEEE, Vol. 68, No. 5, pp. 593-619, May 1980.

[21] L. R. Welch, "Lower Bounds on the Maximum Cross Correlation of Signals," IEEE transactions on Information Theory, Vol. IT-20, No. 3, 1974.

[22] D. V. Sarwate, "Bounds on Cross Correlation and Auto Correlation of sequences," IEEE Transactions on Information Theory, Vol. IT-25, No. 6, 1979.

[23] V. M. Sidelnikov, "Cross Correlation of Sequences," Probl. Kybern. Vol. 24, 1971.

[24] M. Stular and S. Tomazic, "Maximum Periodic Correlation of Pseudo-Random Sequences in CDMA," 10th Mediterranean Electrotechnical Conference, Vol. 1, pp. 420-423, 2000.

[25] V. DaSilva, E. S. Sousa, "Performance of Orthogonal CDMA Codes for quasi-Synchronous Communication Systems," ICUPC, pp. 995-999, 1993.

[26] C. Chen, K. Yao and E. Biglieri, "Optimal Spread Spectrum Sequences-Constructed from Gold Codes," IEEE GLOBECOM, Vol. 2, pp. 867-871, 2000.

[27] H. Donelan and T. O'Farrell, "Method for Generating Sets of Orthogonal Sequences," Electronics Letters, Vol. 35, No. 18, pp. 1537-1538, 1999.

[28] D. Gerakoulis and S. Ghassemzadeh, "Extended Orthogonal Code Designs with Applications in CDMA," 6th International Symposium on Spread Spectrum Techniques and Applications, Vol. 2, pp. 657-661, Sept. 2000.

[29] A. Miranda, S. Marques and F. Cercas, "On the Performance of TCH Sequences in DS-CDMA Systems," 5th International Symposium on Spread Spectrum Techniques and Applications, Vol. 3, pp. 818-822, Sept. 1998.

[30] J. A. L. Inacio, J. A. B. Gerald and M. D. Ortigueira, "New PN Even Balanced Sequences for Spread-Spectrum Systems," EURASIP journal on Wireless Communications and Networking, pp. 447-458, 2005.

[31] R. Yarlagadda and J. E. Hersley, "Analysis and Synthesis of Bent Sequences," IEE Transactions, Vol. 136, No. 2, pp. 112-123, March 1989.

[32] X. Zeng, L. Hu, Q. Liu and Y. Zhu, "Binary Sequences with Optimal Correlations and Large Linear Span," IEEE International Conference on Communications, Vol. 1, pp. 385-390, June 2006.

[33] P. Viswanath and V. Anantharam, "Optimal sequences and Sum Capacity of Synchronous CDMA Systems," IEEE Transactions on Information theory, Vol. 45, No. 6, pp. 1984-1991, Sept. 1999.

[34] S. Ulukus, R. D. Yates, "Iterative Construction of Optimum Signature Sequence Sets in Synchronous CDMA Systems," IEEE Transactions on Information theory, Vol. 47, No. 5, pp. 1989-1998, July 2001.

[35] H. Donelan, T. O'Farrell, "Families of ternary sequences with aperiodic zero correlation zones for MC-DS-CDMA," Electronics Letters, Vol. 38, No. 25, pp. 1660-1661, Dec. 2002.

[36] P. Z. Fan, N. Suehiro, N. Kuroyanagi and X. M. Deng, "Class of Binary Sequences with Zero Correlation zone," Electronics Letters, Vol. 35, No. 10, pp. 777-789, May 1999.

[37] R. Appuswamy and A. K. Chaturvedi, "Mutually Orthogonal Sets of ZCZ Sequences," Electronics Letters, Vol. 40, No. 18, pp. 1133-1134, Sept. 2004.

[38] J. A. Davis and J. Jedwab, "Peak-to-Mean Power Control in OFDM, Golay Complementary Sequences and Reed-Muller Codes," IEEE Transactions on Information Theory, Vol. 45, No. 7, pp. 2397-2417, Nov. 1999.

[39] A. V. Oppenheim and R. W. Schafer, Discrete-Time Signal Processing, Prentice-Hall, 2nd Edition, 1999.

[40] A. Papoulis, Signal Analysis, McGraw-Hill, New York, NY, 1977.

[41] H. Harada and R. Prasad, Simulation and Software Radio for Mobile Communications, Artech House, 2002.

[42] S. Verdu, Multiuser Detection, Cambridge University Press, 1998.

[43] R. Poluri and A. N. Akansu, "New Orthogonal Binary User Codes for Multiuser Spread Spectrum Communications," Proc. of EUSIPCO, pp. 1-4, Sept. 2005.

[44] R. Poluri and A. N. Akansu, "New Linear Phase Orthogonal Binary Codes for Spread Spectrum Multicarrier Communications," IEEE, VTC, pp. 1-5, Sept. 2006.

[45] R. Poluri and A. N. Akansu, "Walsh-like Nonlinear Phase Orthogonal Transforms for CDMA Communications," Asilomar Conference on Signals, Systems, and Computers, pp. 2214-2218, Nov. 2006.

[46] A. N. Akansu and R. Poluri, "Walsh-like Nonlinear Phase Orthogonal Transforms for Direct Sequence CDMA Communications," IEEE Transactions on Signal Processing, to appear in 2007.

[47] Website for the new binary codes and their comparative BER performance (http://web.njit.edu/~ali/NewCodes.html).

[48] S. Moshavi, "Multi-User Detection for DS-CDMA Communications," IEEE Communications Magazine, pp. 124-136, Oct. 1996.

[49] G. Woodward and B. S. Vucetic, "Adaptive Detection for DS-CDMA," Proceedings of IEEE, Vol. 86, No. 7, pp. 1413-1432, July1998.

[50] B. Sklar, "Rayleigh Fading Channels in Mobile Digital Communication Systems Part I: Characterization," IEEE Communications Magazine, pp. 90-100, July 1997.

[51] B. Sklar, "Rayleigh Fading Channels in Mobile Digital Communication Systems Part II: Mitigation," IEEE Communications Magazine, pp. 102-109, July 1997.

[52] M. K. Simon and M. S. Alouini, Digital Communications over Fading Channels, Wiley series in Telecommunications and Signal Processing, 2004.

[53] C. Komninakis, "A Fast and Accurate Rayleigh Fading Simulator," IEEE GLOBECOM, Vol. 6, pp. 3306-3310, 2003.

[54] T. S. Rappaport, Wireless Communications: Principles and Practice, 2nd Edition, Prentice Hall, 2001.

[55] T. Lang and X. Chen, "Comparison of Correlation Parameters of Binary Codes for DS/CDMA Systems," ICCS, Singapore, pp. 1059-1063, 1994.

[56] R. L. Frank, "Polyphase Codes with Good Nonperiodic Correlation Properties," IEEE Transactions on Information Theory, Vol. 9, No. 1, pp. 43-45, Jan. 1963.

[57] L. Lu and V. K. Dubey, "Extended Orthogonal Polyphase Codes for Multicarrier CDMA System," IEEE Communications Letters, Vol. 8, No. 12, pp. 700-702, Dec. 2004.

[58] M. Darnell and A. H. Kemp, "Synthesis of Multilevel Complementary Sequences," Electronics Letters, Vol. 24, No. 19, pp. 1251-1252, Sept. 1988.

[59] Q. K. Trinh, P. Fan and E. M. Gabidulin, "Multilevel Hadamard Matrices and Zero Correlation Zone Sequences," Electronics Letters, Vol. 42, No. 13, pp. 748-750, June 2006.

[60] C.-P. Liang, et. al, "Nonlinear Amplifier Effects in Communications Systems," IEEE, Transactions on Microwave Theory and Techniques, Vol. 47, No. 8, pp. 1461-1466, Aug. 1999.

[61] M. Chrysochoos and J. Kim, "Performance Analysis of an MC-CDMA Broadcasting System under High Power Amplifier Non-Linearities, Part I: System Proposal," IEEE Transactions on Broadcasting, Vol. 46, No. 4, pp. 256-262, Dec. 2000.

[62] R. Poluri and A. N. Akansu, "Short Length CDMA Codes for Wireless Sensor Networks," accepted to IEEE, Sarnoff Conference, 2007.

[63] Zigbee Protocols: http://www.zigbee.org.

[64] H. Hotelling, "Analysis of a Complex of Statistical Variables into Principal Components," Journal of Educational Psychology, Vol. 24, pp. 417-441 and 498-520, 1993.

[65] W. Ray and R. M. Driver, "Decomposition of the K-L Series Representation of a Stationary Random Process," IEEE Transactions on Information Theory, IT-16, pp. 663-668, 1970.

[66] S. M. Kay, Modern Spectral Estimation: Theory and Application, 1st Edition, Prentice Hall, 1991.

[67] I. J. Good, "The interaction algorithm and practical Fourier Analysis," J. Roy. Statist. Soc., B20, No. 2, pp. 361-372, 1958.

[68] W. C. Y. Lee, "Mobile Signaling Error Rate Caused by Jammers at VHF," IEEE VTC, Vol. 31, pp. 240-260, 1981.

[69] A. A. Ali and I. A. Al-Kadi, "On the Use of Repetition Coding with Binary Digital Modulations on Mobile Channels," IEEE Transactions on Vehicular Technology, Vol. 38, No. 1, pp. 14-18, Feb. 1989.

[70] S. Hara, R. Prasad, "Design and Performance of Multi-carrier CDMA System in Frequency Selective Rayleigh Fading Channels," IEEE Transactions on Vehicular Tech., Vol. 48, No.5, pp 1584-1595, Sep. 2002.

[71] S. M Alamouti, "A Simple Transmitter Diversity Scheme for Wireless Communications," IEEE Journal on Selected Areas Communication, Vol. 16, pp. 1451-1458, Oct. 1998.

[72] I. Chih-Lin and R. D. Gitlin, "Multi-code CDMA Wireless Personal Communications Networks," IEEE International Conference on Communications, Vol. 2, pp. 1060-1064, June 1995.